OPTIMIZATION OF CONTINUOUS POST-TENSIONED CONCRETE BRIDGE GIRDERS WITH VARIABLE DEPTH

BY

MOHAMMED ALI MOHAMMED AL-OSTA

A Thesis Presented to the

DEANSHIP OF GRADUATE STUDIES

KING FAHD UNIVERSITY OF PETROLEUM & MINERALS

DHAHRAN, SAUDI ARABIA

In Partial Fulfillment of the
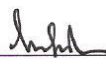Requirements for the Degree of

MASTER OF SCIENCE

In

CIVIL ENGINEERING

APRIL, 2009

KING FAHD UNIVERSITY OF PETROLEUM & MINERALS
DHAHRAN 31261, SAUDI ARABIA
DEANSHIP OF GRADUATE STUDIES

This thesis, written by **MOHAMMED ALI MOHAMMED AL-OSTA** under the direction of his thesis advisor and approved by his thesis committee, has been presented to and accepted by the Dean of Graduate Studies, in partial fulfillment of the requirements for the degree of **MASTER OF SCIENCE** in **CIVIL ENGINEERING**
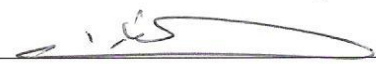
Thesis Committee

Prof. Abul Kalam Azad (Advisor)
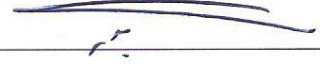
Dr. Husain J. Al-Gahtani (Co-Advisor)

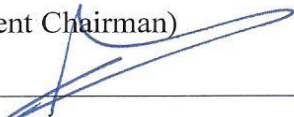Prof. Alfarabi Sharif (Member)

Dr. Ahmad S. Al-Gahtani (Member)

Dr. Maher A. Bader (Member)

Dr. Husain J. Al-Gahtani
(Department Chairman)

Dr. Salam A. Zummo
(Dean of Graduate Studies)

13|6|09

Date

بسم الله الرحمن الرحيم

DEDICATED
TO MY FATHER, MOTHER, WIFE AND MY
CHILDREN AND TO MY BROTHERS AND SISTERS

ACKNOWLEDGMENT

TABLE OF CONTENTS

LIST OF TABLES

LIST OF FIGURES

ix

THESIS ABSTRACT

NAME: **MOHAMMED A. MOHAMMED AL-OSTA**

TITLE: **OPTIMIZATION OF CONTINUOUS POST-TENSIONED CONCRETE BRIDGE GIRDERS WITH VARIABLE DEPTH.**

DEPARTMENT: **CIVIL ENGINEERING**

DATE: **April, 2009**

Post-tensioned single-cell concrete box girders of variable depth are used in continuous bridges to achieve both economy and aesthetics. To determine the minimum prestressing for a given bridge deck profile, the minimum cost design of a continuous single box girder of non-uniform depth is achieved through a constrained optimization procedure. This study considers both two and three span continuous bridge girders subjected to American Association of State Highway and Transportation Officials (AASHTO-96) HS Bridge loading. Both short and long tendons are used in order to obtain the optimum prestressing force. The nonlinear problem is solved by transforming it into a linear one by using a new design variable, which proportions long and short tendons.

A computer code (**PCPCBGND**) is developed by using a standard FORTRAN for analysis and optimum structural design of bridge girders where a gradient search technique is used to solve iteratively the optimization problem. The design variables include: interior to exterior span ratio for three-span, the depth profile of the cross-section, tendon eccentricities, and prestressing force. The total cost of the member

considered is the cost of structural materials (concrete and prestressing steel), excluding the formwork. The design constraints are the prescribed limits of working stresses, the strength, and serviceability requirements. Several examples are solved by using the design required by the American Institute (ACI-343R-95) to demonstrate applications and some important findings. The study shows that optimum prestressing is attained only at an optimum proportion of long and short tension. Furthermore, for an economical design, the ratio of interior to exterior span for a three-span continuous girder should be from 1.30 to 1.40.

MASTER OF SCIENCE DEGREE
KING FAHD UNIVERSITY OF PETROLEUM AND MINERALS
DHAHRAN, SAUDI ARABIA

ملخص الرسالة

الإســـــــــم : محمد علي محمد الأسطى

عنوان الرسالة : التصميم الامثل للجسور الخرسانية المستمرة المسبقة الشد ذات العمق المتغير

التخصـــــص : الهندسة المدنية

تاريخ التخرج : إبريل 2009م

تستخدم الجسـور المستمرة المسبقة الشد ذات العمق المتغير و المقطع الخرساني الصندوقي احـادي الفتحـة لتحقيـق كـلاً مـن الإقتصـاد والجمـال. لتحديد الحدّ الأدنى مـن مقدار الشد الـلازم للجسـور المعطاة ، صـممت الجسـور المستمرة المسبقة الشد ذات العمق المتغير و المقطع الخرسـاني الصـندوقي احـادي الفتحـة بكلفـة أدنى وخاضـعه لتقييدات معينـة و ذلـك باسـتخدام خطـوات تحقيـق مثلـى. هـذه الدراسـة تاخـذ فـي الاعتبـار الجسـور المستمرة المكونـة مـن بحرين وثلاثـة بحـور ومعرضـة لاحمـال وفقـاً للجمعيـة الأمريكيـة للطرق HS-20(AASHTO-96). حيـث تـم اسـتخدام نـوعين مـن الكـابلات ، كاملـة وقصـيرة الطـول للوصـول الـى افضل منظومـة لهـا و الحد الأدنى مـن مقدار الشد الـلازم. حيث تـم حل المسألة اللاخطية بتحويلها الـى مسـألة خطية وذلك باستخدام متغير جديد وهو النسبة مابين الكابلات الطويلة والقصيرة.

لقد تـم تطـوير برنـامج (**PCPCBGND**) باسـتخدام لغـة الفـورتران وذلـك لتحليـل وايجـاد التصـميم الامثل باسـتخدام تقينيـة البحـث المتـدرج (gradient search technique) . حيث شـملت متغيـرات التصـميم النسبة مـابين البحـر الـداخلي والبحـر الخـارجي فـي حالـة الجسـور ذات الثلاثـة بحـور ، سـماكة الكمـرة علـى طـول الجسـر ، وضـع الكـابلات الهندسـي و مقدار الشد الـلازم . أخـذت التكلفـة الكليـة للمـواد الانشـائية للجسـر ممثلـة بكلفـة الخرسـانة وكلفـة الحديد المشـدود فقط ولـم تؤخـذ كلفـة الشدات . امـا بالنسبة لتقييدات التصـميم فقد شـملت عـدم تجـاوز الحـدود المسـموح بهـا للاجهـادات ، قـدرة التحمـل للعـزوم والقص و متطلبـات التشـغيل. العديد مـن الامثلـة صـممت طبقـاً لمواصفات المعهدالامريكي (ACI-343R-95) لعـرض امكانيـة البرنـامج ولتوضـيح اشـياء مهمـة. حيث وضـحت الدراسـة أن مقدار الشد المثـالي يمكـن تحقيقـه فقـط باسـتخدام نسـبة

مثاليـة مـابين الكـابلات الطويلـة والقصـيرة المشـدودة. عـلاوة على ذلـك وجـد أن التصـميم الأقتصـادي للجسـور

ذات الثلاثـة بحـور يمكـن التوصـل اليـه عنـدما تكـون النسبة مـابين البحـر الـداخلي والبحـر الخـارجي تتـرواح مـا

بين 1.3 و 1.4 .

درجة الماجستير في العلوم
والمعادن للبترول فهد الملك جامعة
31261 – الظهران
المملكة العربية السعودية

CHAPTER ONE

INTRODUCTION

1.1 General

Prestressed concrete is used widely in concrete construction due to its economy, reliable structural resistance, ductility and durability. The technique of prestressed concrete is now widely used in all types of structures and structural components. These can range from simple beams and floor slabs to large oil platform structures and innovative bridge forms (Hulse and Mosley, 1987).

Prestressed concrete, particularly box girder construction which is often used in bridges, allows the use of architectural treatments, such as curved surfaces and finishes that enhance the appearance of the structure. Box girders, moreover, provide one excellent method of concealment for unsightly utilities. Post-tensioning in the box girders extends the usefulness and versatility of concrete by allowing longer spans, fewer and thinner columns, and better proportioned sections, enhancing the overall appearance of the structure (Western Concrete Reinforcing Steel Institute, 1971).

Box girder construction also affords many advantages in terms of safety, appearance, maintenance, and economy. Long spans may be constructed economically, thereby reducing the number of piers and eliminating shoulder obstacles at overpasses. Obstacle elimination greatly enhances the recovery area for out-of-control vehicles. Box girders may consist of a single cell for a two-lane roadway, multiple cells for multiple-

lane roadways, or single or multiple cells with cantilever arms on both sides to provide the necessary roadway width, and to reduce the substructure cost and minimize right-of-way requirements. For box girders in general, the longer spans have been cast-in-place because of the need for greater and variable depths, while the shorter spans lend themselves to constant depth precast units (ACI-343R-95).

Modern structural engineering tends to progress toward more economical structures by using numerical mathematics for optimization. Optimization is a branch of numerical mathematics which is used to identify optimal settings of elements' parameters, properties, time-variant processes, etc., while simultaneously considering constraints. Optimization is becoming more important and useful for designing more economical structures in terms of cost (Arora, 2004).

Optimization involves minimizing or maximizing an objective function, subject to a set of applicable constraints. For a bridge section the objective function can be: minimum production costs, minimum life cycle costs, minimum weight, and maximum stiffness. The list of constraints for a feasible design can be: choice of material, admissible stresses, admissible displacements (deformations), load cases, and supports.

1.2 Significance of the Study

The design of a continuous prestressed concrete bridge is a time-consuming process if the bridge girders are of variable depth. As numerous safe designs are possible, it is of interest to seek an optimal solution based on minimum material cost. In the present study, an optimization procedure is prescribed for adoption in practical design.

The prescribed approach will enable designers to achieve low-cost design of a continuous non-uniform bridge girder having a prescribed length.

1.3 Scope and Objectives

The scope of this study is to optimize the design of continuous post-tensioned concrete bridge girders having two or three spans subject to the HS Bridge loading of the American Association of State Highway and Transportation Officials (AASHTO). The system will be capable of analyzing and designing an economical prestressed concrete single cell continuous box-girder (Figure 1.1). These girders are symmetric about the transverse center line, as is common in bridges. This implies equal spans for a two-span continuous bridge girder and an equal exterior span for a three-span girder. The total cost of structural materials (concrete and prestressing steel) will be taken as the objective function. The constraints include: prescribed limits of working stresses, ultimate shear and ultimate moment capacities, severability, cross-sectional dimensions, and tendons profile to ensure that the minimum concrete cover to tendons is maintained throughout the whole bridge girder.

The primary objectives of this study are as follows:

1- Develop a generalized computer program to find an optimum design of continuous post-tensioned concrete bridge girders with variable depth having two or three spans.

2- Provide informative data about the optimum span ratio in a three-span continuous bridge girder, which would assist an engineer to choose the spans

close to the optimum value.

3- Provide informative data about the optimum depth ratios relative to the total length of the bridge.

4- Highlight the optimum tendon arrangement of short and long tendons.

1.4 Limitations

This study is limited to the following conditions:

- The two or three-span continuous post-tensioned prestressed bridge girders have parabolically varying depth.

- The only cross-sectional dimensions variable for the single cell of box-girder is the depth h, which varies along the length. All other dimensions (Figure 1.1) are assumed to be prescribed.

- The tendon profile consists of parabolic segments.
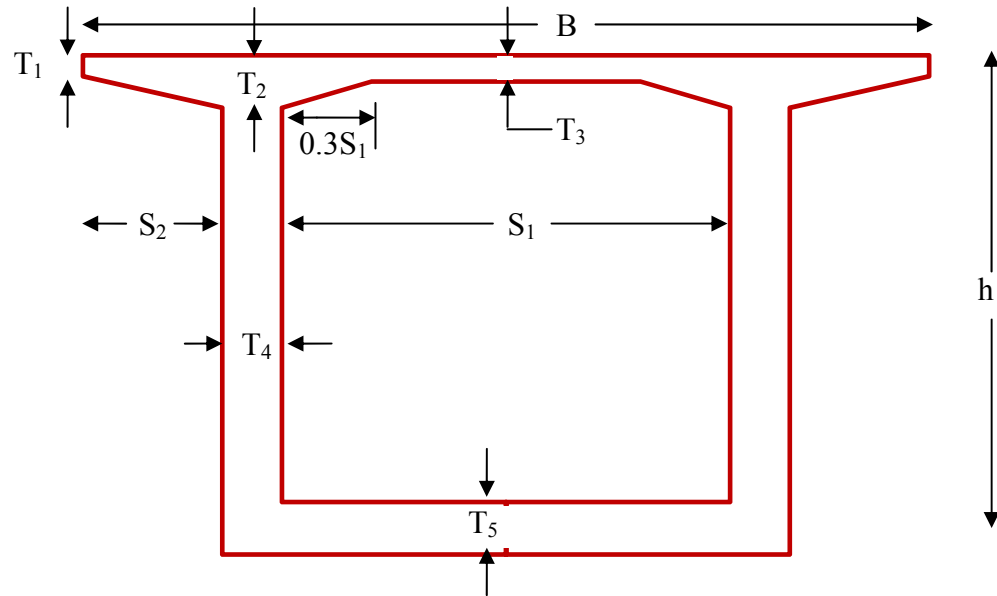
Figure 1.1 Typical Cross-Section of the Box Girder

1.5 Research Methodology

To accomplish the above objectives, this research will use a methodology comprising the following phases (Figure 1.2):

1. Literature Review

    - Optimum design of prestressed concrete bridge girders.

    - Numerical methods for optimization of prestressed concrete.

    - Linear and nonlinear optimization in conjunction with the 'gradient technique'.

2. Analysis of Prestressed Concrete:

    - Identification of prestress loss in prestressed concrete.

    - Identification of secondary moment due to prestressing at the transfer and service stages.

- Identification of design requirements in prestressed concrete elements.

3. Formulation of the Optimum Design:

    - Definition of the design variables (optimization variables).

    - Identification of optimization criteria.

    - Identification of the inequality, equality constraints and upper and lower bounds on design variables.

    - Provide an optimization procedure.

4. Computer Code for Optimization

    - Development of a subroutine to analyse the system for uniform load.

    - Development of a subroutine to analyse the system for AASHTO HS Bridge loading.

    - Development of a subroutine to calculate the maximum and the minimum design forces at each of the ten division stations along a span.

    - Development of a subroutine to calculate the tendon eccentricities of prestressed concrete at each of the ten division stations along a span.

    - Development of a subroutine to calculate the frictional loss of prestressed concrete at each of the ten division stations along a span.

    - Development of a subroutine to calculate the secondary moment due to prestressing at the transfer and service stages.

    - Development of a subroutine to calculate the stresses at the transfer and service stages for each of the ten division stations along a span.

    - Development of a subroutine to optimize the system.

5. Applications, Results and Discussion

- Solution of example bridge girders for different lengths to obtain the optimum values of the design variables of these examples.

- Investigations on the influence of span ratio on the total cost of structural materials (concrete and prestressing steel) for three-span bridge girders.

- Investigations on the influence of tendon arrangement (short or long) on the cost of prestressing steel for bridge girders.

- Investigations on the influence of depth on the total cost of structural materials (concrete and prestressing steel) for bridge girders.
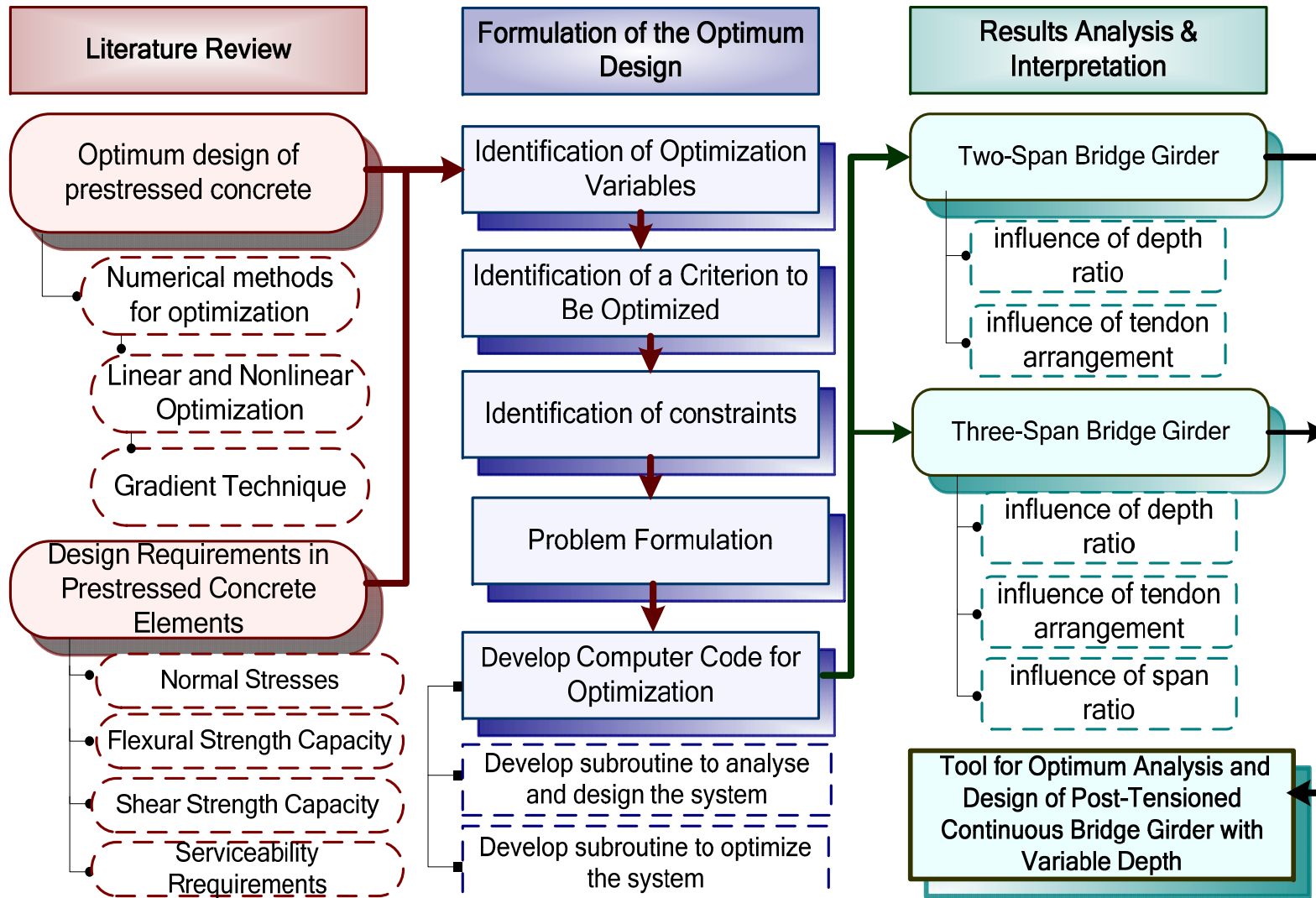
Figure 1.2 Flow Chart of Research Methodology

CHAPTER TWO

LITERATURE REVIEW

A considerable amount of literature is available on the optimum prestress design for a bridge girder. Many optimization criteria have been introduced, such as minimum weight, initial camber and recently minimum cost. This chapter reviews some recent and previous works of the optimal design of prestressed concrete bridge girders and slab decks of simply supported and continuous beams, with pre-tensioned or post-tensioned members.

A method was developed for the optimum design of prestressed indeterminate beams with uniform cross-section. The design variables were prestressing force, tendon configuration and cross-sectional dimensions. A transformation of variables was employed to reduce the optimization to a solution of a linear programming problem. The total cost of the system was the cost of concrete and prestressing steel (Kirsch, 1972).

An interactive design and analysis algorithm for simply supported prestressed concrete girders was devised by using linear programming to arrive at the optimum girder cross-section and prestressing strand design. The path of the strands by specifying the strand hold-down points and associated strand centroid eccentricity can be determined by using the kern boundaries (Johnson, 1972).

A computer program using the direct search method was developed to calculate optimum geometric configurations of prestressed concrete box girders of uniform depth

along the span length: (a) with nonlinear constraint conditions involving stresses and deflections; (b) with specified inputs on loading, unit costs and overall size; and (c) with checks on buckling, shear and ultimate section strength. The system was composed of identical simple spans, each of length l, placed end to end, together with their supporting piers (Touma and Wilson, 1972).

An optimal design of indeterminate prestressed concrete systems was developed in a nonlinear programming form. The design variables were the concrete dimensions, tendon coordinates, and prestressing force. The constraints were related to various behavior and design requirements, and the objective function represented the overall cost. The total cost included the concrete and prestressing steel. The problem was formulated on a two-level optimization, where the concrete dimensions were optimized in the second level, and the tendon variables prestressing force and tendon coordinates were determined in the first level (Kirsch, 1985).

An application of generalized geometric programming was presented for the optimal design of a prestressed concrete box bridge girder for a balanced cantilever bridge. The actual costs of construction (consisting of prestressing, formwork and concrete) were minimized. The design problem was formulated in accordance with the British Code of practice CP-110. The constraints variables were bending and shear stresses, and geometric criteria (Yu et al, 1986).

An optimization procedure for the design of structures was developed. This work was based on the work done by Barr, using an algorithm called GALL based on the geometric programming theory to solve large engineering design-related optimization

problems. The optimization procedure was applied successfully to solve optimally structural design problems in large reinforced concrete and prestressed concrete structures and to determine the sensitivity of the design to parameter values (Barr et al, 1986).

The design of three-span continuous prestressed concrete girders was formulated as a mathematical programming problem with the possibility of parabolically varying depth in each span. The design variables were prestressing force, seven geometrical concrete section dimensions, and tendon eccentricities at the supports and mid-spans. The total cost of the system was the cost of concrete and prestressing steel. Long cables running throughout the whole length of beam were used, which was neither practical nor economical (Hussain and Bhatti, 1986).

An algorithm to minimize prestressing steel in concrete slabs was presented. This was based on elastic theory, and it used the finite element method. The influence-line method and the equivalent-load approach were reviewed, and the latter was employed to compute the effects of prestressing. Non-uniform tendon layouts were used to minimize cable weight of concrete slabs, but this problem required iteration, since the moments and the prestressing force of a section depend on the tendon layout (Kuyucular, 1991).

A method was presented for optimization of prestressed concrete bridge decks for a given fixed geometry. The design variables included the sizes of the prestressing cables and the cable profile. A simple procedure of linear optimization was used to obtain the 'best' cable profile, by combining a series of feasible cable profiles. A non-linear

programming for optimization, namely 'the steepest gradient method' was used to solve this problem. This problem was to find the sizes and geometries of the prestressing cables as well as the longitudinal variation of the concrete section (Quiroga and Arroyo, 1991).

An optimum design of prestressed concrete beams was presented for simply supported beams having three different sections. Minimum weight and minimum cost optimization formulations were used to solve the problem. The minimum cost of the problem included the costs of concrete, steel and forming. In the minimum weight problem, the weights of concrete and steel were considered. The design variables included the prestressing force and the width of the cross-section (rectangular sections), or the width of the web (flanged sections). The constraints were the working stresses, deflections, ultimate strength, buckling, and section adequacy requirements (Erbatur et al, 1992).

An approach was presented for the optimization of prestressed concrete structures with two or more (possibly conflicting) objectives which must simultaneously be satisfied. The most relevant objective function was adopted as the primary criterion, and the other objective functions were transformed into constraints by imposing some lower and upper bounds on them. The projected Lagrangian algorithm was then used to solve the single-objective optimization problem. The results show that increasing the prestressing force and decreasing the slab depth made successive improvements of the minimum cost, but the opposite trend occur on improving the minimum initial camber (Lounis and Cohn, 1993).

A practical approach was presented for nonlinear design for continuous

prestressed concrete structures and to identify its potential benefits. The conflict was demonstrated between desirable plastic redistribution (at ultimate limit state) and zero or limited cracking (at serviceability limit state) for fully prestressed concrete structures. The problem was solved by using the Lagrangian algorithm. The design problem was simplified by adopting the maximum practical eccentricities at all critical sections for the tendon layout (Cohn and Lounis, 1993).

An optimum design was presented for the optimization of simply supported partially prestressed un-symmetric I-shaped concrete girders. The design variables included prestressing steel, non-prestressing steel and spacing between shear reinforcements. Both cracked and uncracked sections were assumed. The constraints variables were flexural stresses, fatigue stresses, crack width, ductility, initial camber, deflection due to both dead and live loads, ultimate moment capacity of the section with respect to cracking moment and factored loads, and the ultimate shear strength (Khaleel and Itani, 1993).

Three levels of optimization were applied for superstructure design of short- and medium-span highway bridge systems: (1) level 1 - component optimization; (2) level 2 - structural configuration optimization; and (3) level 3 - overall system optimization. Levels 1 and 2 identified the best solutions for specific components (precast I-girders, voided and solid slabs, single- and two-cell box girders) and layouts (for precast I-girder: one, two, and three; simple or continuous spans). Level 3 selected the overall best system for given bridge lengths, widths, and traffic loadings. Only single-span, cast-in-place prestressed concrete box girders with one or two cells and with constant depth were investigated (Cohn and Lounis, 1994).

An effective formulation was developed for optimum design of two-span continuous partially prestressed concrete beams. The design variables were prestressing forces along the tendon profile, which may be jacked from one end or both ends with flexibility in the overlapping range and location, and the induced secondary effects. The imposed constraints variables were the flexural stresses, ultimate flexural strength, cracking moment, ultimate shear strength, reinforcement, limits cross-section dimensions, and cable profile geometries (Al-Gahtani et al, 1995).

A method for automatic design of continuous post-tensioned bridge decks with two equal spans, constant depth, a straight platform and cast in place monolithically in only one construction phase was presented by using two steps. In the first step, the optimal prestressed force for feasible prestressed layout was obtained by means of linear programming techniques. In the second step, the prestress geometry and minimum force were automatically found by steepest descent optimization techniques (Utrilla and Samartin, 1997).

A two-level design procedure was developed for indeterminate structure prestressed concrete structures. In the first level, the prestressing force and the tendon coordinates were optimized. In the second level, the concrete dimensions were selected. The first-level problem was solved by using a linear programming form, but the minimum concrete dimensions were determined by solving a simple explicit nonlinear programming problem (Kirsch, 1997).

An approach was presented for multicriteria fuzzy optimization of a prestressed concrete bridge system considering cost and aesthetic feeling. For discrete sets of span

ratio and girder height at the intermediate support of the superstructure, the minimum total construction costs were obtained by solving the minimum construction cost problems of the superstructure and substructure for given span ratio and girder height. A long cable along the whole span, and very short cable only at maximum positive and negative moments, were used in this system. The design variables of superstructure included the parabolic prestressing force, the linear partial prestressing forces, the thickness of the bottom slab of the box section and the tendon eccentricities of parabolic prestressing cable. The constraints variables of superstructure (box girder) were stress and cracking constraints in the serviceability limit state and the flexural-strength and ductility constraints in the ultimate limit state (Ohkubo et al, 1998).

A computer program was developed to find the optimum design of three-span continuous post-tensioned beams of a prescribed total length for pseudo slab-type decks with constant depth. The design variables included cable layout, which would yield minimum prestressing steel and span ratio. The problem of optimization was solved by using linear programming in conjunction with the 'gradient technique'. The two types of tendons, full length and short length, were used to find the best tendon arrangement. The constraints variables were the limits of permissible stresses both at the initial stage of prestressing and at the final stage, which must be satisfied at all sections throughout the beam (Azad and Qureshi, 1999).

Deterministic design was presented for simply supported prestressed concrete girder bridges. A set of geometrical dimensions, girders spacing, amount of prestressing loses and tendon profile were optimized. The constraints variables were flexural stresses at initial and final stages, crack width, initial camber, deflection due to both dead and live

load, total loses, ultimate moment capacity with respect to the factored loads and cracking moment, and the ultimate shear strength (Barakat et al, 2002).

A general approach was presented for the single objective reliability-based optimum (SORBO) design of simply supported prestressed concrete beams (PCB). Several limit states were considered, such as permissible tensile and compressive stresses at both initial and final stages, prestressing losses, ultimate shear strength, ultimate flexural strength, cracking moment, crack width, and the immediate deflection and the final long-term deflection. The design variables included six geometrical dimensions that shape the PCB cross-section and one that represents the amount of prestressing steel (Barakat et al, 2003).

A method for the total cost optimization of precast prestressed concrete I-beam bridge systems was presented by taking into account the costs of the prestressed concrete, deck concrete, prestressing steel of I-beam, deck reinforcing steel, and formwork. The problem was formulated as a mixed integer-discrete nonlinear programming problem, and it was solved using the robust neural dynamics model of Adeli and Park. The total cost of the system included the cost of the concrete, reinforcement prestressed and non-prestressed, concrete deck formwork, and fabrication of the prestressed I-beams. The design variables were the number of beams, the cross-sectional area of the precast prestressed I-beams, the area of the prestressing steel slab thickness, the cross-sectional area of the deck steel, and the surface area of the formwork (Sirca and Adeli, 2005).

Review of the literature implies that many researchers have been working in this direction to find the optimum prestress design for a bridge girder but most of them did

not consider the variation of the prestressing force along the tendon profile and the resulting secondary moments due to prestressing. Almost no research has yet been done on optimization of the design of post-tensioned continuous bridge girders of prescribed total length and with variable depth. Ohkubo et al. (1998) use multicriteria fuzzy optimization of only a three-span continuous prestressed concrete bridge system considering cost and aesthetic feeling. The prestressing loss was assumed to be 15% and the design involved the use of long parabolic cable along the whole span and very short linear partial cable only at maximum positive and negative moments. This system was neither practical nor economical, because it needs more anchorages and the prestressing is more difficult. In other words, the assumed prestressing arrangement is not very practical for routine design.

CHAPTER THREE

ANALYSIS OF PRESTRESSED CONCRETE

3.1 General

In this chapter, a brief introduction to analysis of prestressed concrete elements is given.

The prestressing force applied to a post-tensioned member varies not only with time but also along the length of the member due to loss of prestressing force from various factors.

3.2 Loss of Prestressing

Loss of prestress in general is defined as the difference between the initial prestress in the prestressing steel and the effective prestress in the member. This definition of prestress loss includes both immediate loss at transfer stage and time-dependent loss at service stage. The loss of prestressing force can be divided into two categories (Figure 3.1):

- Immediate elastic loss during the fabrication or construction process, due to elastic shortening of the member, anchorage losses, and frictional losses:

$$\text{Instantaneous loss at a section} = P_J - P_i$$

- Time-dependent losses such as creep, shrinkage, and those due to

temperature effects and steel relaxation:

$$\text{Time-dependent loss} = P_i - P_e$$

where

$P_J =$ prestressing force at the jacking end.

$P_i =$ initial prestressing force in prestressing tendon after transfer at a particular section.

$P_e =$ final prestressing force in prestressing tendon after all losses.

Immediate Losses | Time-Dependent Losses

P_J → P_i → P_e

Jacking Force | Prestressing Force Immediately after Transfer | Final or Effective Prestressing Force
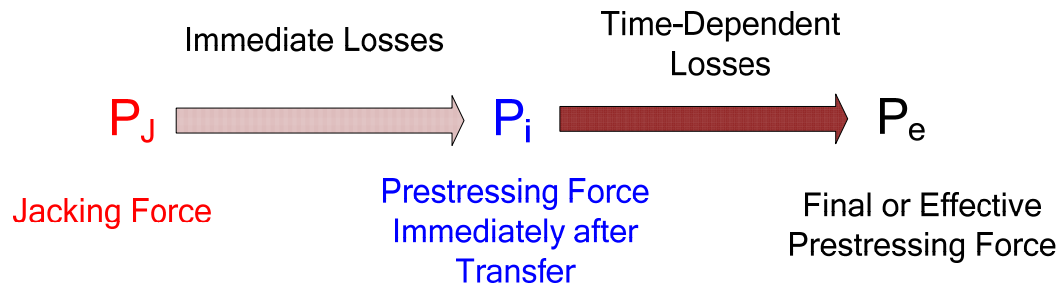
Figure 3.1 Loss of Prestressing Force

Immediate Elastic Loss (at Transfer Stage)

These losses occur at the transfer stage, and they include (Qureshi, 1995):

- the friction loss due to curvature and wobble effects,

- the elastic shortening loss,

- the anchorage seating loss due to tendon slippage during anchoring.

3.2.1 Loss due to Friction

Loss due to friction occurs in a post-tensioning member due to friction between the tendons and the surrounding concrete ducts. It is affected by the global tendon profile (curvature effect), and local deviation (wobble effect).

The loss due to curvature, ΔP_c, at a location is

$$\Delta P_c = P_J (1 - e^{-\mu\theta_i}) \tag{3.1}$$

and the loss due to wobble, ΔP_w, is

$$\Delta P_{wi} = P_J (1 - e^{-Kl_i}) \tag{3.2}$$

Thus, the total loss due to friction, ΔP_{fi}, at any location along the tendon is given by

$$\Delta P_{f_i} = P_J (1 - e^{-(\mu\theta_i + Kl_i)}) \tag{3.3}$$

where

P_J = prestressing force at the jacking end.

θ_i = the change in angle between the tangents of tendon from the jacking end to the location i, where the friction loss is calculated.

μ = coefficient of friction between the tendon and the duct.

K = coefficient of friction between the tendon and the surrounding concrete.

l_i = the projected length of the tendon from the jacking end to the location i, where the friction loss is calculated.

So the prestressing force at any station *i* after friction loss becomes:

$$P_i = P_J - \Delta P_{f_i}$$ (3.4)

3.2.2 Loss due to Elastic Shortening of Concrete

For post-tensioned members with one tendon or with two or more tendons stressed simultaneously, the elastic deformation of the concrete occurs during the stressing operation before the tendons are anchored. In this case, elastic shortening losses are zero. In a member containing more than one tendon, and where the tendons are stressed sequentially, the elastic deformation losses vary from one tendon to another, and are a maximum in the tendon stressed first and a minimum (zero) in the tendon stressed last. Immediately after transfer, the change in strain in the prestressing steel $\Delta \varepsilon_p$ caused by elastic shortening of the concrete is equal to the strain in the concrete at the steel level, ε_{cp}, which can be expressed mathematically as follows:

$$\varepsilon_{cp} = \frac{\sigma_{cp}}{E_c} = \Delta \varepsilon_p = \frac{\Delta \sigma_{es}}{E_p}$$ (3.5)

Therefore the loss of stress in post-tensioned member is equal to

Post-tensioned: $\Delta P_{es} = \frac{E_p}{E_c} \sigma_{cp} \times A_{ps} \times 0.5$ (3.6)

in which $\sigma_{cp} = -\frac{P_i}{A_c} - \frac{e_p^2 . P_i}{I_c} + \frac{e_p . M_o}{I_c}$ (3.7)

where

ΔP_{es} = losses of prestressing force due to elastic shortening in post-tensioned member.

E_c, E_p = elastic modulus of concrete and steel, respectively.

$P_i = A_{ps}.\sigma_{pi}$ = initial prestressing force at transfer.

ε_{cp} = strain in concrete at prestressing steel level due to elastic shortening.

σ_{cp} = stress in concrete at the centroid of tendons at station.

A_c, A_{ps} = gross area of concrete section and prestressing steel , respectively.

I_c = moment of inertia of concrete section at station.

e_p = the distance from the centroidal axis of the section to the tendon profile at the being considered station.

It is clear that the loss due to elastic shortening varies along the tendon profile because it is affected by many factors such as prestressing steel, cross-sectional dimensions, and bending moment due to self-weight.

3.2.3 Loss due to Anchorage Seating

In post-tensioned members, when the prestressing force is transferred from the jack to the anchorage, some slip occurs. This results in loss of prestress. The amount of slip depends on the type of anchorage, and it is usually specified by the manufacturer of the anchorage. Generally, the magnitude of the anchorage seating loss ranges between 1/4 of inch and 3/8 of inch for two-piece wedges (Abul-Feilat, 1991). The loss of prestress force due to slip has more effect on a short prestressed concrete member than on a long one, and it should not be ignored in the design. This can be expressed as follows:

$$\Delta P_{sl} = E_p \frac{\Delta s}{L} \times A_{ps} \tag{3.8}$$

where

ΔP_{sl} = loss of prestressing force due to anchorage seating.

E_p = elastic modulus of prestressing steel.

A_{ps} = gross area of prestressing steel at the relevant station.

L = the length of tendon.

Time-Dependent Loss (at Service Stage)

These losses occur at the service stage, and they include (Qureshi, 1995):

- the loss due to creep of concrete,

- the loss due to relaxation of prestressing steel,

- the loss due to shrinkage of concrete.

3.2.4 Loss due to Concrete Creep

The deformation in the concrete at the level of the tendon is called creep. This creep strain depends on the stress in the concrete at that level. It is a function of the magnitude of the applied load, its duration, the properties of concrete including its mixture proportions, curing conditions, the age of the element at first loading, and environmental conditions.

The loss of prestressing force due to concrete creep can be represented as

$$\Delta P_{CR} = C_t \frac{E_p}{E_c} \times \sigma_{cp} \times A_{ps} \tag{3.9}$$

It can be observed that the loss of prestressing force due to concrete creep depends on the creep coefficient at time t, C_t and stress in concrete at the centroid of tendons, σ_{cp}.

The creep coefficient at time t, C_t is given by:

$$C_t = \frac{t^{0.6}}{t^{0.6} + 10} C_u \tag{3.10}$$

The relationship between creep strain ε_{CR} and elastic strain ε_{EL} is called creep coefficient C_u and it is given by:

$$C_u = \frac{\varepsilon_{CR}}{\varepsilon_{EL}} \tag{3.11}$$

The stress in concrete at the centroid of tendons σ_{cp} is defined as

$$\sigma_{cp} = -\frac{P_e}{A_c} - \frac{e_p^2 . P_e}{I_c} + \frac{e_p . M_t}{I_c} \tag{3.12}$$

where

$P_e = RP_i = A_{ps} . \sigma_{pe} =$ effective prestressing force at service stage.

R = factor representing the total loss of prestressing force, $R = \dfrac{P_e}{P_i}$.

M_t = bending moment due to total load at that station.

Other variables are as defined before.

3.2.5 Loss due to Steel Stress Relaxation

If a tendon is stretched and held at a constant length (constant strain), the development of creep strain in the steel is exhibited as a loss of elastic strain, and hence a

loss of stress. This loss of stress in a specimen subjected to constant strain is known as relaxation. Relaxation in steel is dependent on the stress level, and it increases as the stress level increases. Relaxation losses depend on the quality of the steel, and they can vary in the range from 3% to 8% (Caprani, 2006/7).

The loss increment due to steel stress relaxation at any stage can be expressed as

$$\Delta P_{SR} = Pi \frac{(\log t_2 - \log t_1)}{C_R} (\frac{f_{pi}}{f_{py}} - 0.55) \qquad (3.13)$$

where

f_{pi} = the initial stress of tendon steel.

f_{py} = the yield strength of tendon steel.

C_R = Coefficient depends on type of tendon steel, where

C_R = 10 and C_R = 45 for stress-relieved and low-relaxation tendons, respectively.

t_1, t_2 = the time at the beginning and end of that time interval from jacking to the time when loss is being considered.

3.2.6 Loss due to Concrete Shrinkage

Shrinkage is affected by many factors, such as mixture proportions, type of aggregate, type of cement, curing time, time between the end of external curing and application of prestressing, and size and shape. The average value of nominal ultimate shrinkage strain is $(\varepsilon_{sh})_u$ = 820 x 10^{-6} in/in as stipulated by the Prestressed Concrete Institute. For post-tensioned members, the loss in prestressing due to shrinkage is less than the loss in pre-tensioned members since some shrinkage has already taken place before post-tensioning members. The PCI gives a general expression for loss due to

shrinkage as follows:

$$\Delta f_{psh} = 8.2 \times 10^{-6} K_{sh} E_{ps} (1 - 0.06 \frac{V}{S})(100 - RH) \qquad (3.14)$$

where RH = relative humidity, $\frac{V}{S}$ = volume-surface ratio, and K_{sh} = factor depending

on time from end of moist curing to application of prestress. See Table 3.1 (Nawy, 2006).

Table 3.1 Value of K_{sh} for Post-Tensioned Members

from end of moist curing to application of prestress, days	1	3	5	7	10	20	30	60
K_{sh}	0.92	0.85	0.8	0.77	0.73	0.64	0.58	0.45

Adjustment of shrinkage losses for standard conditions as a function of time t in days, after 7 days for moist curing and 3 days for steam curing, can be expressed mathematically as follows:

- Moist curing, after 7 days

$$(\varepsilon_{sh})_t = \frac{t}{35 + t}(\varepsilon_{sh})_u \qquad (3.15)$$

where $(\varepsilon_{sh})_u$ is the ultimate shrinkage strain, and t = time in days after shrinkage is considered.

- Steam curing, after 1 to 3 days

$$(\varepsilon_{sh})_t = \frac{t}{55 + t}(\varepsilon_{sh})_u \qquad (3.16)$$

3.2.7 Lump-Sum Estimates of Losses

Many thousands of successful prestressed structures have been built on the basis of lump-sum estimates of losses. This approach is suitable where member sizes, span,

materials, construction procedures, amount of prestress force and environmental conditions are not out of the ordinary. For such conditions, the American Association of State Highway and Transportation Officials has recommended the lump-sum estimates of losses for fully prestressed post-tensioned box girder as 25 *Ksi* with an average value of 23 *Ksi*. The loss due to friction is excluded, and so it should be computed and added to the previous value to get the total loss of the prestressed concrete member (Nilson, 2004).

The total loss of the prestressed concrete member, excluding loss due to friction, can be taken as 19% (Gail, 2000).

3.3 Tendon Arrangement

3.3.1 Tendon Profile

The profile of tendons in general varies along the bridge to follow the bending moment, and this variation affects the indeterminate moments. In a continuous span with variable depth, the bending moment along the span varies considerably, due to the changing moment of inertia, resulting in a significant difference between maximum positive and negative moments. The optimum tendon profile will have to follow this trend to counter the stresses due to bending moments. The tendon profiles for exterior and interior spans are shown in Figures 3.2 and 3.3.

In this study, the girder profile along the length is assumed to have parabolic depth variation, and the tendon geometry is also assumed to have a parabolic profile which consists of small segments whose coordinates can be represented mathematically by using the following expressions taking into account the variation of the depth as

shown in Figures 3.2 and 3.3 (Khachaturian and Gurfinkel, 1969).

a) Typical endspan:

$x = 0$ to $x = \alpha l_1$:

$$e(x) = -\frac{(\beta_0 - \beta_1)e_b}{(\alpha l_1)^2}x^2 + \frac{2(\beta_0 - \beta_1)e_b}{\alpha l_1}x - \beta_0 e_b + (yt(x) - y_d) \tag{3.17}$$

$x = \alpha l_1$ to $x = (1 - \alpha_1)l_1$:

$$e(x) = \frac{(1 + \beta_1)e_b}{(1 - \alpha)(1 - \alpha - \alpha_1)l_1^2}x^2 - \frac{2\alpha(1 + \beta_1)e_b}{(1 - \alpha)(1 - \alpha - \alpha_1)l}x$$

$$+ \frac{\alpha^2(1 + \beta_1)e_b}{(1 - \alpha)(1 - \alpha - \alpha_1)}x - \beta_1 e_b + (yt(x) - y_d) \tag{3.18}$$

$x = (1 - \alpha_1)l_1$ to $x = l_1$:

$$e(x) = -\frac{(1 + \beta_1)e_b}{\alpha_1(1 - \alpha)l_1^2}x^2 + \frac{2(1 + \beta_1)e_b}{\alpha_1(1 - \alpha)l_1}x - \frac{(1 + \beta_1)e_b}{\alpha_1(1 - \alpha)} + e_b + (yt(x) - y_d) \tag{3.19}$$

b) Typical symmetrical interior span:

$x = -\dfrac{l_2}{2}$ to $x = -(\dfrac{1}{2} - \alpha_2)l_2$:

$$e(x) = -\frac{2(1 + \beta_2)e_b}{\alpha_2 l_2^2}x^2 - \frac{2(1 + \beta_2)e_b}{\alpha_2 l_2}x - \frac{(1 + \beta_2)e_b}{2\alpha_2} + e_b + (yt(x) - y_d) \tag{3.20}$$

$x = -(\dfrac{1}{2} - \alpha_2)l_2$ to $x = (\dfrac{1}{2} - \alpha_2)l_2$:

$$e(x) = \frac{2(1 + \beta_2)e_b}{(\dfrac{1}{2} - \alpha_2)l_2^2}x^2 - \beta_2 e_b + (yt(x) - y_d) \tag{3.21}$$

$x = (\dfrac{1}{2} - \alpha_2)l_2$ to $x = \dfrac{1}{2}l_2$:

$$e(x) = -\frac{2(1 + \beta_2)e_b}{\alpha_2 l_2^2}x^2 + \frac{2(1 + \beta_2)e_b}{\alpha_2 l_2}x - \frac{(1 + \beta_2)e_b}{2\alpha_2}x + e_b + (yt(x) - y_d) \tag{3.22}$$

where

$yt(x)$, y_d are the distance from the centroidal axis to the top fibre of the section at distance x and at exterior support, respectively. The symbols β_0 to β_2 are eccentricity

factors and α to α_2 are the length factors for tendon geometry. *e(x)* is the distance from the centroidal axis of tendon to the centroidal axis of cross-section at distance *x*.

3.3.2 Long and Short Tendons

In a continuous span, the maximum negative moment at the interior support is generally greater than the maximum positive moment near the midspan. The demand of required prestressing steel at the interior support is greater than the area of prestressing steel at the maximum positive moment location. Thus the use of the same area of the prestressing steel (same number of tendons) throughout the whole bridge is not economical. The problem is solved by using variable depth and a combination of long tendons running throughout the whole length (*L*) and short tendons running to a specified length of the bridge girder (*Ls*). The layouts of long and short tendons in two and three span are shown in Figures 3.4 and 3.5, respectively.

The total prestressing force at the jacking end is denoted by P_l in long tendons and by P_s in short tendons. Hence the total of prestressing force at the jacking end will be denoted as P_J.
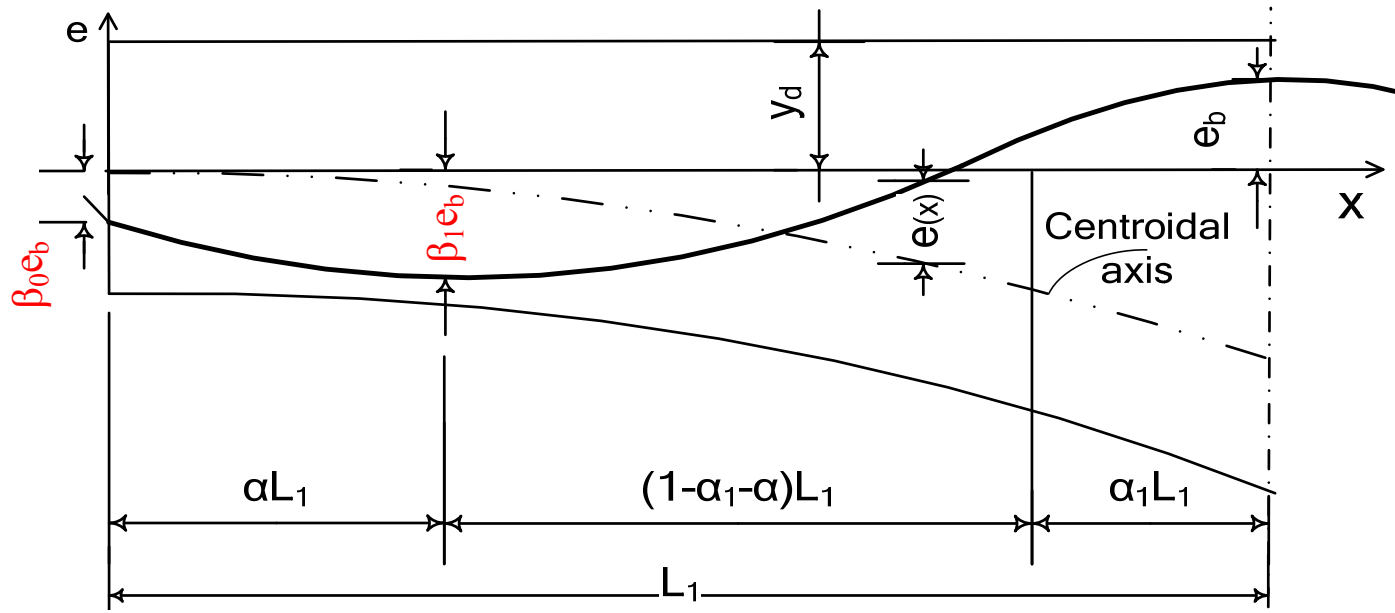
Figure 3.2 Variation of Tendon Profile in Exterior Span
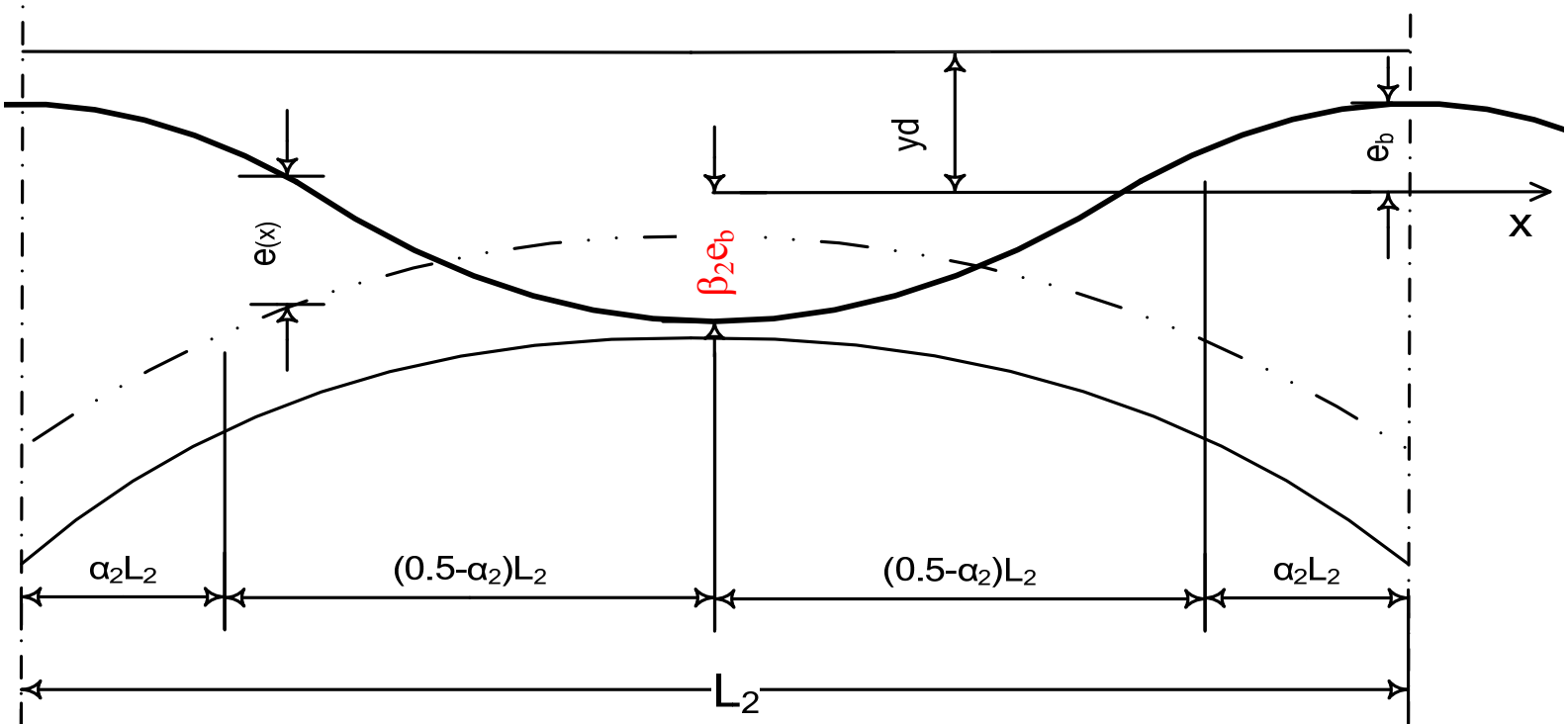
Figure 3.3 Variation of Tendon Profile in Interior Span
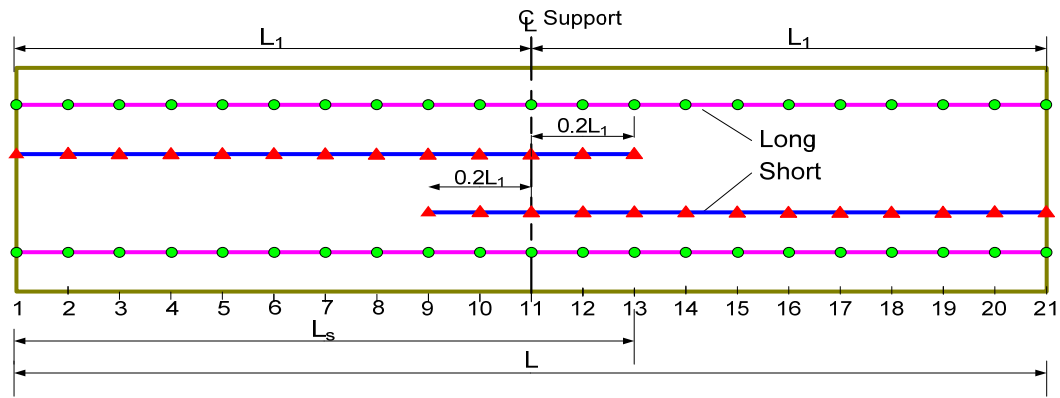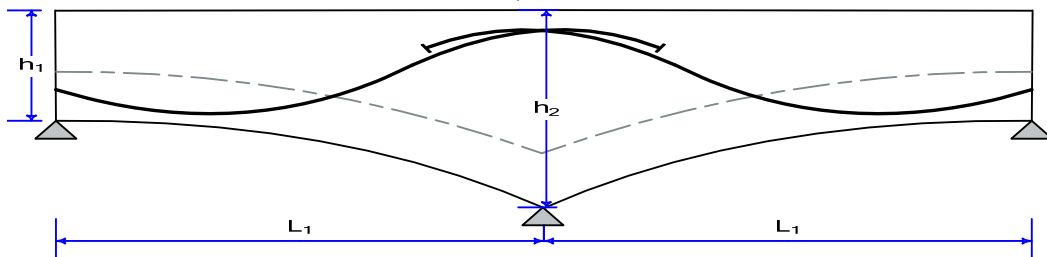
Figure 3.4 Layout of Long and Short Tendons for Two-Span Continuous Bridge Girder
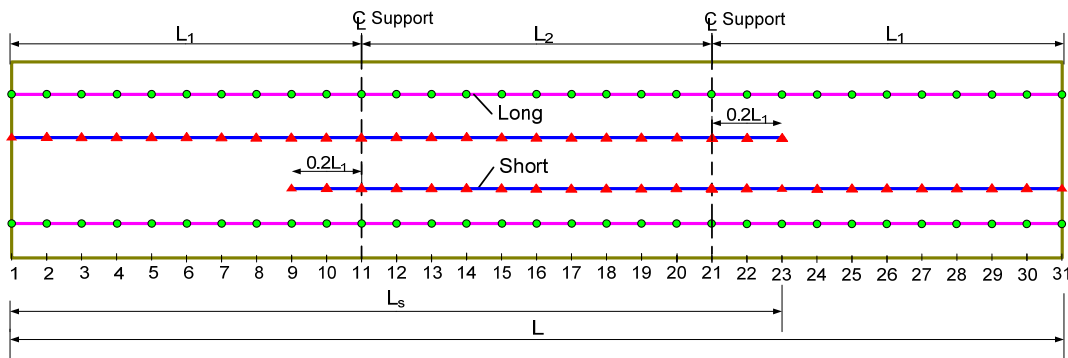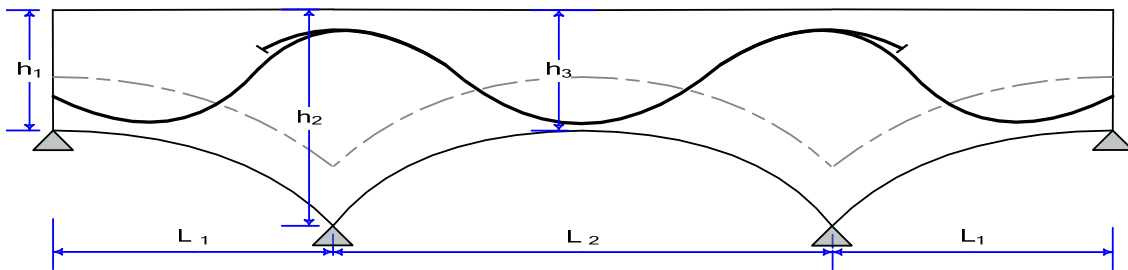
Figure 3.5 Layout of Long and Short Tendons for Three-Span Continuous Bridge Girder

3.4 Secondary Moment

In continuous beams, an additional moment results from the prestress force itself and this moment is often referred to as the secondary moment, and the support reaction due to prestressing force must be included in the overall analysis of the beam. The term ''secondary'' is somewhat misleading, since sometimes the moments are not secondary in magnitude but play a most important part in the stresses and strength of the beam. The value of secondary moment is dependent upon the tendon geometry and prestressing.

This value could be positive or negative. If the positive moment exists, it will increase the positive moment in the midspan and decrease the negative moment at the interior support, and vice versa. The secondary moment has to be evaluated at the transfer and service stages of loading to be considered in the design of the member.

3.4.1 Analysis to Determine Secondary Moment

The calculation of the secondary moment M_s can be done in several ways. Due to the complication of tendon profile, and the variability of prestress force along the tendon and depth of cross-section, the appropriate method to determine M_s is the unit load method of structural analysis.

The secondary moment and the net prestressing moment can be calculated as follows:

1- First, each span is divided into ten equal divisions. The primary prestressing moment M_p from the chosen tendon profile is calculated at each station.

2- The primary prestressing moment is used to determine the secondary moment by using the unit load method. For a numerical integration, Simpson's rule is used.

3- From the support moments, the net prestressing moment at a station can be computed as

$$M_{pnet} = M_p - M_s \tag{3.23}$$

3.4.2 Unit Load Method

Two-Spans Continuous Bridge Girder

The redundant support moments M_b due to primary prestressing moment M_p can be calculated from the condition that the slope at the interior support b is zero due to symmetry. This is the unit load method (Figure 3.6.a):

Equating Slope at ' b ':

$$\int_0^{L_1} \frac{M_{px} \, m_{bx}}{EI} \partial x \;+\; M_b \int_0^{L_1} \frac{m_{bx}^{\,2}}{EI} \partial x \;=\; 0 \tag{3.24}$$

The integral can be calculated by using Simpson's rule.

Three-Spans Continuous Bridge Girder:

In three-span continuous girders, the redundant support moments M_b and M_c due to the primary prestressing moment M_p can be calculated by solving two simultaneous equations. These equations can be written by equating slopes at ' b ' and ' c '

and by using the unit load method (Figure 3.6.b). However, as only symmetric three spans are considered, $M_b = M_c$. This leads to the solution of only one equation (Azad, 2006).

Equating Slope at ' b ':

$$\theta_{bl} + \theta_{br} = 0 \tag{3.25}$$

$$\int_0^{L_1} \frac{M_{px} m_{bx}}{EI} \partial x + M_b \int_0^{L_1} \frac{m_{bx}{}^2}{EI} \partial x + \int_0^{L_2} \frac{M_{px} m_{bx}}{EI} \partial x +$$

$$M_b \int_0^{L_2} \frac{m_{bx}{}^2}{EI} \partial x + M_c \int_0^{L_2} \frac{m_{bx} m_{cx}}{EI} \partial x = 0 \tag{3.25.1}$$

where

M_{px} = primary moment at x on the span.

m_{bx} = moment at x due to unit moment at b .

m_{cx} = moment at x due to unit moment at c .

Evaluation of the integral can be accomplished as before by using Simpson's rule as

$$\int_a^b f(x)dx = \frac{h}{3}\left[f(x_0) + 4 \sum_{\substack{i=1 \\ i=odd}}^{n-1} f(x_i) + 2 \sum_{\substack{i=2 \\ i=even}}^{n-2} f(x_i) + f(x_n) \right] \tag{3.26}$$

where $f(x_0)$ = value of $f(x)$ at the first station, numbred zero and $f(x_i)$ = value of $f(x)$ at station i ($i = 1,....,10$)
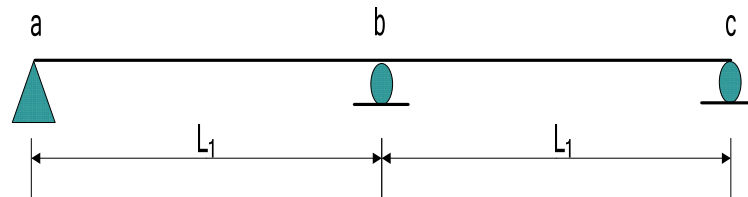
(a) Two-span
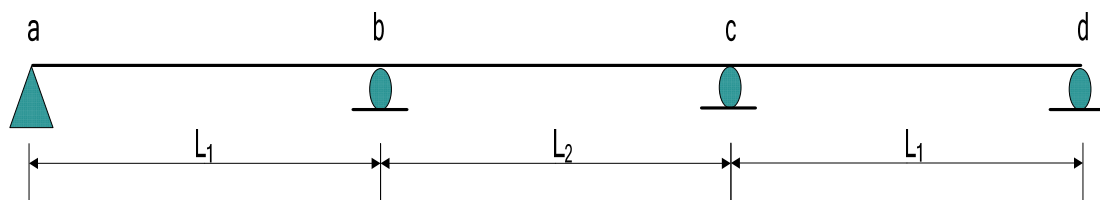
(b) Three-span

Figure 3.6 Unit Load Method for Analysis

3.5 Design Requirements for Prestressed Concrete Members

In the design of prestressed concrete members, the main considerations are

1. normal stresses due axial and flexure force under service load,

2. flexural capacity under ultimate load,

3. shear strength capacity,

4. serviceability requirements (camber and deflection).

3.5.1 Normal Stresses Due to Axial and Flexure Force

Sign Convention of Normal Stresses:

The positive sign will be considered for tensile stresses and allowable tensile stresses, whereas the negative sign will be considered for compressive stresses and allowable compressive stresses.

Normal stresses in a concrete section are due to the applied loads (live and dead) and to the prestressing force. These stresses are maximum at the extreme fiber of the cross-section (at top and bottom of cross-section). These stresses have to be considered in the design of prestressed concrete at two stages of loading. The first stage is the transfer stage or initial conditions, where the initial prestressing force and the secondary moment after the immediate losses are acting with the self-weight of the member. The second stage is called the service stage, at which the effective prestressing force (with secondary moment) after all losses are acting with the self-weight of member and the superimposed dead and live load.

a) At Transfer Stage:

$$f_i^b = -\frac{P_i}{Ac} + \frac{(\pm P_i e \pm M_O \pm M_{si})}{S_b} \tag{3.27}$$

$$f_i^t = -\frac{P_i}{Ac} - \frac{(\pm P_i e \pm M_O \pm M_{si})}{S_t} \tag{3.28}$$

b) At Service Stage:

$$f_s^b = -\frac{P_e}{Ac} + \frac{(\pm P_e e \pm M_T \pm M_{se})}{S_b} \tag{3.29}$$

$$f_s^t = -\frac{P_e}{Ac} - \frac{(\pm P_e e \pm M_T \pm M_{se})}{S_t} \tag{3.30}$$

where

f_i^t, f_i^b are top and bottom stresses in cross-section at transfer stage, respectively.

f_s^t, f_s^b are top and bottom stresses in cross-section at service stage, respectively.

P_i, P_e are initial and effective total prestressing force at transfer and services stages, respectively.

S_t, S_b are section modulus at top and bottom of cross-section, respectively.

Ac is the area of the concrete cross-section.

e is the distance from the centroidal axis of the section to the tendon profile.

M_{si}, M_{se} are initial and effective secondary prestressing moments at transfer and services stages , respectively.

M_o, M_T are bending moments due to self-weight and total load, respectively.

These stresses vary along the beam due to variation in prestressing force, cross-section and the applied moment from the loads. Thus, these stresses have to be calculated

at each station, and checked to ensure that they are less than the allowable stresses.

3.5.2 Ultimate Flexural Strength

The ultimate flexural strength of prestress concrete member requires calculating the value of prestressing steel stress at failure f_{ps} . This stress can be determined either by using the ACI-318-05 approximate formulae or by using the more accurate method called strain compatibility analysis.

The ACI-318-05 recommends the use of the following formula for bonded prestressing tendons, in lieu of the more exact method,

$$
f_{ps} = f_{pu} \left\{ 1 - \frac{\gamma_p}{\beta_1} \left[\rho_p \frac{f_{pu}}{f_c'} + \frac{d}{d_p} (\omega - \omega') \right] \right\} \tag{3.31}
$$

This equation may be used, provided that f_{ep} is not less than $0.5 f_{pu}$.

In this thesis, strain compatibility was adopted. This method provides a more accurate value of f_{ps} than the value specified in ACI-318-05's approximate formulae, and it requires the stress-strain curve of the prestressing steel. Since computer code is implemented as in this thesis, mathematical equations can be used to represent the stress-strain curve of the prestressing steel. These mathematical equations can be written for the idealized stress-strain diagram or can be obtained from other references, such as (PCI, 2004).

Strain Compatibility Method

As the stress-strain for prestressing steel is nonlinear after proportional limit, the

exact value of f_{ps} is not known at failure, unlike ordinary reinforced concrete *RC*. The failure condition is assumed when the strain in concrete reaches ε_{cu} :
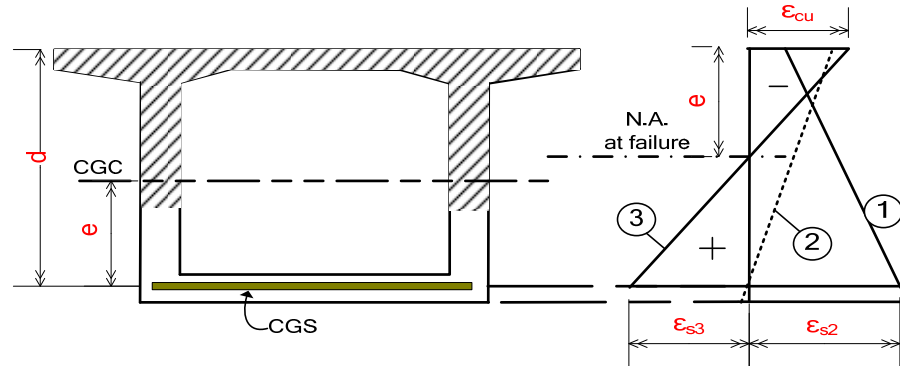
Figure 3.7 Strain during Loading Stages

Successive iterations are used to solve this problem as follows:

1) The initial strain of steel due to prestress alone is calculated by

$$\varepsilon_{ps1} = \frac{f_{pe}}{E_{ps}} \tag{3.32}$$

2) The strain in the tendon when concrete reaches cracking (decompressed) is

$$\varepsilon_{ps2} = \frac{P_e}{A_c E_c} + \frac{e_p^{\,2}.P_e}{I_c} \tag{3.33}$$

3) The steel stress, f_{ps}, at failure is assumed so that $f_{ps} \leq f_{pu}$.

4) The depth of the stress block at failure ' a ' can be calculated from the equilibrium of the tensile and compressive forces acting on the section, as follows:

$$T_{ps} = C_c \tag{3.34}$$

in which C_c is the compressive force acting on concrete segments which are expressed in terms of the stress block depth 'a' and T_{ps} is the tensile force acting on prestressing steel.

Depending on the assumed value of f_{ps} and the sign of bending moment (top or bottom flange in compression) this value will be calculated and checked to find out whether the neutral axis lies within the top or bottom flange or the web. Then, the depth of the neutral axis c can be obtained from:

$$c = \frac{a}{\beta_1} \qquad\qquad (3.35)$$

5) The strain at ultimate condition is

$$\varepsilon_{ps3} = \varepsilon_{cu} \frac{d - c}{c} \qquad\qquad (3.36)$$

6) The total strain at failure is

$$\varepsilon_{ps} = \varepsilon_{ps1} + \varepsilon_{ps2} + \varepsilon_{ps3} \qquad\qquad (3.37)$$

7) The actual stress of prestressing f_{ps} is calculated, depending on ε_{ps} and checked with the trial value. If close agreement is observed, the actual stress of prestressing f_{ps} is used to calculate the ultimate flexural strength. Otherwise the steps from (3) to (7) will be repeated until the desired accuracy is reached. Then the last value for f_{ps} will be used.

8) The ultimate flexural strength of the section M_{ur} is calculated by the moment equilibrium of the tensile and compressive forces acting on the

section.

3.5.3 Shear Strength Capacity

Generally cracking of prestressing concrete as well as reinforced concrete members can arise from two causes:

- Flexure-shear cracking

- Web-shear cracking

Both these crackings are essentially diagonal. During the design process, these two types of shear strength criteria have to be verified.

Flexure-shear cracking

For a member in bending, the flexural cracking first develops at the maximum moment region, and it propagates vertically. This crack becomes inclined in the combined stress region with an increase in the load. The presence of shear stress causes the cracks to be inclined. When the cracks develop to a sufficient height, the member may fail in shear-compression failure. The total shear force V_{ci} that would produce flexure-shear failure according to ACI-318-05 is:

$$V_{ci} = 0.6\sqrt{fc'}b_w d + V_d + \frac{V_i M_{cr}}{M_{max}}$$ (3.38)

But V_{ci} need not be taken as less than

$$1.7\sqrt{fc'}b_w d$$ (3.39)

where

M_{max} = maximum factored moment at section due to externally applied loads, *in-lb*

V_i = factored shear force at section due to externally applied loads occurring simultaneously with M_{max}, *lb*

M_{cr} = moment causing flexural cracking at section due to externally applied loads, which is given by

$$M_{cr} = (I/y_t)(6\sqrt{fc'} + f_{pe} - f_d)$$ (3.40)

where

f_{pe} = compressive stress in concrete due to effective prestress forces only (after allowance for all prestress losses) at extreme fiber of section where tensile stress is caused by externally applied loads in *psi*

$$f_{pe} = \frac{P_e}{A_c}(1 + y_t \frac{e}{r^2})$$ (3.41)

f_d = stress due to unfactored self-weight, at extreme fiber of section where tensile stress is caused by externally applied loads in *psi*

$$f_d = \frac{y_t M_o}{I_c}$$ (3.42)

M_o = moment due to unfactored self-weight at section

y_t = distance from centroidal axis to extreme fiber in tension in inches.

I_c = moment of inertia of concrete cross-section in inches.

Web-shear cracking

This type of cracking may occur in a thin web member of a heavily prestressed member, especially near the support. If the principal tensile stress in the web is large enough, cracks will develop in the web and will propagate diagonally, causing the failure of the member.

The nominal shear strength provided by concrete when diagonal cracking results from excessive principal tensile stress in web is V_{cw}. This shear strength is increased by the vertical component of the effective prestressing force, V_p , and is given by

$$V_p = P_e \sin \theta \qquad (3.43)$$

where

P_e = the effective prestress force acting at that section, and

θ = the angle between the slop of the tangent to the tendon profile and the horizontal C.G.C line at that station.

Therefore, V_{cw} as recommended by ACI-318-05 is

$$V_{cw} = (3.5\sqrt{fc'} + 0.3f_{pc})b_w d + V_p \qquad (3.44)$$

where

f_{pc} = compressive stress in concrete (after allowance for all prestress losses) at the centroid of the cross-section resisting externally applied loads, or at the junction of web and flange when the centroid lies within the flange, which is given as

$$f_{pc} = \frac{P_e}{A_c}$$ (3.45)

The shear strength provided by the concrete V_c is assumed equal to the lesser of V_{ci} and V_{cw} .

The ACI-318-05 stipulates shear strength V_s shall not be taken as greater than $8\sqrt{fc'}b_w d$, or else the cross-sectional dimensions must be modified to satisfy this condition

where

V_s = nominal shear strength provided by shear reinforcement and is given by

$$V_s = \frac{V_u - V_c}{\phi}$$ (3.46)

V_u = maximum factored shear force at section due to externally applied loads

ϕ = strength reduction factor.

3.5.4 Serviceability Requirements

Control of deflections

Deflection calculations shall consider dead load, live load, prestressing, erection loads, concrete creep and shrinkage, and steel relaxation.

The AASHTO specification recommends that, for a superstructure member having simple or continuous spans deflection, the deflection due to service live load plus impact shall not exceed 1/800 of the span (AASHTO, 1996).

The ACI-343R-95 stipulates minimum recommended thicknesses for superstructure prestressed members, unless computation of deflection indicates that a lesser thickness can be used without any effects. Table 3.2 (ACI-343R-95)

Table 3.2 Recommended Minimum Thickness for Constant Depth Members*

Superstructure type	Minimum depth **	
	ft	m
Bridge slabs with main reinforcement parallel or perpendicular to traffic	$\dfrac{L + 10}{30}$	$\dfrac{L + 3}{30}$
	But not less than 0.542(0.164)	
T-girders	$\dfrac{L + 9}{18}$	$\dfrac{L + 2.75}{18}$
Box girders	$\dfrac{L + 10}{20}$	$\dfrac{L + 3}{20}$

* When variable depth members are used, table values may be adjusted to account for change in relative stiffness of positive and negative moment sections.

** Recommended values for continuous spans. Simple spans should have about a 10 percent greater depth.

L = Span length of member in *ft* (*m*).

- Computation of immediate deflections which occur immediately on application of load should be computed by the usual methods or formulas for elastic deflections, and by using the moment of inertia of the gross

concrete section for uncracked sections.

- Additional long-time deflection should be computed, taking into account the stresses in the concrete and steel under the sustained load, including the effects of creep and shrinkage of the concrete and relaxation of the steel.

In calculating the deflection, the ACI Committee 435-R suggests the equation of ACI-318-05 to calculate the modulus of elasticity of concrete E_c when there no test is available (ACI-435-R-95):

$$E_c = 57000\sqrt{fc'} \tag{3.47}$$

where

fc' = specified concrete strength of concrete in *psi*

Camber

Camber is dependent on many factors: the profile of prestressing tendons and force, initial losses due to elastic shortening, anchorage seating, relaxation of the prestressing tendons, time-dependent effects of creep, shrinkage, and the constant sustained applied loading of the girder self-weight. Because of the complex nature of these factors, it is satisfactory to use an approach that calculates the time-dependent change in the effective prestressing force over many discrete time steps (Hinkle, 2006).

Several "multiplier methods" are currently available to predict camber growth in prestressed concrete girders. These methods are very simplistic in that the instantaneous elastic deflection or various components of deflection are increased by multipliers. The

AASHTO-LRFD Design Specification includes a recommended method, in addition to the PCI Bridge Design Manual, which includes two recommended methods. The first method described by the PCI Bridge Design Manual is based on previous work by Martin (1977) Table 3.3 (PCI, 2004). The second is a more detailed method developed by Tadros et al (1985). It allows for using a creep coefficient specific to the concrete mix, as well as using a prestress loss component of deflection based on calculated values (Hinkle, 2006).

Table 3.3 PCI Manual Multiplier Method - based on Martin (1977)

	Without Composite Topping	**With Composite Topping**
At erection:		
1. Deflection (downward) component-apply to the elastic deflection due to the member weight at release of prestress.	1.85	1.85
2. Camber (upward) component-apply to the elastic camber due to prestress at the time of release of prestress.	1.80	1.80
Final:		
3. Deflection (downward) component-apply to the elastic deflection due to the member weight at release of prestress.	2.7	2.4
4. Camber (upward) component-apply to the elastic camber due to prestress at the time of release of prestress.	2.45	2.2
5. Deflection (downward)-apply to elastic deflection due to superimposed dead load only.	3.0	3.0
6. Deflection (downward)-apply to elastic deflection caused by the composite topping.	--	2.3

3.6 Geometrical Dimensions Requirements

AASHTO Standard Specifications for Highway Bridges recommends minimum dimensions of box girders as follows (AASHTO, 1996).

3.6.1 Top Flange

AASHTO recommends the minimum dimension of the top flange thickness as 1/30 of the clear distance between fillets or webs, but not less than 6 inches, except that the minimum thickness may be reduced to 5.5 inches for factory-produced precast pre-tensioned elements.

3.6.2 Bottom Flange

AASHTO recommends that the minimum thickness of the bottom flange shall be 1/30 of the clear distance between fillets or webs but not less than 5.5 inches, except that the minimum thickness may be reduced to 5 inches for factory-produced precast pre-tensioned elements.

3.6.3 Width of Bridge

The recommended roadway width for freeway overpasses is as follows (Barker and Puckett, 2007):

Table 3.4 Typical Roadway Width for Freeway Overpasses

Roadway	Width (ft)	Width (m)
Lane width	12.0	3.6
Right shoulder width		
Four lanes	10.0	3.0
Six and eight lanes	10.0	3.0
Left shoulder width		
Four lanes	4.0	1.2
Six and eight lanes	10.0	3.0

3.7 Range of application of bridge

Table 3.5 Range of Application of Bridge Type by Span Length
(Barker and Puckett, 2007)

Span, ft (m)	Bridge Type
0-150 (0-45)	Precast pre-tensioned I-beam conventional
100-300 (30-90)	Cast-in-place post-tensioned box-girder conventional
100-300 (30-90)	Precast balanced cantilever segmental, constant depth
200-600 (60-180)	Precast balanced cantilever segmental, variable depth
200-1000 (60-300)	Cast-in-place cantilever segmental
800-1500 (240-450)	Cable-stay with balanced cantilever segmental

CHAPTER FOUR

FORMULATION OF THE OPTIMUM DESIGN

4.1 General

The problem under consideration deals with the optimum design of a cast-in-place, post-tensioned, two or three-span continuous and fully prestressed concrete bridge girder with variable depth. The general formulation of the optimum design problem involves three steps, as follows:

1- Definition of the design variables (optimization variables)

$$[X] = \lfloor X_1, X_2, ..., X_i, ..., X_n \rfloor \tag{4.1}$$

2- Identification of a criterion to be optimized F(x)

3- Identification of the inequality/equality constraints and the upper and lower bounds on design variables.

$$g_k(X) \geq 0, \qquad k = 1,...., j \tag{4.2}$$

$$h_k(X) = 0, \qquad k = 1,...., m \tag{4.3}$$

$$X_i^l \leq X \leq X_i^u \tag{4.4}$$

where

$[X]$ = vector representing the design variables, which minimize the objective function.

n = the total number of design variables.

X_i^l = the lowest bound for the ith design variables.

X_i^u = the highest bound for the ith design variables.

j = the total number of inequality highest constraints.

m = the total number of equality highest constraints .

      For any system, there can be many feasible designs, and some are better than others. To compare different designs, we must have a criterion. The criterion must be a scalar function whose numerical value can be obtained once a design is specified, i.e. it must be a function of the design variable (vector *X*) and influenced directly or indirectly by the variables of the design problem (Arora, 2004).

4.2 Design Variables

      The design variables are the set of variables that describe the system. In general, they are referred to as optimization variables. They are considered as free because any value can be assigned to them. Different values for the variables produce different designs. In this thesis, the term "design variables" will be used to indicate all unknowns of the optimization problem, and they will be represented in the vector *X*. In the problem under investigation, there are four design variables as follows:

4.2.1 Structural Configuration

The girders are symmetric about the transverse center line, as is common in bridges. In the two-span continuous bridge girder, the optimum design would have both spans equal. For the three-span girder, many choices exist for the length of the interior span, depending on the ratio of interior span to exterior span.

X_1 = the length of the external span, L_1, Figure 4.2.

X_2 = the length of the internal span (for three-span girder), L_2, Figure 4.2.

X_3 = the ratio of interior span to exterior span in three-span girder, ε.

4.2.2 Geometrical Dimensions

The width of the bridge girder depends on the number of lanes to be provided. In this study, the length and thickness of overhangs, the thickness of the web, and the thickness of the bottom and top slab, are all assumed to be known. Therefore, the variables in the cross-sectional dimensions are the depths of the section, which are variable along the length of the bridge. The variation in depth is assumed to be parabolic.

X_4 = the depth of the section at the jacking end, h_1, Figures 4.1 and 4.2.

X_5 = the depth of the section at interior support, h_2, Figures 4.1 and 4.2.

X_6 = the depth of the section at the midspan of the interior span (for a three-span bridge), h_3 Figure.4.2.

4.2.3 Tendon Arrangement

For economical prestressing, the prestressing tendons consist of long (full-length) and short tendons.

X_7 = the total prestress force at the jacking end in long tendons running throughout the whole span, P_l

X_8 = the total prestress force at the jacking end in short tendons running to specified distance of the span, P_s .

X_9 = the proportion of prestressing forces at the jacking end in short and long tendons, λ

4.2.4 Profile of Prestressing Tendon

The profile used is a parabolically varying tendons profile configuration which consists of small segments whose coordinates can be represented mathematically as explained in chapter 5.

The design variables of this profile are as illustrated in Figures 4.3 and 4.4 and as follows:

X_{10} = the distance from the centroidal axis of the section to the tendon profile at the jacking end, $\beta_0 e_b$.

X_{11} = the distance from the jacking end to the maximum deflected point in the tendon layout, αL_1

X_{12} = the distance from the centroidal axis of the section at the jacking to the tendon profile at the maximum deflected point of exterior span, $\beta_1 e_b$

X_{13} = the distance from the interior support to the point of tangent to both the parabolas on the left side, $\alpha_1 L_1$

X_{14} = the distance from the centroidal axis of the section at the jacking to the tendon profile at the interior support, e_b

X_{15} = the distance from the interior support to the point of tangent to both the parabolas on the right side, $\alpha_2 L_1$

X_{16} = the distance from the centroidal axis of the section at the jacking to the tendon profile at the maximum deflected point of interior span, $\beta_2 e_b$

The whole set of the design variables can be expressed in vector form as:

$$X = \{ X_1, X_2, ..., X_i, ..., X_n \} \tag{4.5}$$

where

X = vector of design variables.

$X_i = i^{th}$ design variable.

n = total number of design variables, which is 16 in this study.

4.3 Optimization Criteria

Such a criterion is usually called the objective function of the optimum design problem, which needs to be minimized or maximized depending on the problem requirements. In this research, the criterion (objective function) that will be minimized is the total cost of structural materials, prestressing steel and structural concrete. Costs related to formwork and anchorages of tendons are not included in this work.

Since the cost of prestressing steel depends on the volume of prestressing steel (V_p), which is proportional to the prestressing force of tendons, the cost objective function F can be written as:

$$F = C_c V_c + C_p \gamma V_p \qquad (4.6)$$

in which F is the total cost of material for the bridge girder (objective function), C_c is the cost of concrete per unit volume, C_p is the cost of prestressing steel per unit weight, and γ is the unit weight of the prestressing steel. The costs of prestressing steel and concrete are taken from the reference (Sirca and Adeli, 2005). V_c and V_p are the total volume of concrete and prestressing steel, respectively.

If P_l and P_s are the total prestressing force in the long tendons and short tendons respectively, the total volume of prestressing steel is given in terms of the prestressing force as:

$$V_p = z(P_l L + 2 P_s L_s) \qquad (4.7)$$

where z is given by $As/P_J{*}$, As = the area of one tendon, $P_J{*}$ = prestressing force at the

jacking end of one tendon, and L = length of a long tendon . The length of a short tendon L_s is determined from a practical consideration of anchorage. L_s is assumed to have the prescribed value shown in Figures 3.4 and 3.5 as:

for two-span L_s = 0.6L

for three-span $L_s = \dfrac{L}{(\varepsilon + 2)}(\varepsilon + 1.2)$

where ε = ratio of L$_2$/L$_1$

A nondimensional variable λ is introduced as:

$$\lambda = 1 + \frac{2P_s}{P_l} \tag{4.8}$$

The variable λ is always ≥ 1, which is a key parameter that assigns the proportion of prestressing forces of short and long tendons. $\lambda = 1$ indicates that all tendons are long with no short one, and $\lambda > 1$ indicates both long and short tendons. Eq. 4.7 takes the form:

$$V_p = zP_lL(1 + \frac{L_s}{L}(\lambda - 1)) \tag{4.9}$$

Eq. 4.6 becomes:

$$F = C_c \sum (A_{ci}l_i) + C_p \gamma P_l z\{L + (\lambda - 1)L_s\} \tag{4.10}$$

for two-span

$$F = C_c \sum (A_{ci}l_i) + C_p \gamma P_l zL \{0.4 + 0.6\lambda\} \tag{4.10.a}$$

for three-span

$$F = C_c \sum (A_{ci} l_i) + C_p \gamma P_l zL \{1 + (\lambda - 1) \frac{(\varepsilon + 1.2)}{(\varepsilon + 2)}\} \qquad (4.10.b)$$

A_{ci} is the area of concrete cross-section at considering station, and l_i is the length of division at the relevant station.

The total prestressing force at the jacking end is

$$P_J = P_l + P_s \qquad (4.11)$$

From Eqs. 4.8 and 4.11,

$$P_l = P_J \frac{2}{(\lambda + 1)} \quad ; \quad P_s = P_J \frac{(\lambda - 1)}{(\lambda + 1)} \qquad (4.12)$$

For a given λ, Eq. 4.12 prescribes the distribution of forces in the long and short tendons.

Equation 4.10 shows that when $\lambda = 1$ all tendons are long with no short one ($P_s = 0$). The use of λ transforms the objective function (Eq.4.10) into a linear function of two variables, the depth of cross-section and P_l for a chosen λ.

4.4 Constraints

The design of any structural problem must have many functional constraints such as limits of working stresses, strength, and serviceability requirements as well as code requirements. In this thesis, the constraints include: prescribed limits of working stresses, ultimate shear and ultimate moment capacities, serviceability, cross-sectional dimensions constraints and tendons profile constraints, to ensure that the minimum concrete cove to tendons is maintained throughout the bridge girder.

4.4.1 Geometrical Constrains

This type of constraints consists of two sub-types as follows:

Tendon Profile for Continuous Span

These constraints ensure that the profile is within the top and bottom concrete boundaries of the cross-section. This can be expressed mathematically as:

$$e(x) \leq Y_i - d_c \qquad (4.13)$$

where

$e(x)$ is the distance from the centroidal axis of the section to the tendon profile at distance x.

Y_i is the distance of top or bottom fibre from the centroidal axis of the section.

d_c is the minimum concrete cover.

Cross-sectional dimensions

This requires that the depth of cross-section h_i is not less or greater than the lower and upper limits respectively. This can be expressed mathematically as:

$$h^l \leq h_i \leq h^u \qquad (4.14)$$

where

h^l is the lowest bound for the depth.

h^u is the highest bound for the depth .

4.4.2 Flexural Stresses in Concrete Section

The flexural stresses at the top and bottom of the cross-section at the transfer and service stages must not be greater than the prescribed limits of working stresses. This can be expressed mathematically as:

i) At Transfer Stage

$$f_i^b = -\frac{P_i}{Ac} + \frac{(\pm P_i e \pm M_o \pm M_{si})}{S_b} \leq f_{ci}, f_{ti} \tag{4.15}$$

$$f_i^t = -\frac{P_i}{Ac} + \frac{(\pm P_i e \pm M_o \pm M_{si})}{S_t} \leq f_{ci}, f_{ti} \tag{4.16}$$

ii) At Service Stage

$$f_s^b = -\frac{P_e}{Ac} + \frac{(\pm P_e e \pm M_T \pm M_{se})}{S_b} \leq f_{cs}, f_{ts} \tag{4.17}$$

$$f_s^t = -\frac{P_e}{Ac} + \frac{(\pm P_e e \pm M_T \pm M_{se})}{S_t} \leq f_{cs}, f_{ts} \tag{4.18}$$

where

f_i^t, f_i^b are top and bottom stresses in cross-section at transfer stage .

f_s^t, f_s^b are top and bottom stresses in cross-section at service stage .

f_{ci}, f_{ti} are allowable compressive and tensile stresses in concrete at transfer stage.

f_{cs}, f_{ts} are allowable compressive and tensile stresses in concrete at service stage .

P_i, P_e are initial and effective total prestressing force at transfer and service stages.

S_t, S_b are section modulus at top and bottom of cross-section .

Ac is the area of the concrete cross-section.

e is the distance from the centroidal axis of the section to the tendon profile .

M_{si}, M_{se} are initial and effective secondary prestressing moments at the transfer and service stages.

M_{ot}, M_T are bending moments due to self-weight and total load.

4.4.3 Ultimate Flexural Strength Constraint

The ACI-318-05 requires that the ultimate moment due to load plus secondary moment due to prestressing force must be less or at least equal to ultimate moment capacity of the prestressing member. This can be expressed mathematically as:

$$(M_u + M_{se}) \leq \phi M_{nr} \tag{4.19}$$

where

M_{se} is the effective secondary prestressing moment at the service stage.

M_u is the ultimate bending moment due to the total load.

ϕM_{nr} is the ultimate capacity of the resisting moment provided by the cross-section.

Constraint on the Minimum Amount of Flexural Reinforcement

To ensure that a reserve of strength exists after initial cracking, the girders should contain sufficient flexural reinforcement at the critical sections. If the girders do not

contain enough reinforcement, they may fail abruptly with rupturing of the reinforcement immediately after cracking. According to ACI-318-05, the minimum amount of flexural reinforcement in steel reinforced members should be controlled by:

$$\phi M_{nr} \geq 1.2 M_{cr} \tag{4.19a}$$

where

M_{cr} = moment causing flexural cracking at section due to externally applied loads, which is given by:

$$M_{cr} = (I/y_t)(7.5\sqrt{fc'} + f_{pe} - f_d) \tag{4.19b}$$

The requirement given by Equation 4.19a can be waived when the factored moment of resistance, ϕM_{nr} is at least 33 percent greater than the moment due to factored loads, $(M_u + M_{se})$ .i.e. when

$$\phi M_{nr} \geq 1.33(M_u + M_{se}) \tag{4.19c}$$

The other variables are as defined before.

4.4.4 Ultimate Shear Strength Constraint

The shear strength to be carried by stirrups must not exceed the maximum value in ACI-318-05. This can be expressed mathematically as:

$$\phi Vs \leq \phi(8\sqrt{fc'}b_w d) \tag{4.20}$$

where

ϕVs is the ultimate shear strength provided by stirrups .

fc' is the specified concrete strength of concrete in psi.

b_w is the width of the web .

d is the depth from the centroidal of prestressing steel to extreme compression fiber but not less than $0.8h$.

4.4.5 Deflection Constraint

The deflection constraints are defined by the following equations:

- Maximum deflection constraint at prestressing transfer is

$$-\frac{l}{800} \leq \delta_{transfer} \leq \frac{l}{800} \tag{4.21}$$

- Maximum deflection constraint at prestressing service is

$$-\frac{l}{800} \leq \delta_{service} \leq \frac{l}{800} \tag{4.22}$$

- Maximum deflection constraint due service live plus impact is

$$-\frac{l}{800} \leq \delta_{ll} \leq \frac{l}{800} \tag{4.23}$$

where $l =$ is the span length, in ft.

4.5 Problem Formulation

The optimization problem is to minimize the cost function F (Eq. 4.10), subject to specified constraints for geometry, stresses, ultimate flexure and shear capacities and deflection. These constraints are nonlinear functions of h, P_l and e, and so the problem is

a constrained nonlinear one, and it can be solved by transforming it to a linear one in the following manner.

By assigning a trial feasible cross-section, the first term of the objective function Eq.4.10, $[C_c \Sigma A_{ci} l_i]$, becomes a constant, and F becomes a function of $C_p \gamma P_l z\{ L+ (\lambda\text{-}1) L_s\}$, which means that only the minimum prestressing force P_l and the proportion of long and short tendons λ have to be found. For an assumed value of λ, the problem becomes the finding of minimum P_l and the corresponding layout shown in Figures 4.3 and 4.4.

As the search for the optimum solution begins with an initial feasible tendon profile, the eccentricity e at each station is known. Consequently, the constrained equations of working stresses become linear in P_l and a linear program can be easily used to find P_l satisfying all constraints.

The optimization procedure begins with a feasible design, and it progressively updates the design variables through the use of a gradient vector to minimize the objective function Eq. 4.10, subject to the conditions of strength and serviceability. The search procedure is as follows.

Reducing the problem to a linear one is useful in the building of a repetitive program (algorithm) to search for the optimum solution.

4.5.1 Optimization Procedure

(1) The process begins with a feasible design by assigning initial values to all variables $\{h_1, h_2, h_3, e_b, \beta_0, \beta_1, \beta_2, \alpha, \alpha_1, \alpha_2, \lambda, \varepsilon\}$.

in which $\{h_1, h_2, h_3, e_b, \beta_0, \beta_1, \beta_2, \alpha, \alpha_1 \text{ and } \alpha_2\}$ are shown in Figures 4.1, 4.2, 4.3 and 4.4, and ε is the ratio of interior span to exterior span for a three-span bridge deck. The symbols h_1 to h_3 are the depth of the box girder, β_0 to β_2 are the eccentricity factors, and α to α_2 are the length factors for the tendon geometry.

(2) The span ratio ε is taken initially as 1.0 (this implies equal spans).

(3) Each span is divided into ten equal divisions, and the maximum and minimum values of design forces at each station are calculated from a structural analysis by using applicable service loads.

(4) The initially chosen cross-section is first checked for its adequacy by the following equations:

$$S_b \geq \frac{M_t - RM_o}{f_{ts} + Rf_{ci}} \tag{4.24}$$

$$S_t \geq \frac{M_t - RM_o}{f_{cs} + Rf_{ti}} \tag{4.25}$$

where S_b, S_t = the section modulus at bottom and top; M_t, M_o = the bending moment due to total load and self-weight; f_{ti}, f_{ts} = allowable tensile stress in concrete during initial and service stages; f_{ci}, f_{cs} = allowable compressive stress in concrete during initial and service stages; and R = factor representing the total loss of prestressing force , $R = \dfrac{P_e}{P_i}$

(5) The initial value of λ is taken as 1.0 (this indicates that all tendons are long with no short one).

(6) Based on the chosen tendon geometry, the minimum value of the prestressing force P_l at the jacking end is determined by using linear programming satisfying all constraints.

(7) For the chosen cross-section and for the selected λ, the profile of the tendon is then modified to a new one by recalculating the new geometry of the tendons by using the gradient search method until the optimum value of prestressing force P_l, is found satisfying all constraints. The new geometry of the tendon X_m at ($n+1$) step is calculated from

$$X_m^{(n+1)} = X_m^{(n)} + \zeta \Delta P^{(n)}$$
(4.26)

in which ζ = maximum incremental step permitted and $\Delta P^{(n)}$ is the gradient vector at the step n.

(8) The entire steps 6-7 are repeated for small incremental values of λ until a value of λ and corresponding values of P_l and the geometry of the tendons, and the optimum value of F (Eq 4.10) are obtained satisfying all constraints.

(9) The depths of cross-section (h_1, h_2 and h_3) are then gradually modified to new ones by recalculating the depths of cross-section by using the gradient method of the search, and the entire steps 1-9 are repeated until a value of h and the minimum F are obtained satisfying all constraints. The new vector of design variables h_j at ($i+1$) step is calculated from

$$h_j^{(i+1)} = h_j^{(i)} + \psi \Delta F^{(i)}$$
(4.27)

in which ψ = maximum incremental step permitted and $\Delta F^{(i)}$ is the gradient vector at the step i.

Finally, to find the optimum span ratio ε, the entire steps (1) to (9) are repeated for incremental values of span ratio, until a value of ε and the global minimum F are obtained satisfying all constraints.

4.5.2 Gradient Method of Optimization

Steepest Descent is a well-known iterative minimization method. This method is applied to find the optimum prestressing force of long tendons at the jacking end P_l, the corresponding optimum tendon profile, and the optimum depth as follows:

(1) For the given tendon profile, the variables of tendon profile are divided into categories, where $\{\beta_n\}$ relates to the eccentricities and $\{\alpha_n\}$ relates to the tendon's segment length. At the iteration i, the prestressing force $(P_l)_i$ can be found by linear programming.

(2) Then, the derivatives of P_l with respect to the variables $\{\beta_n\}$ and $\{\alpha_n\}$ are calculated by the finite difference method.

$$P_l'(\beta_n) = \frac{P_l(\beta_n^{i+1}) - P_l(\beta_n^i)}{\Delta \beta_n} \tag{4.28}$$

$$P'_l(\alpha_n) = \frac{P_l(\alpha_n^{i+1}) - P_l(\alpha_n^i)}{\Delta \alpha_n} \tag{4.29}$$

where, at iteration i^{th}, $P_l'(\alpha_n)$ and $P_l'(\beta_n)$ are calculated by a given small fixed

incremental value for the variables $\{\beta_n\}$ and $\{\alpha_n\}$.

(3) This step is applied to each variable $\{\beta_{n-1}, 2, \ldots\ldots\ N\}$ and
$\{\alpha_{n-1}, 2, \ldots\ldots\ N\}$ and the gradients of P_l with respect to these
variables are obtained as follows:

$$P_l'(\beta) = \left\{-\frac{\Delta P_l^i}{\Delta\beta_1}, -\frac{\Delta P_l^i}{\Delta\beta_2}, \ldots\ldots\ \ldots\ldots, -\frac{\Delta P_l^i}{\Delta\beta_N}\right\} \tag{4.30}$$

$$P_l'(\alpha) = \left\{-\frac{\Delta P_l^i}{\Delta\alpha_1}, -\frac{\Delta P_l^i}{\Delta\alpha_2}, \ldots\ldots\ \ldots\ldots, -\frac{\Delta P_l^i}{\Delta\alpha_N}\right\} \tag{4.31}$$

(4) The new value of each variable is calculated from the given equation:

$$X_{\beta 1}^{(i+1)} = \beta_1^i + \xi_{\beta 1}\frac{\Delta P_l^i}{\Delta\beta_1}, \ldots\ldots\ldots, X_{\beta N}^{(i+1)} = \beta_N^i + \xi_{\beta N}\frac{\Delta P_l^i}{\Delta\beta_N} \tag{4.32}$$

$$X_{\alpha 1}^{(i+1)} = \alpha_1^i + \xi_{\alpha 1}\frac{\Delta P_l^i}{\Delta\alpha_1}, \ldots\ldots\ldots, X_{\alpha N}^{(i+1)} = \alpha_N^i + \xi_{\alpha N}\frac{\Delta P_l^i}{\Delta\alpha_N} \tag{4.33}$$

where $\xi_{\beta n} > 0$ is obtained from the following expression:

$$\xi_{\beta n} \leq \frac{\Delta\beta}{\max_n\left|\dfrac{\Delta P_l^i}{\Delta\beta_n}\right|} \tag{4.34}$$

and $\xi_{\alpha n} > 0$ is obtained from the following expression:

$$\xi_{\alpha n} \leq \frac{\Delta\alpha}{\max_n\left|\dfrac{\Delta P_l^i}{\Delta\alpha_n}\right|} \tag{4.35}$$

(5) This procedure is repeated until ΔP_l^i is less than the admissible error for
all the variables and the optimum value of P_l is obtained satisfying all

constrains.

(6) To find the optimum depth and corresponding optimum of cost function, the derivatives of F (objective function) with respect to the depth $\{h_n\}$ are calculated by the finite difference method.

$$F'(h_n) = \frac{F(\beta_n^{i+1}) - F(h_n^{i})}{\Delta h_n} \qquad (4.36)$$

where, at iteration i^{th}, $F'(h_n)$ are calculated by a given small fixed incremental value for the variables $\{ h_n \}$.

(7) This step is applied to each variable $\{ h_2$ and $h_3 \}$, and the gradients of F with respect to these variables are obtained as follows:

$$F'(h) = \left\{ -\frac{\Delta F^i}{\Delta h_2}, -\frac{\Delta F^i}{\Delta h_N} \right\} \qquad (4.37)$$

The new value of each variable is calculated from the given equation:

$$h_2^{(i+1)} = h_2^{i} + \psi_{h2} \frac{\Delta F^i}{\Delta h_2}, \ldots\ldots\ldots, h_N^{(i+1)} = h_N^{i} + \psi_N \frac{\Delta F^i}{\Delta h_N} \qquad (4.38)$$

where $\psi_N > 0$ is obtained from the following expression:

$$\psi_{hn} \leq \frac{\Delta h}{\max_n \left| \frac{\Delta F^i}{\Delta h_n} \right|} \qquad (4.39)$$

(8) This procedure is repeated until ΔF^i is less than the admissible error for all the variables and the optimum value of F is obtained satisfying all constrains.

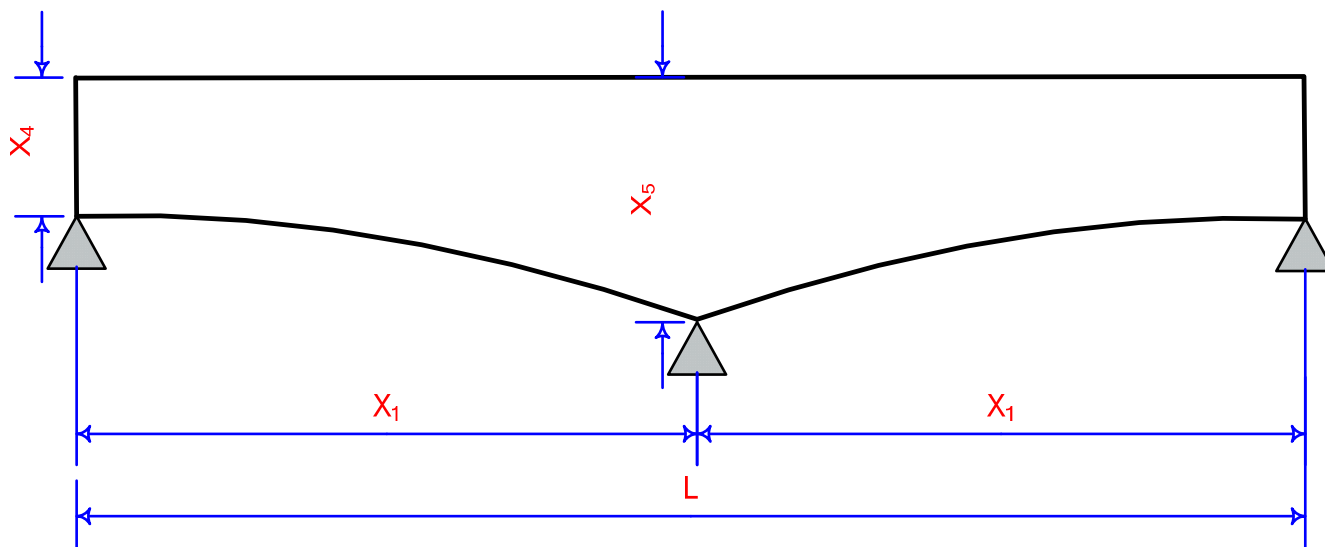**Figure 4.1** Design Variables in Cross-Sectional Dimensions and Structural Configuration of Two-Span Continuous Bridge girders
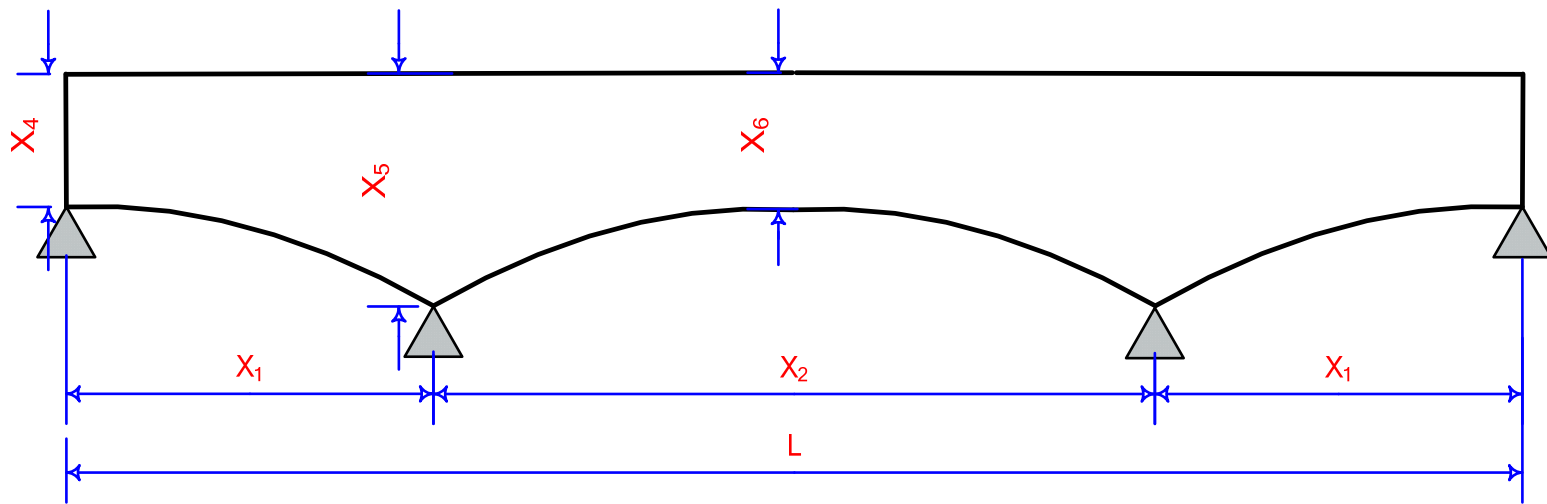
Figure 4.2 Design Variables in Cross-Sectional Dimensions and Structural Configuration of Three-Span Continuous Bridge girders
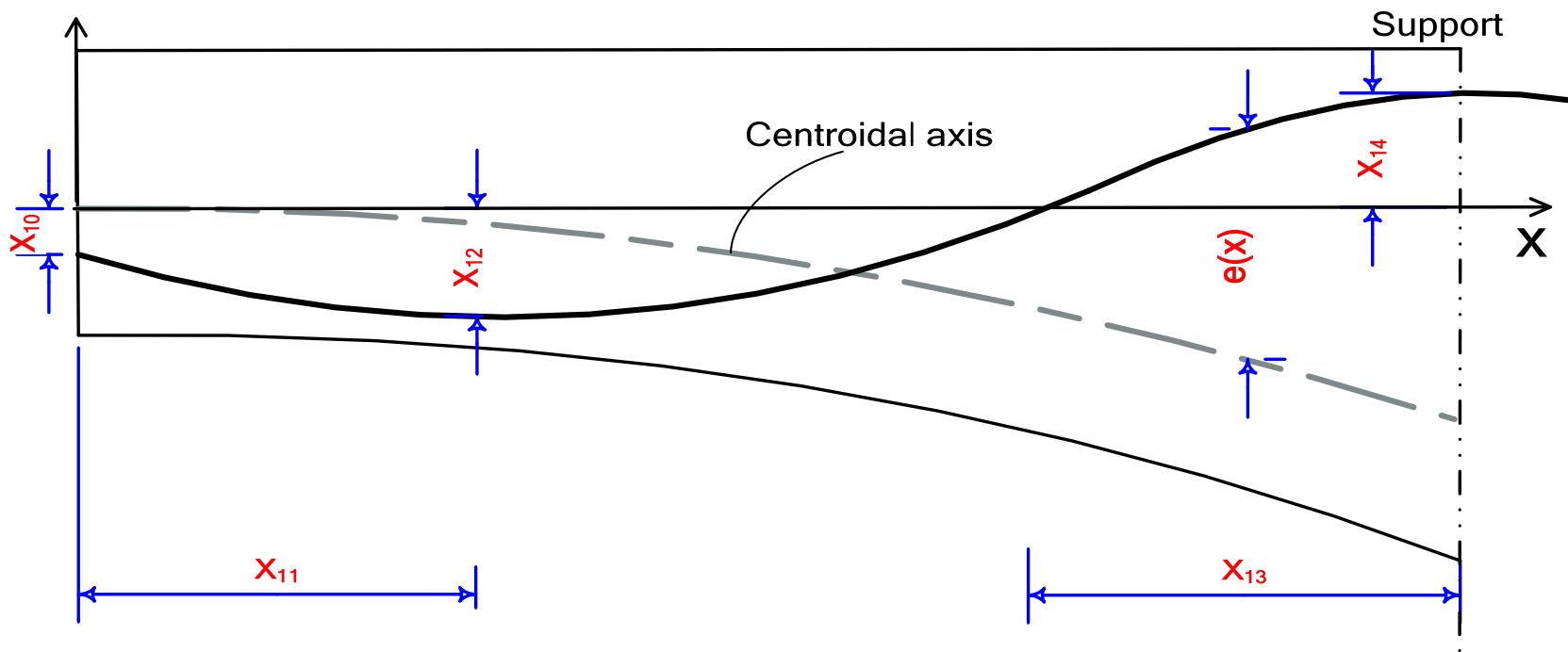
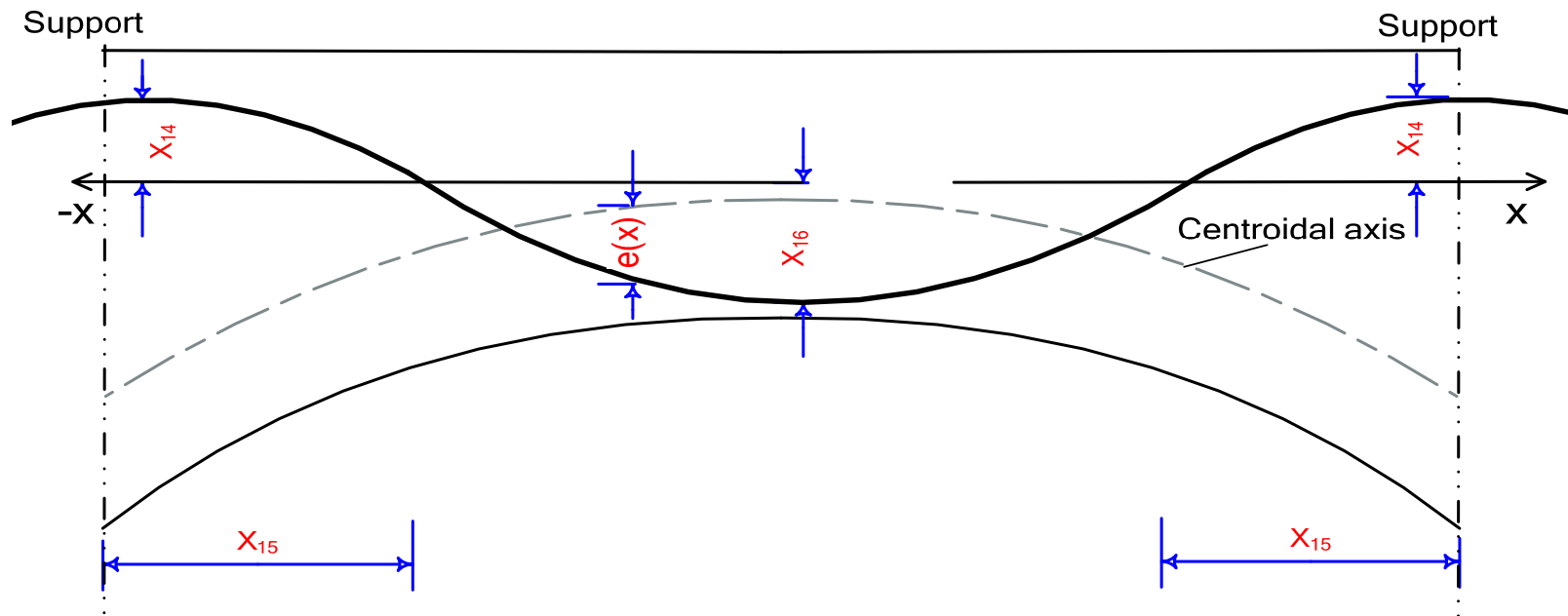**Figure 4.3** Design Variables in Exterior Span of Continuous Bridge girders

Figure 4.4 Design Variables in Interior Span of Continuous Bridge girders

CHAPTER FIVE

COMPUTER CODE FOR ANALYSIS AND

OPTIMIZATION

5.1 General

Many tools for optimization are easy and ready to use, such as the MATLAB Optimization toolbox which implements several methods. However, MATLAB code is not as efficient as compiled C or FORTRAN code, and it is appropriate for small to medium scale problems only (Karim, 2003). Therefore a standard FORTRAN is chosen in the present study to develop a computer code for optimization where the criterion to be optimized is an indirect function of some design variables.

5.2 FORTRAN Program

For optimization of the problem under investigation, a computer code has been developed by using a standard FORTRAN, and it is called **PCPCBGND** (Program for Continuous Post-tensioned Concrete Bridge Girder of Non-uniform Depth). This program can handle both two- and three-span continuous bridge girders having a single-cell box cross-section subject to the AASHTO-HS Bridge loading. The cross-section may have uniform or variable depth. It is important to point out that PCPCBGND is sensitive to the initial value of design variables that are entered by the user for the first design cycle. Where the initial values are away from the optimum solution, a longer time will be taken

to reach the optimum solution, but a good starting value will reduce this time.

The problem begins with an initial feasible point in the design space by assigning initial values to all design variables through the subroutine DATA. Then, a gradient search technique is used to solve the optimization problem iteratively.

The first part of the program is to prepare the analysis module which predicts and demonstrates the behavior and response of the structure under subjected load. This module analyzes the structure for the initial value of all variables, and it generates all the necessary information that will be used in other subroutines of cost function and constraints. For this purpose, a general bridge analysis routine called BRDANA is used for linear elastic analysis of the bridge girder. The program was first checked by comparing results with the STAAD Pro package. Sample results are shown in Appendix A to show that this program is fairly accurate. For the initial value of all variables, the bridge is idealized as (n) straight elements, the linear analysis is conducted, and the member end forces for each element are calculated. The maximum and minimum values of shear force, bending moment and deflection, $\{V_{max},\ M_{max},\ M_{min},\ \delta_{max},\ \delta_{min}\}$ are obtained.

Then, the subroutine PRESTD is developed to calculate eccentricities, frictional and other losses, secondary moment, initial and final working stresses, bearing capacities for moment and shear, and initial and final deflections at each station along the bridge girder .

After that, the required data for optimization are available. Finally, the subroutine ALLOPT is used to find the optimum value of the objective function as follows:

1. For the initial values of the proportion of prestressing forces in short and long tendons, $\lambda = 1.0$ (all tendons long with no short tendons), depth h_1, h_2, h_3, initial tendon profile and span ratio, $\varepsilon = 1.0$, the program carries on iteration till the optimum profile of prestressing tendon and the corresponding minimum of prestressing force at the jacking end P_l are obtained satisfying all constraints.

2. Then, the program changes λ to a new value and it continuous the iteration till the optimum profile of prestressing tendon and the corresponding minimum of prestressing force at the jacking end P_l are obtained satisfying all constraints . This step and subroutine PRESTD are repeated till the optimum value of λ and the corresponding optimum profile of prestressing tendon and the optimum of prestressing force P_l are obtained.

3. The depths of cross-section (h_1, h_2 and h_3) are then gradually changed to new depths by recalculating the depths of the cross-section by using the gradient method of the search. The previous steps and the subroutine BRDANA are repeated till the optimum values of h_1, h_2 and h_3 are obtained satisfying all constraints.

4. Finally, the span ratio ε is changed to a new one, and all subroutines are repeated, till the optimum value of ε is obtained.

5.2.1 Flow Chart

The program consists of subroutines as illustrated by the flow-chart shown in Figures 5.1, 5.2, 5.3, 5.4, 5.6 and 5.7. These routines are as follows:

1. SDATA: reads and writes the data of the design variables and the data of bridge girder spans, loads, geometry, material properties and unit cost of material.

2. BRDANA: calculates the minimum and maximum of shear force, bending moment and deflection by calling the following subroutines:

   - SEPROES: calculates the geometrical properties of the concrete cross-section at each station.

   - STIFF: calculates the stiffness matrix for each member.

   - BANFAC: calculates the section properties at each station.

   - DELOAD: calculates the end action due to self-weight and superimposed dead load. Then, it calculates the shear force, bending moment and deflection by calling the routines: XDIS, LOADS, BANSOL and RESUTS.

   - LLLOAD: calculates the end action due to live load. Then, it calculates the minimum and maximum of shear force, bending moment and deflection by calling the routines: XDIS, LOADS, BANSOL, RESUTS, MAXULL, MXRESU and FINBM.

3. PRESTD: calculates the prestressing force corresponding to the profile by calling

   - ECCENT: calculates the eccentricities of the tendon profile at each station.

   - FRLOSS: calculates the slope of the tangents to the tendon profile and the frictional losses at all stations.

   - OTHLOS: calculates the total prestressing loss at all stations.

- PRIMPS: calculates the primary prestressing moment, at the transfer and service stages at all stations.

- SECMO: calculates the secondary prestressing moment, at the transfer and service stages at all stations where it calculates numerically by using Simpson's rule.

- CHFEAS: calculates the minimum of the top and bottom modulus for section S^t_{min} and S^b_{min} of the cross-section, and checks the adequacy of chosen initial depth.

- STRESS: calculates the stresses at the top and bottom of the cross-section at the transfer and service stages due to net prestressing moment and load.

- MOMCAP: calculates the stresses of prestressing steel f_{ps} by using strain compatibility, and then calculates the ultimate flexural strength of a section and the cracking moment at each station.

- SHECAP: calculates the shear strength of the concrete cross-section at each station.

- DEFLEC: calculates the maximum deflection due to live load, camber due to prestressing force, and initial and final total deflection at each station.

4. ALLOPT: depending on the number of spans, this routine calls. If span equal to two then it calls routine OPDTWO but otherwise it calls SPANRT.

- OPDTWO: calculates the gradient of the objective function, the new value of design variables, and   finally finds the optimum profile of tendon, the optimum arrangement of long and short tendon, the optimum prestressing force P_l, the optimum depth at interior support, and the optimum depth ratios:

- OPDINT: for the initial constant depth, this routine calculates the minimum object

function, which is the first value of the object function, by calling the routines: BRDANA and OPLEMD1.

- OPLEMD1: calculates the optimum profile of tendon, the optimum arrangement of long and short tendons, and the optimum prestressing force Pl, by calling OPPRSS1.

- OPPOFI1: calculates the optimum profile of tendon and the corresponding optimum prestressing force Pl by calling BRDANA and MINPRF.

- MINPRF: calculates the prestressing force corresponding to the profile that satisfies the constraints.

- SPANRT: calculates the optimum profile of tendon, the optimum arrangement of long and short tendon, the optimum prestressing force, the optimum depth at support, the optimum depth ratios and the optimum span ratio by calling OPDINT, OPLEMD1, and OPPRSS2.

5.3 Design Optimization Software (Excel Solver)

Microsoft Excel Solver incorporates a nonlinear optimization code based on the Generalized Reduced Gradient (GRG) technique. This tool is easy and ready to use, but the whole problem under consideration is difficult to model in Excel Solver because the maximum and minimum values of shear force, bending moment and deflection, $\{V_{max}, M_{max}, M_{min}, \delta_{max}, \delta_{min}\}$ have to be calculated many times during optimization. Thus for a given cross-section, it is employed only to find the minimum prestressing force at the jacking end P_J and the corresponding layout satisfying all constraints. The problem of using Excel Solver is to find the maximum and minimum values of shear force, bending

moment and deflection, $\{V_{max}, M_{max}, M_{min}, \delta_{max}, \delta_{min}\}$ for the given cross-section. This is solved by using the symbolic software Mathematic as follow:

The governing differential equation for deflection of the beam

$$EI \frac{d^4 y}{dx^4} = q(x) \qquad 0 < x < L_1 \qquad (5.1)$$

where

EI = flexural rigidity;

y = the deflection;

$q(x)$ = the distributed load;

L_1 = span length.

The shear force $V(x)$, bending moment $M(x)$ and the deflection $y(x)$ are equal

$$V(x) = \int q(x) dx \qquad (5.2)$$

$$M(x) = \int V(x) dx \qquad (5.3)$$

$$y(x) = \iint \frac{M(x)}{EI} \qquad (5.4)$$

The above equations are subjected to boundary conditions and solved by using the software Mathematic. As the term $\frac{1}{EI}$ is a function of the depth h which is variable, it is better to integrate the above equations symbolically by replacing $\frac{1}{EI}$ with a simple polynomial function of the form:

$$P(x) = \frac{1}{EI} = k_0 + k_1 x^2 + k_2 x^4 + k_3 x^6 + k_4 x^8 \qquad (5.5)$$

in which k_0 to k_4 are factors.

Therefore, the shear force $V(x)$, bending moment $M(x)$ and the deflection $y(x)$ are functional in these factors which are calculated by using Excel Solver as follows:

1) Each span is divided into ten equal divisions.

2) For a given cross-section, the value $\frac{1}{EI}$ and other section properties are known at each distance x.

3) By assigning initial values to all factors K_0 to K_4, the polynomial function $P(x)$ is calculated at each distance x.

4) The square difference $(\frac{1}{EI} - P(x))^2$ is calculated at each distance x.

5) The sum of these differences is calculated and the Excel Solver is used to find the factors K_0 to K_4 that minimize the sum of the difference and the maximum and minimum values of design forces at each station are calculated by using the above equations.

After constructing the module in Excel and for a given λ, the Excel Solver is used to find the minimum prestressing force at the jacking end P_J and the corresponding layout satisfying all constraints. The comparison of the minimum prestressing force P_J using Excel Solver and PCPCBGND is shown in Appendix A.
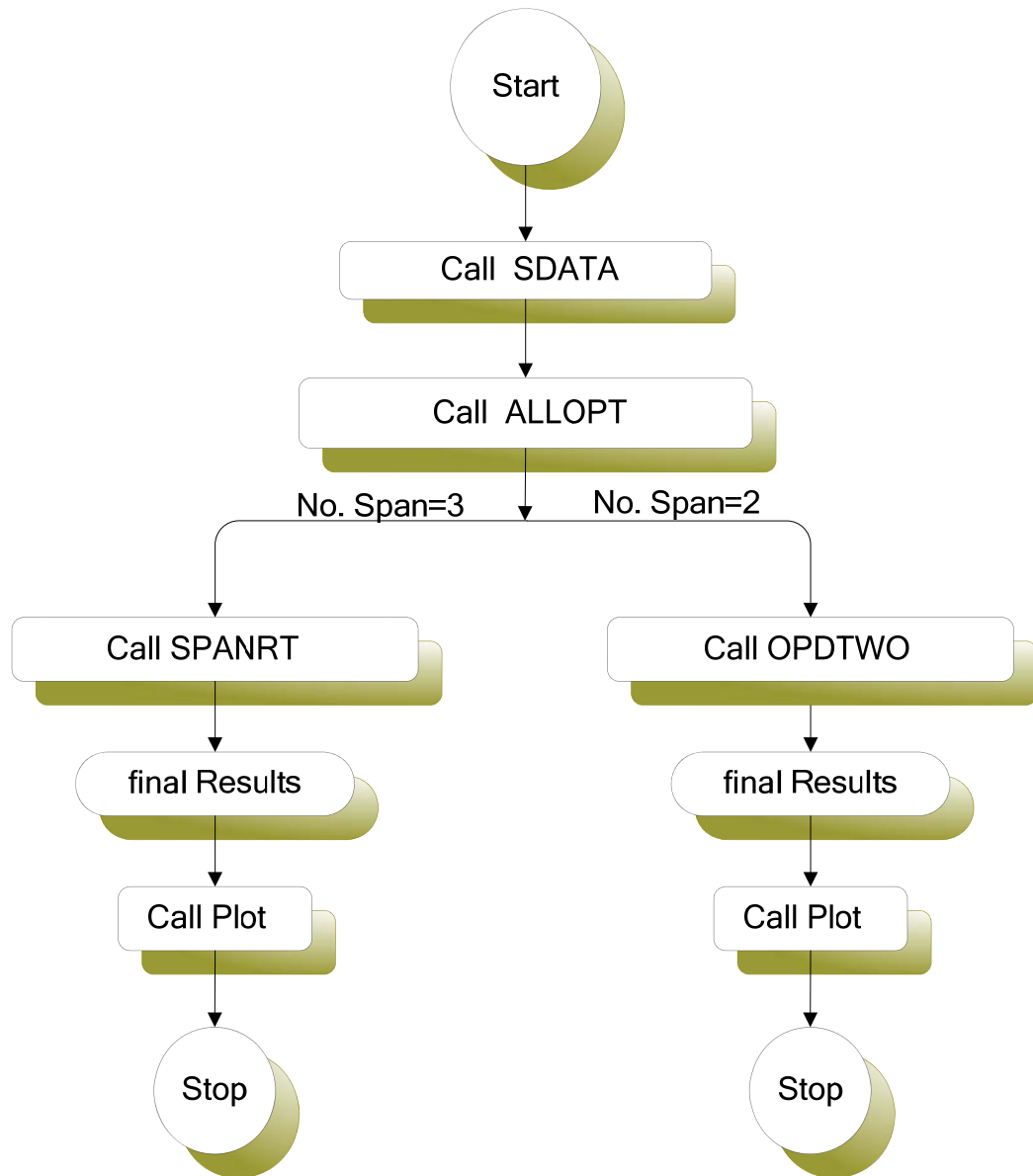
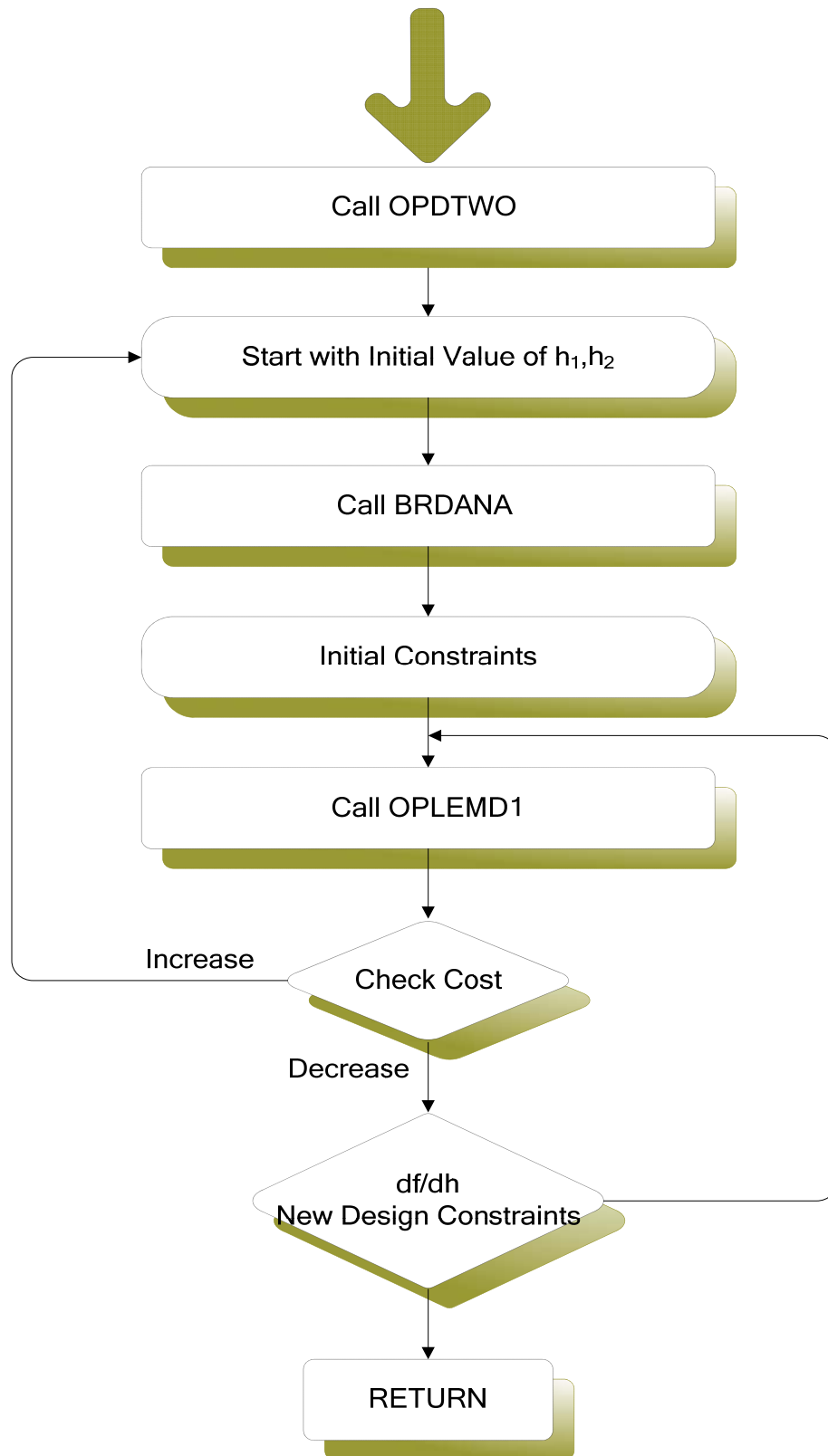**Figure 5.1** Flow Chart of Main Program

Figure 5.2 Flow Chart of Sub-Routine OPDTWO
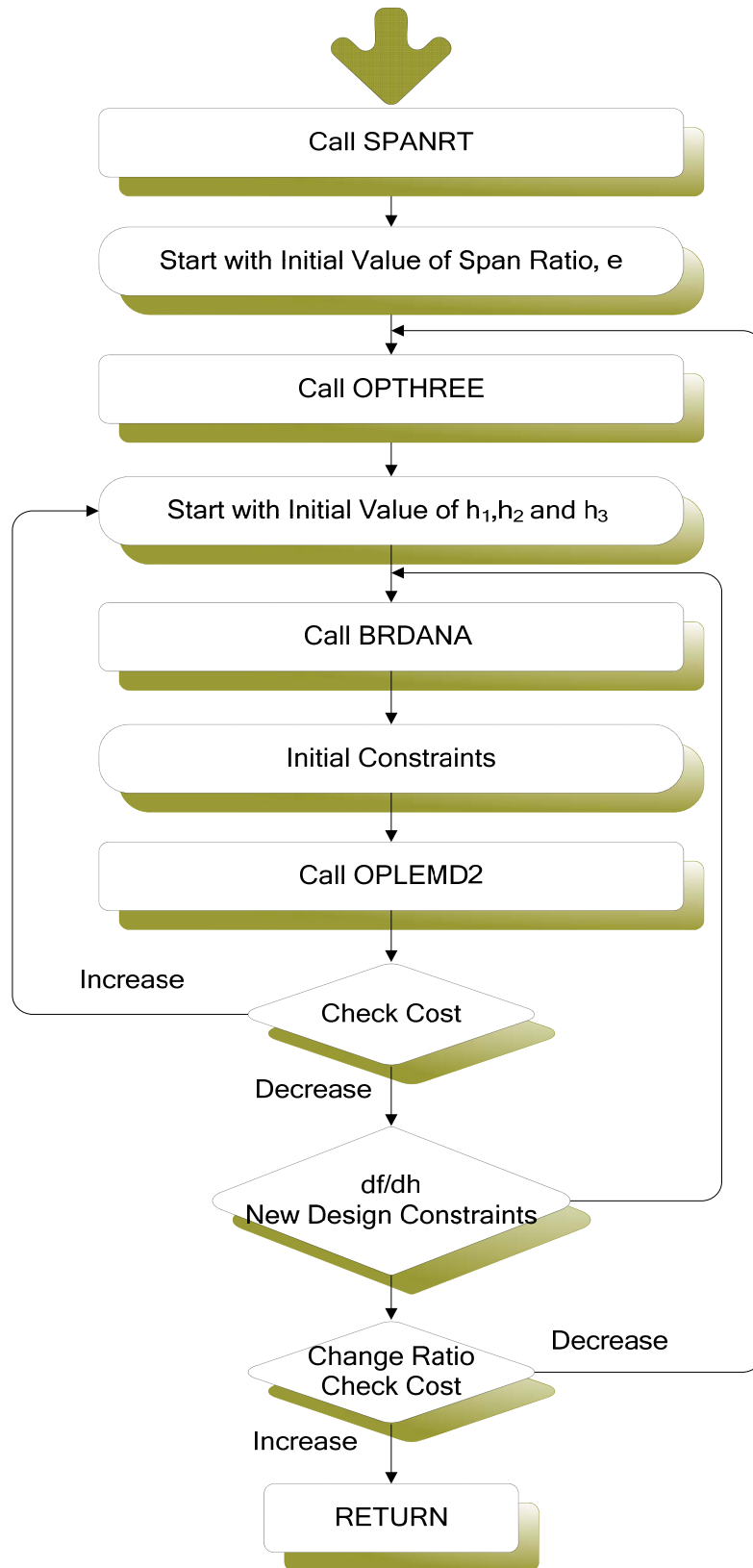
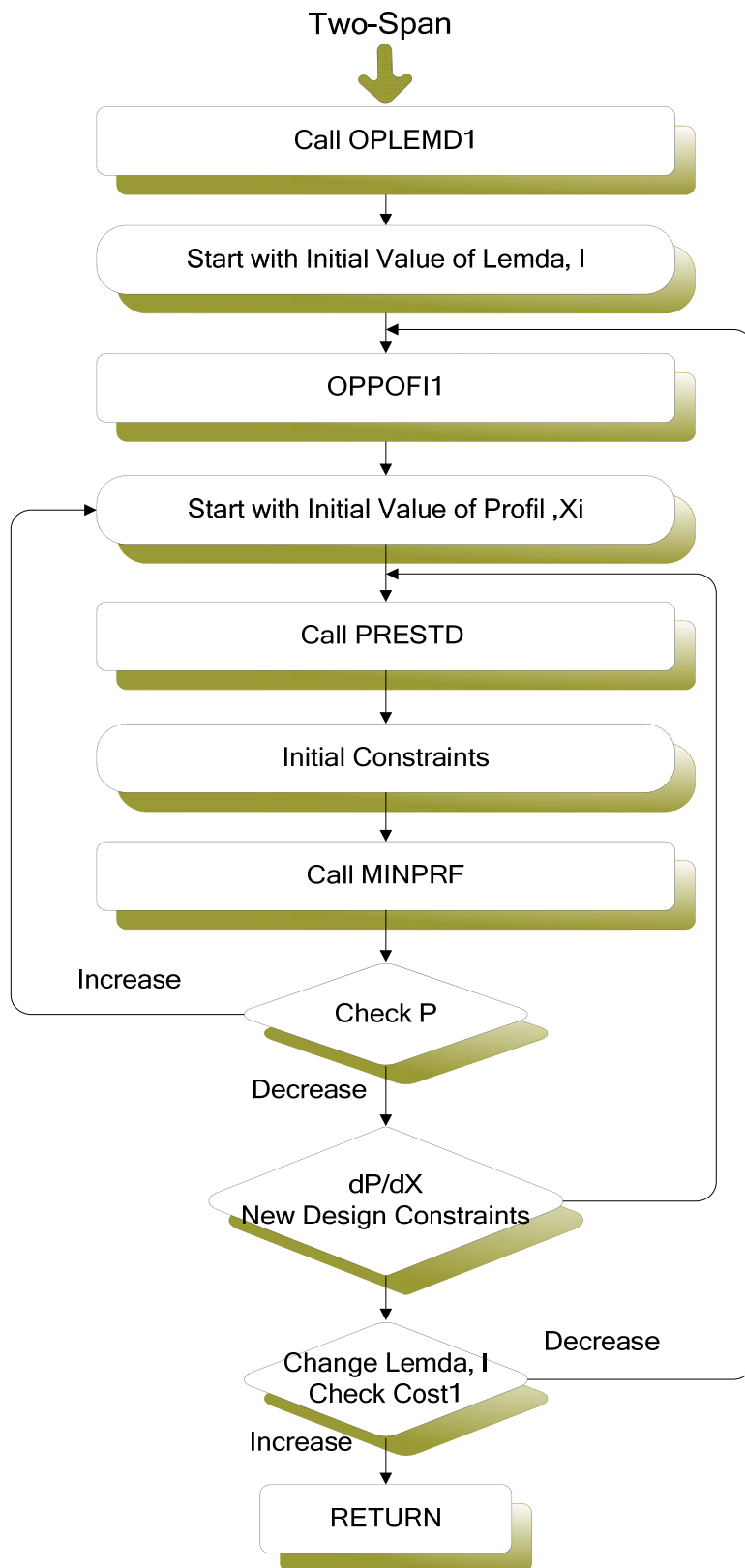**Figure 5.3** Flow Chart of Sub-Routine SPANRT

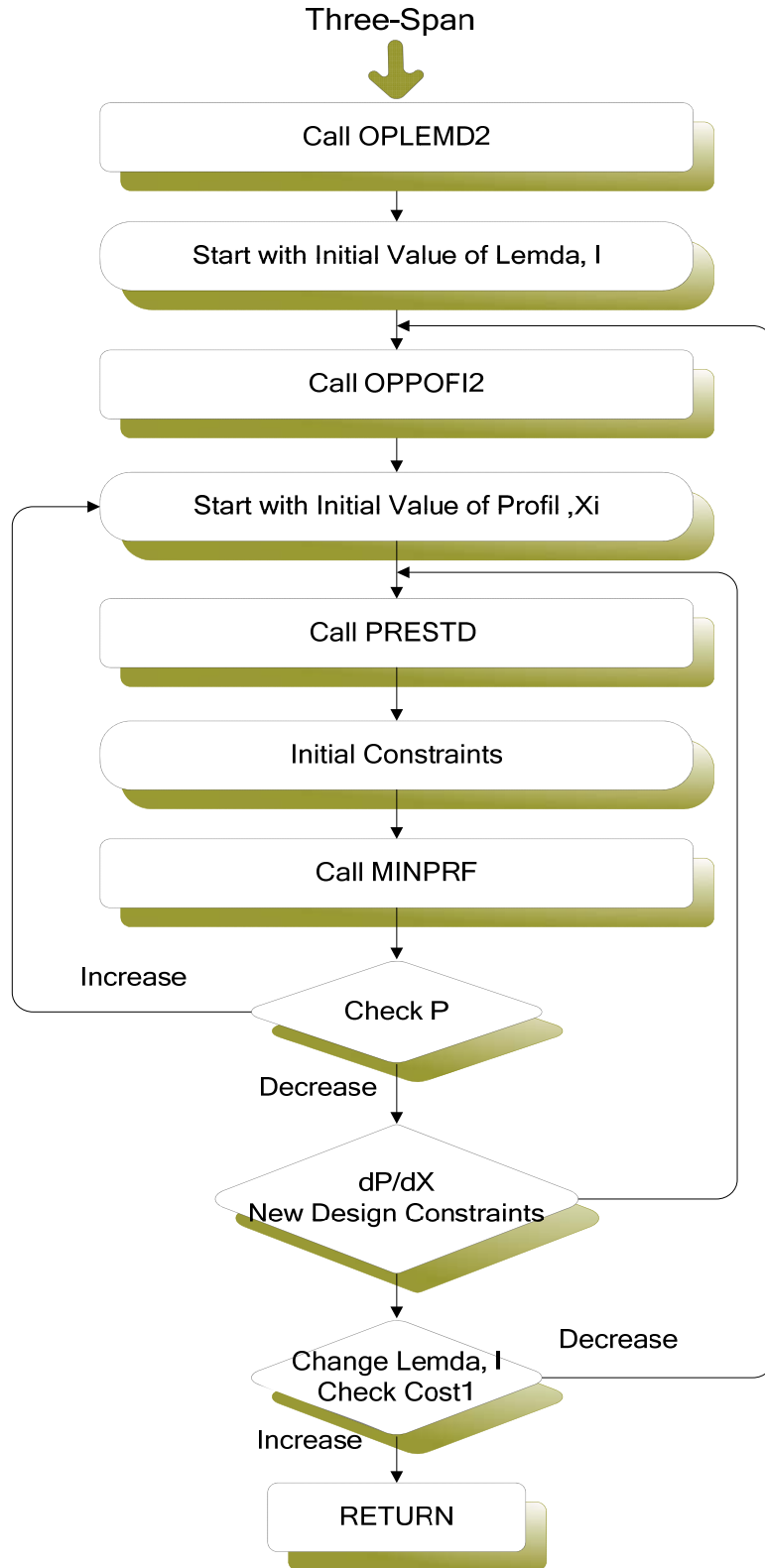**Figure 5.4** Flow Chart of Sub-Routine OPLEMD1

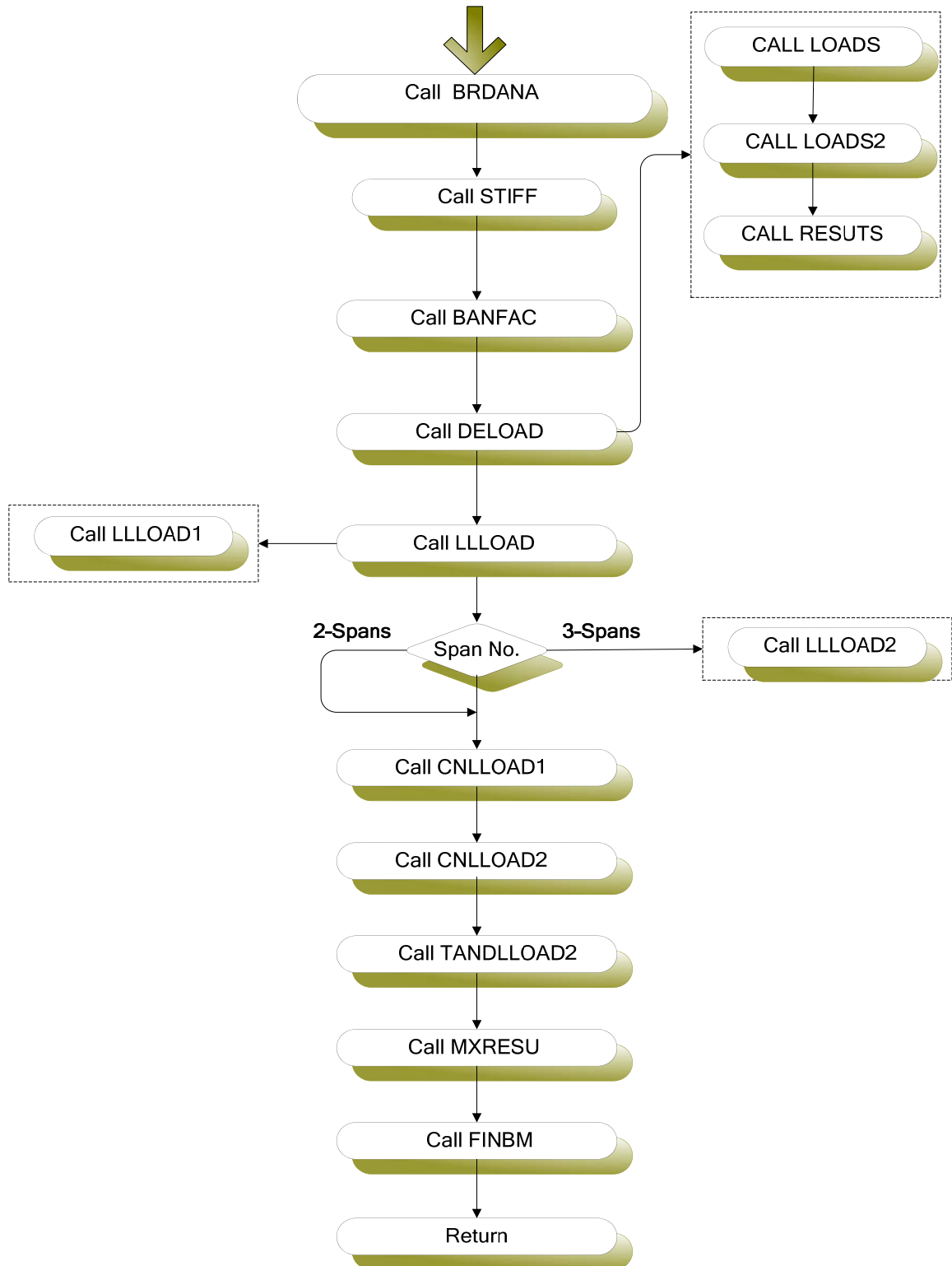**Figure 5.5** Flow Chart of Sub-Routine OPLEMD2

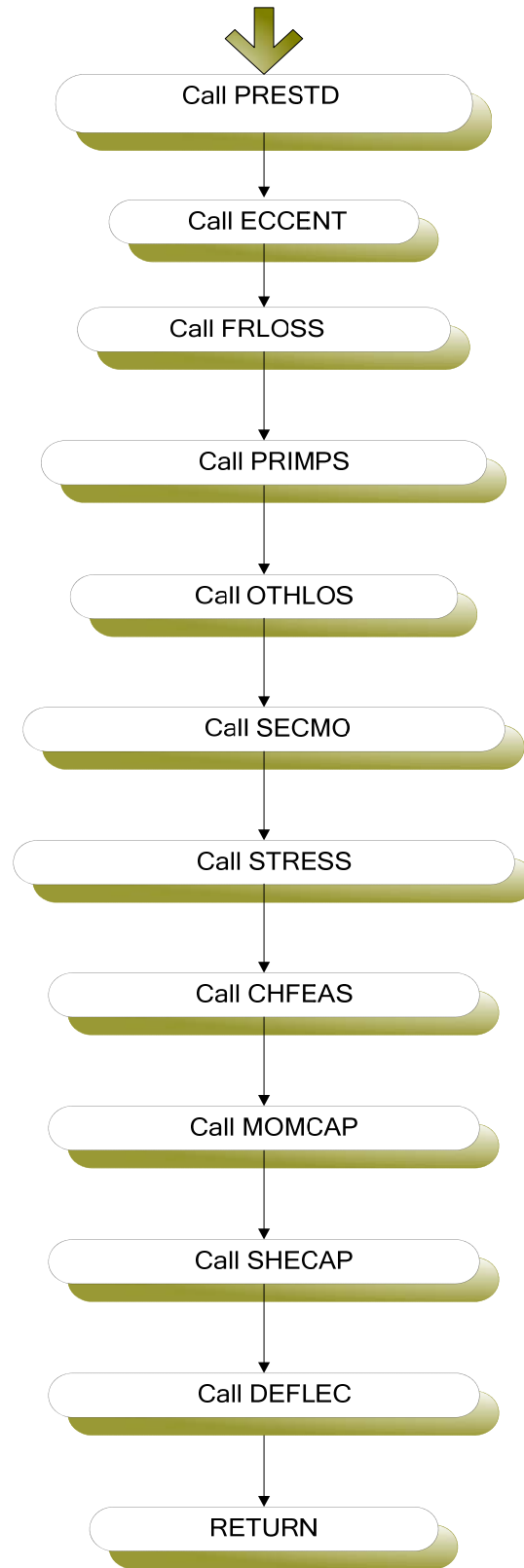**Figure 5.6** Flow Chart of Sub-Routine BRDANA

Figure 5.7 Flow Chart of Sub-Routine PRESTD

CHAPTER SIX

APPLICATION, RESULTS AND DISCUSSION

6.1 General

The PCPCBGND program is used in solving several problems, to show the capabilities of the code in handling analysis, and to obtain the optimum design. For given information about allowable stresses, deflection, strength of concrete, initial value of design variables and other variables, the optimum values are obtained for λ, interior to exterior span ratio for three-span, the depths of the cross-section, tendon eccentricities, and prestressing force P_l. The total cost of the member considered is the cost of structural materials (concrete and prestressing steel), excluding the formwork.

Several examples are considered for two and three spans to establish the reliability and performance of the present computational method in optimizing the design of bridge girders with variable depth for which the optimal solution is obtained analytically. Five cases are studied: four cases with $\lambda > 1$ (both short and long tendons) and one case with $\lambda = 1.0$ (all long tendons). These cases are selected to provide information on the influence of the design variables on optimization. The design variables are studied under the variation of total bridge length, the unit cost of material and proportioning of long and short tendons.

6.2 Two-Span Continuous Girder

6.2.1 Example

General Design Data

The design data and parameters are as follows:

Total length of the bridge $L = 400$ ft (121.6 m)

Each span is equal to $L_1 = 200$ ft (60.8 m)

Loading: the dead load includes: self-weight of the girder, and superimposed load = 500 lb/ft. Live load: AASHTO HS-20

Cross-section: single box girder with dimensions is shown in Figure 6.1.

Tendons profile: parabolic

Material Properties

Concrete

$f_{ci} = 2062 \ psi$, $f_{cs} = 2000 \ psi$

No tensile stress is assumed for concrete

$\gamma_c = 150 \ pcf$

Unit cost of concrete, $C_c = \$ \ 5.75 \ /ft^3$

Prestressing steel

$$f_{pu} = 270 \ Ksi$$
$$f_j = 0.7 f_{pu}$$
$$E_p = 28 \times 10^3 \ Ksi$$

Curvature coefficient of friction $\mu = 0.25$

Wobble coefficient of friction $K = 0.0015$ *per ft*

The loss of prestressing excluding friction is taken as 20%

Unit cost of prestressing steel, C_p =\$ 3.5 /lb

The cost ratio, CR = C_c/C_p = 1.64

(a) Case 1: All Long tendons (λ = 1.0)

In order to study the impact of using a combination of long and short tendons and using all long tendons to reduce the total material cost, this example is solved with $\lambda = 1$ (all long tendons) and $\lambda > 1$ (both short and long tendons). Each span of the bridge girder is divided into 10 equal divisions. The program starts with a feasible design with initial values of the variables $\{ \beta_0, \beta_1, \alpha, \alpha_1, e_b, h_1, h_2 \}$ and $\lambda = 1.0$. The optimum design is searched iteratively, by using the gradient method of the search explained earlier in this study, until the optimum value of each variable is obtained.

The optimum design of this example is attained at depth $h_1 = 8.95 \ ft$ and depth $h_2 = 14.77 \ ft$, with depth ratio of $h_2/h_1 = 1.65$. The optimum tendon profile for this case is plotted in Figure 6.3. It has been observed that the optimum tendon profile is obtained in

this example when the values of design variables are at their upper limits. The variation of the objective function which is the total cost of material (concrete and prestressing steel) with the depth ratio h_2/h_1 is plotted for three values of h_1 ($h_1 = 8.95$ ft, 10.95ft and 11.95ft) in Figure 6.2 to show the effect of incremental values of h_1 on cost. The total cost of material is nondimensionalized as C_{ti}/C_{to}, where C_{ti} is the total cost at $h_2/h_1 = (h_2)_i/h_1$ (the ith step of iteration for $(h_2)_i/h_1$) and C_{to} is the total cost at $h_1 = 8.95$ ft with $h_2/h_1 = 1.65$. The plots show that the cost parameter for material decreases rapidly with increases in the depth ratio h_2/h_1 up to about $h_2/h_1 = 1.65$, and then the total cost increases as h_2/h_1 increases. The plots in Figure 6.2 also show the total cost increases as h_1 increases and a minimum material cost is attained when h_1 is kept as small as practicable. The results indicate that for these values of h_1, the optimum h_2/h_1 ratio appears to lie in the close proximity of 1.65.
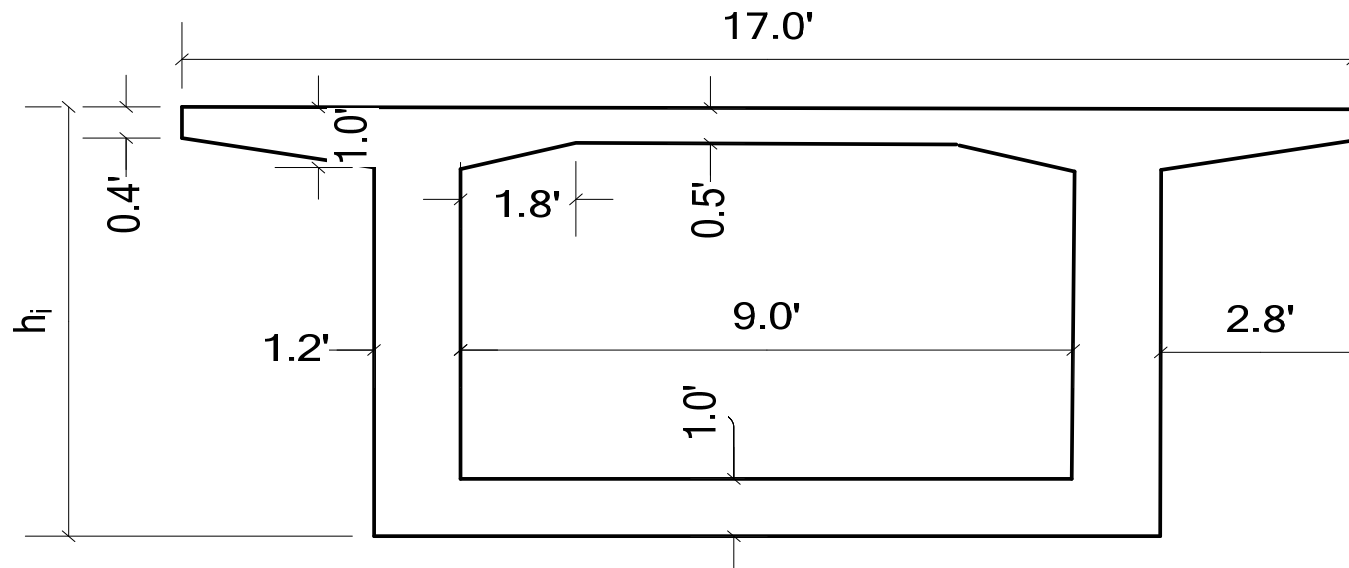
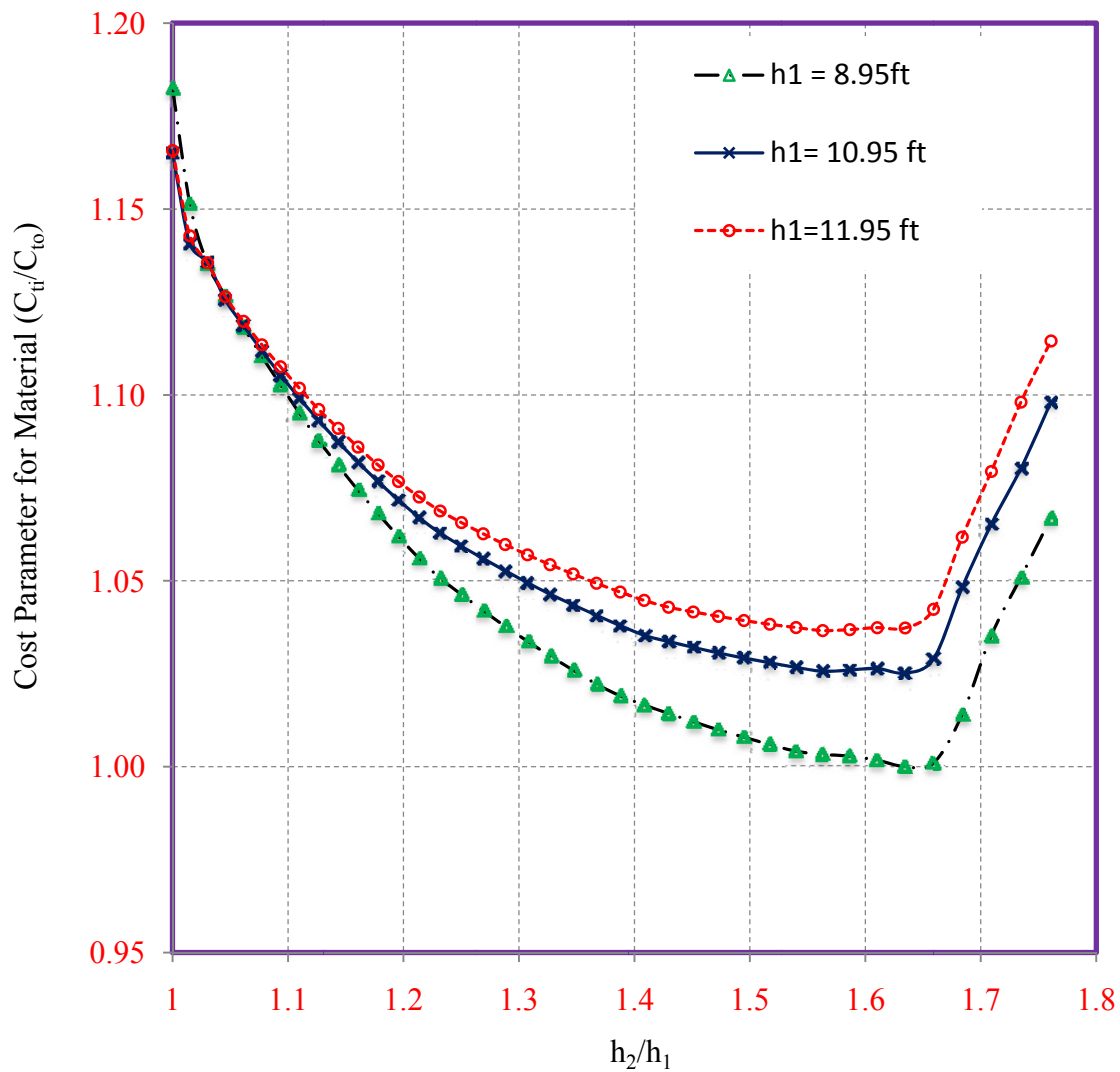**Figure 6.1** Cross-Section of Bridge Girder (ft)

Figure 6.2 Plot of Total Cost versus h_2/h_1 (2-Span of Total Length (400 ft), $\lambda = 1$ and AASHTO HS-20 loads)
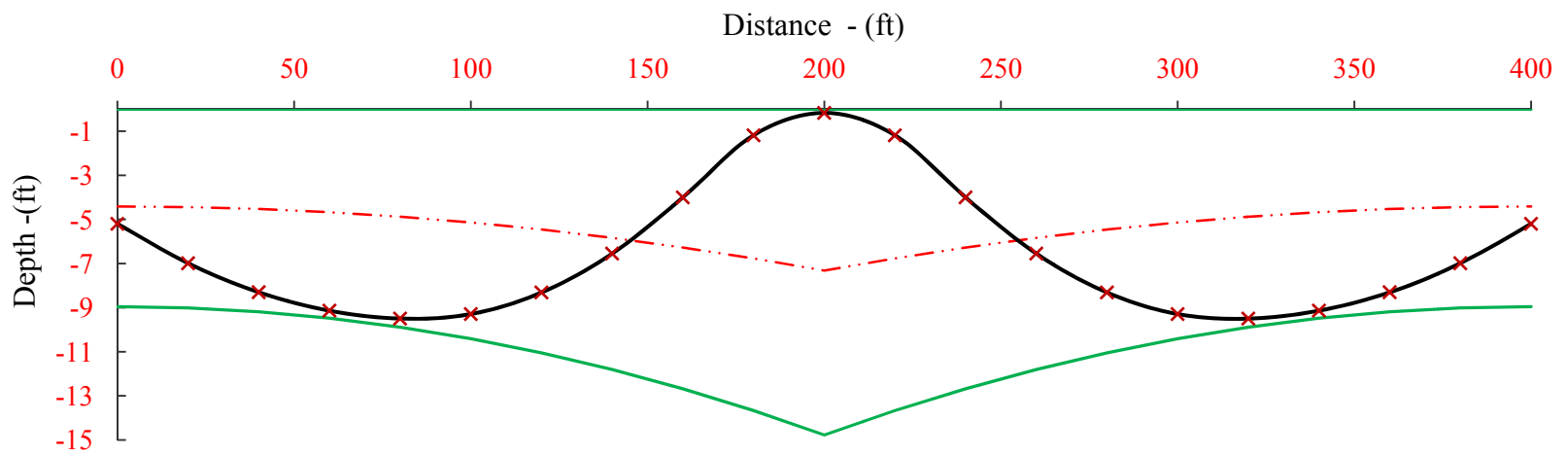
Figure 6.3 Plot of Optimum Tendon Profile (2-Span of Total Length (400 ft), λ = 1 and AASHTO HS-20 loads)

(b) Case 2: Both Long and Short Tendons ($\lambda > 1$)

The previous example is solved again for $\lambda > 1$ using three values of h_1: 8.95 ft, 10.95 ft and 11.95 ft. The optimum design of this example is achieved at depth $h_1 = 8.95$ ft and depth $h_2 = 13.07$ ft, with depth ratio of $h_2/h_1 = 1.46$. The change of the total cost of material with the depth ratio h_2/h_1 is plotted for each h_1 in Figure 6.4. The total cost of material is nondimensionalized as before. Figure 6.4 shows that the cost parameter for material gradually decreases with increases in the depth ratio h_2/h_1 up to about $h_2/h_1 = 1.46$, thereafter the total cost gradually increases as h_2/h_1 increases. The plots in Figure 6.4 also show that for these values of h_1, the optimum h_2/h_1 ratio appears to lie in the close proximity of 1.46. As there is only a small reduction in the material cost by about 3%, it is apparent that for a reasonable non-optimal value of h_1, an economical design can be obtained with an optimum value of λ for the optimum h_2/h_1.

A comparison of Figures 6.2 and 6.4 shows that for a given h_1, the optimum ratio h_2/h_1 is lesser with $\lambda > 1.0$ than with $\lambda = 1.0$. The calculated minimum total material cost for the bridge with $\lambda = 1.0$ is \$ 265,188 at optimum value of $h_1 = 8.95$ ft and $h_2 = 14.77$ ft with depth ratio $h_2/h_1 = 1.65$. The total material cost for the same bridge reduces to \$ 227,123 by using both long and short tendons ($\lambda = 14.0$) for $h_1 = 8.95$ ft and $h_2 = 13.07$ ft ($h_2/h_1 = 1. 46$). This reduction of about 15% achieved due entirely to the use of both long and short tendons.

At optimum value of $h_1 = 8.95$ ft and $h_2 = 13.07$ ft, with depth ratio of $h_2/h_1 = 1. 46$, the cost of prestressing steel versus λ is plotted in Figure 6.5, by nondimensionalizing

the steel cost as C_{psi}/C_{ps1}, where C_{psi} is the cost of prestressing steel at $\lambda = \lambda_i$ (the ith step of iteration for λ) and C_{ps1} is the steel cost at $\lambda=1.0$ to show the influence of λ on cost. It is found that the cost of prestressing steel rapidly decreases as λ increases up to about $\lambda = 9.0$, after which the cost slowly decreases with increases in λ till it becomes flat beyond $\lambda > 13$. The required prestressing force at the jacking end versus λ is plotted in Figure 6.6. The force of prestressing steel is nondimensionalized as P_{Ji}/P_{J1}, where P_{Ji} is the prestressing force at $\lambda = \lambda_i$ (the ith step of iteration for λ) and P_{J1} is the force at $\lambda = 1.0$. The plot is noticed to have a similar trend as expected, with force parameter decreasing with increasing λ until it becomes flat beyond $\lambda = 14.0$.

From Figures 6.5 and 6.6, it is clear that the prestressing force P_J and the cost of prestressing steel decrease slowly with value of $\lambda > 9.0$. As a higher value of λ would increase the cost of anchorage, practically it is preferred to keep λ at a reasonable value. Thus from a practical viewpoint, an economical design can be attained with $\lambda \geq 9.0$, in this case.

From the results presented, it can be concluded that for two-span continuous girders, the use of all full length tendons for prestressing is not an economical arrangement.

6.2.2 Variation in Total Bridge Length

In order to study the effect of total length of bridge on the optimum depth ratio h_2/h_1 and optimum depth at interior support h_2, several designs were performed with different total length of bridge L from 250 ft to 400 ft. The optimum value of h_2 and h_2/h_1 versus the bridge total length L subjected to AASHTO HS-20 loading is plotted in Figure

6.7. It is observed that the optimum depth ratio h_2/h_1 and h_2 increase almost linearly as L increases. The required prestressing force at the jacking end P_J versus λ is plotted in Figures 6.8, which shows that the required prestressing force P_J decreases slowly with higher value of $\lambda \geq 9.0$ for all spans. It can be concluded that, for bridge, a low-cost design can be attained for the chosen section with $\lambda \geq 9.0$ for any value of L.

6.2.3 Effect of Unit Costs on Optimum Solution

To study the effect of unit cost on the optimum values of λ, h_2/h_1 and depth at interior support h_2 for two-span continuous bridge girder, several designs were performed for a bridge of total length $L = 300$ ft with different cost ratio CR from 1.37 to 2.05, in which CR is the ratio of the unit cost of concrete per volume to the unit cost of prestressing steel per weight.

The change in the dimensions h_2 and depth ratio h_2/h_1 resulting from change in the cost ratio CR are shown in Figure 6.9. Although the optimum values of h_2 and h_2/h_1 change with CR, as seen from Figure 6.9, the changes can be considered as small. The variation of prestressing force at the jacking end P_J with λ is shown in Figure 6.10 for different CR shows that the required prestressing force P_J decreases slowly with higher value of $\lambda \geq 9.0$. Hence, it can be concluded that regardless of the assumed value of CR, from a practical viewpoint, a low-cost solution can be attained with $\lambda \geq 9.0$ for two-span symmetrical single box girder.
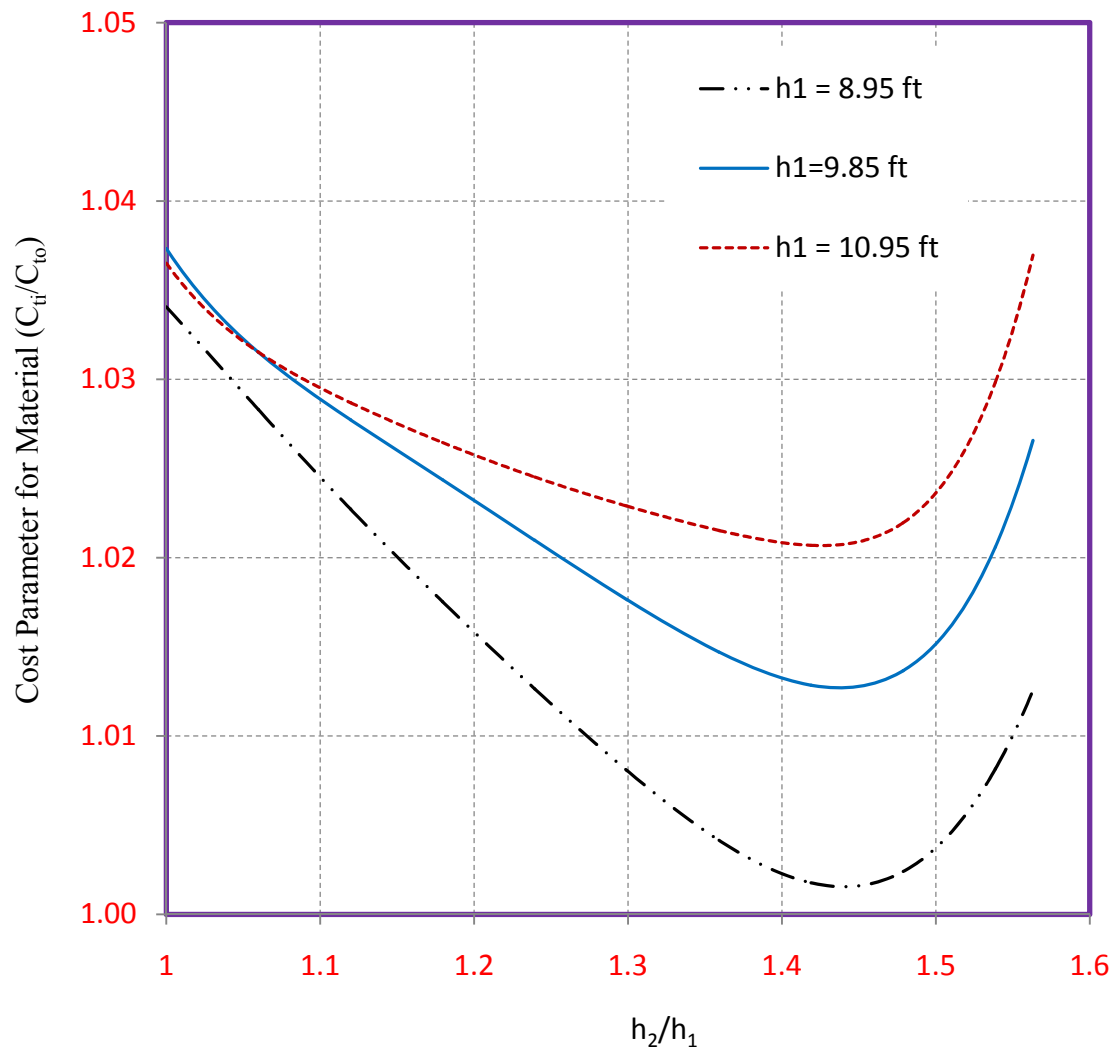
Figure 6.4 Plot of Total Cost versus h_2/h_1 (2-Span of Total Length (400 ft) and AASHTO HS-20 loads)
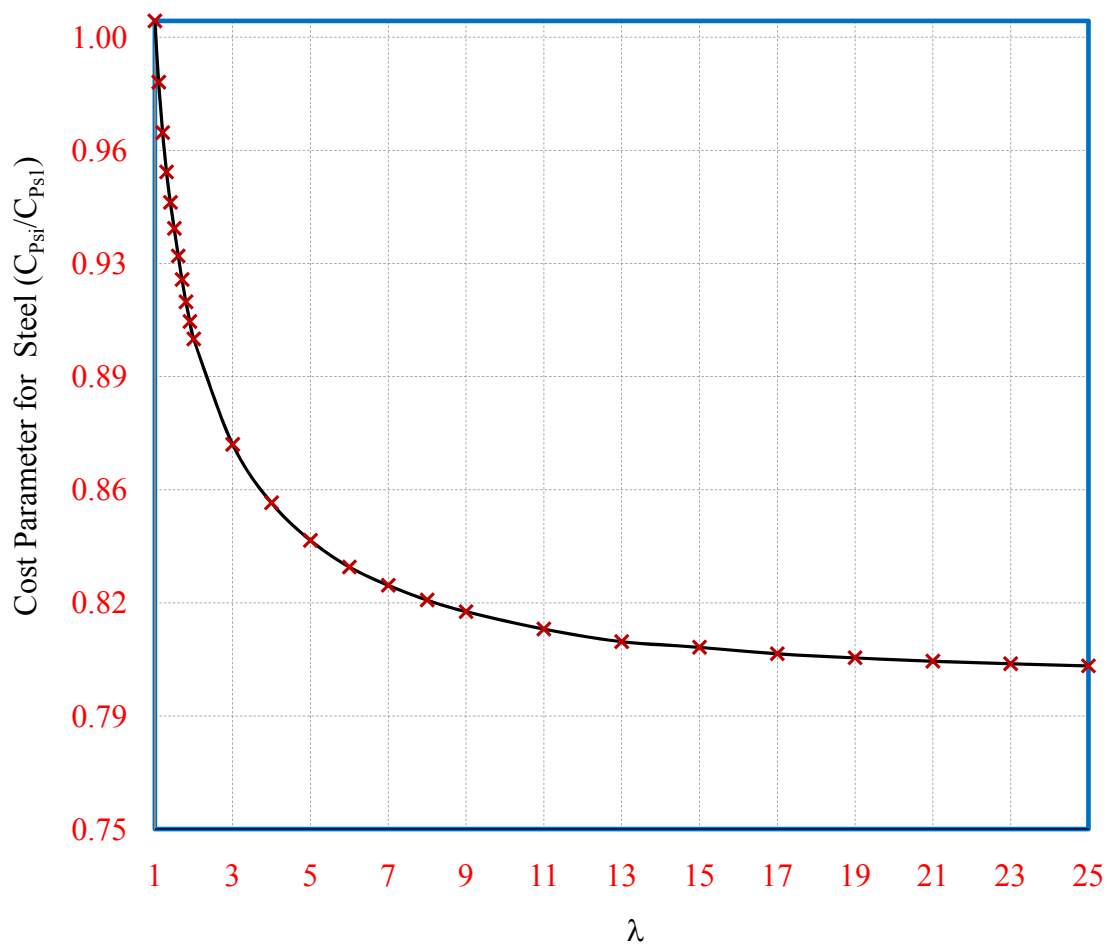
Figure 6.5 Plot of Steel Cost versus λ (2-Span of Total Length (400 ft) and AASHTO HS-20 loads)
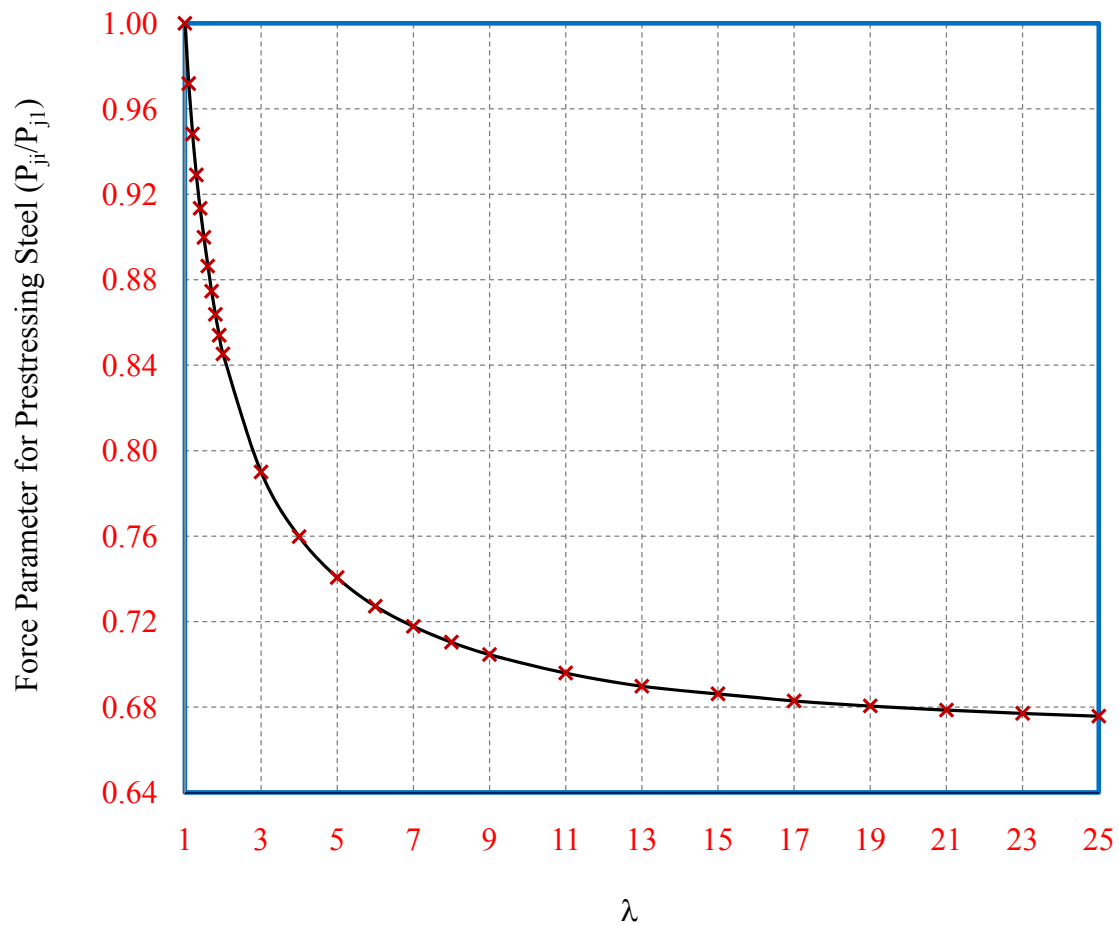
Figure 6.6 Plot of Required Prestressing versus λ (2-Span of Total Length (400 ft) ft and AASHTO HS-20 loads)
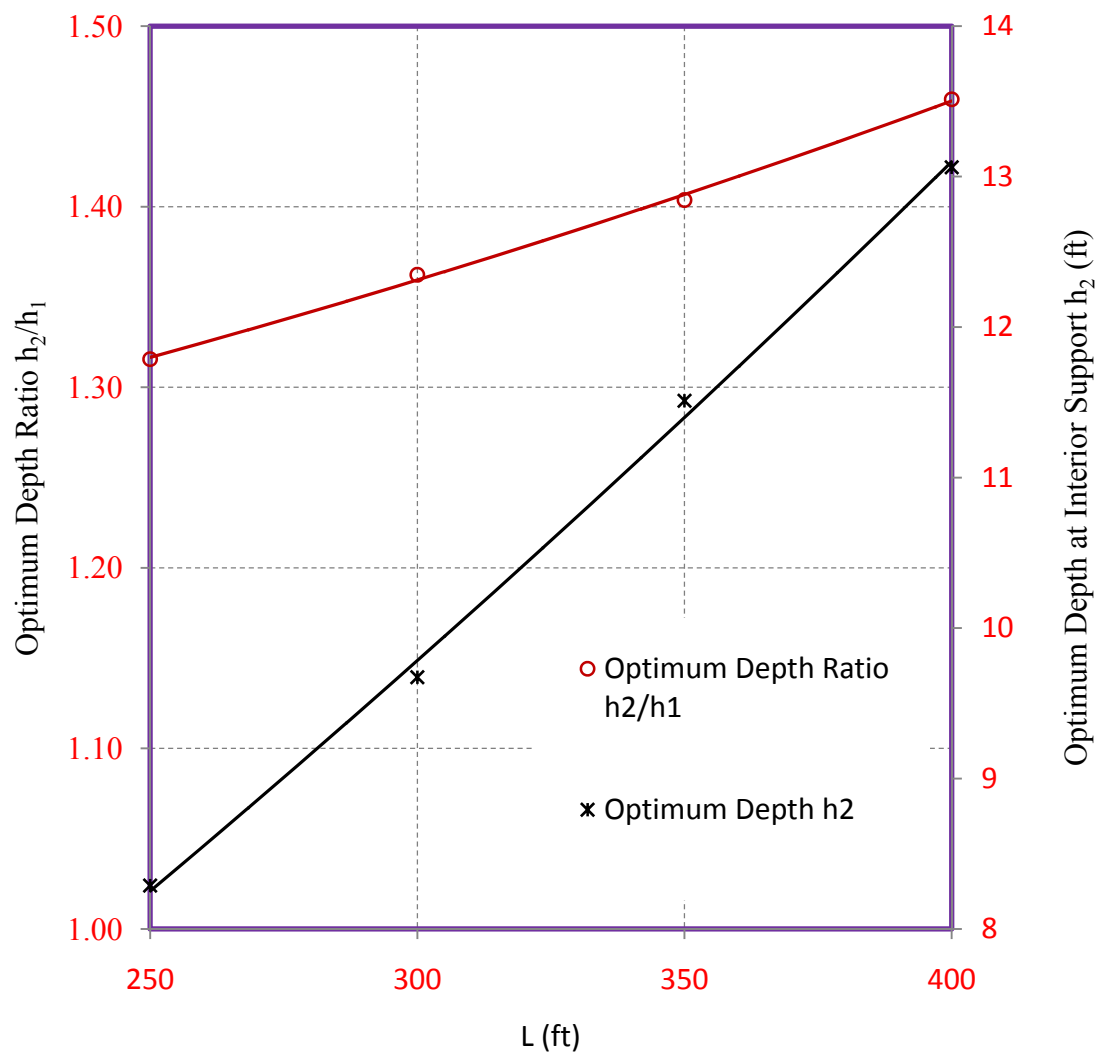
Figure 6.7 Plot of Optimum h_2 and h_2/h_1 versus Total Length of Bridge Girder (2-Span AASHTO HS-20 loads)
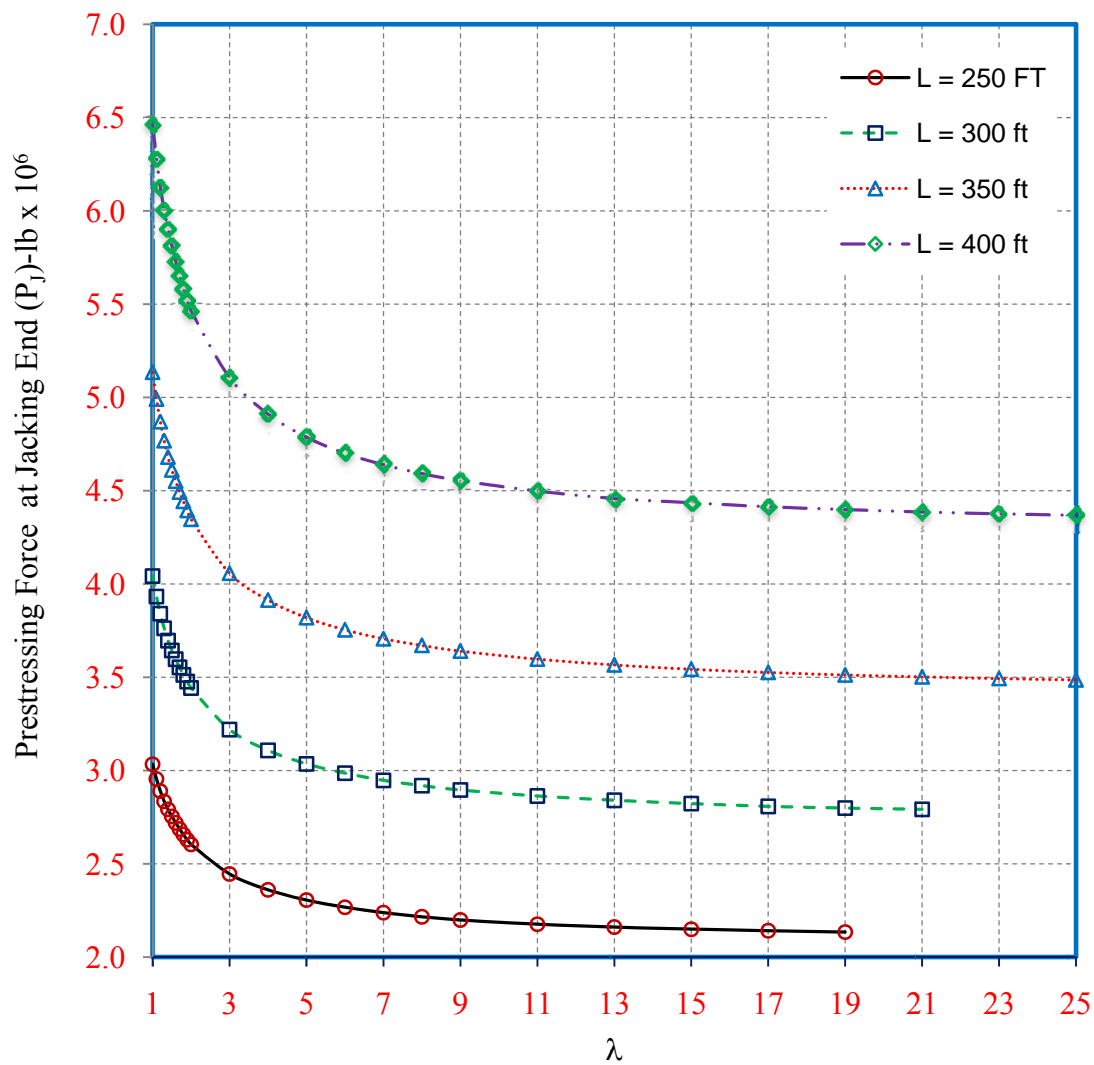
Figure 6.8 Plot of Required Prestressing P_J versus λ (2-Span and AASHTO HS-20 loads, L = 250 ft to 400 ft)
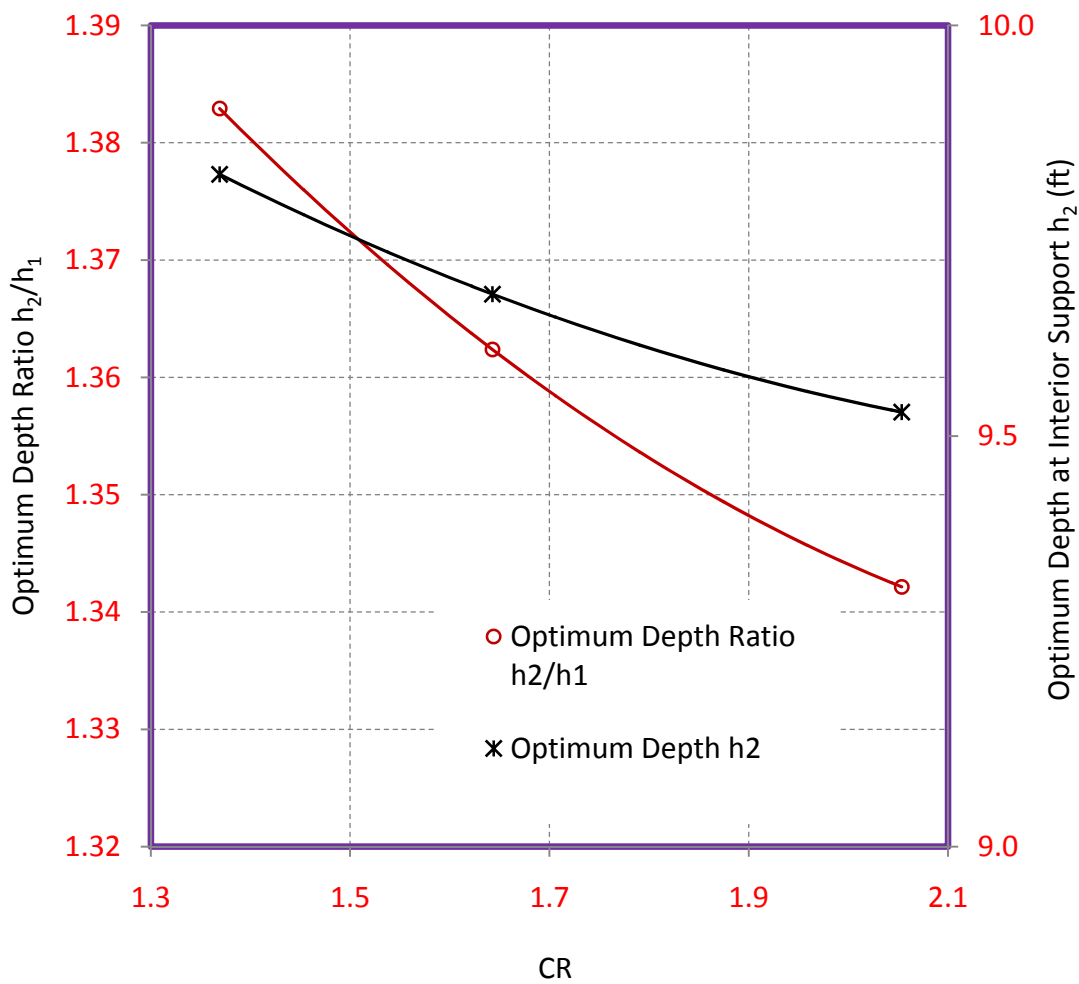
Figure 6.9 Optimum Value of Depth Ratio h_2/h_1 and Depth h_2 versus Ratio of Unit Cost CR (C_c/C_p) (2-Span of Total Length (300 ft) and AASHTO HS-20 loads)

Figure 6.10 Plot of Required Prestressing P_J versus λ for Different CR(C_c/C_p) (2-Span of Total Length (300 ft) and AASHTO HS-20 loads)

6.3 Three-Span Continuous Girder

6.3.1 Example

All design data including the girder cross-section are same as used in the two-span bridge girder except that the total length of the bridge now equals 500 *ft* (152 *m*).

The optimum design of this example is achieved at values of $\varepsilon = 1.34$, $h_1 = 7.1$ *ft*, $h_2 = 17.27$ *ft* and $h_3 = 4.59$ *ft*, with depth ratio of $h_2/h_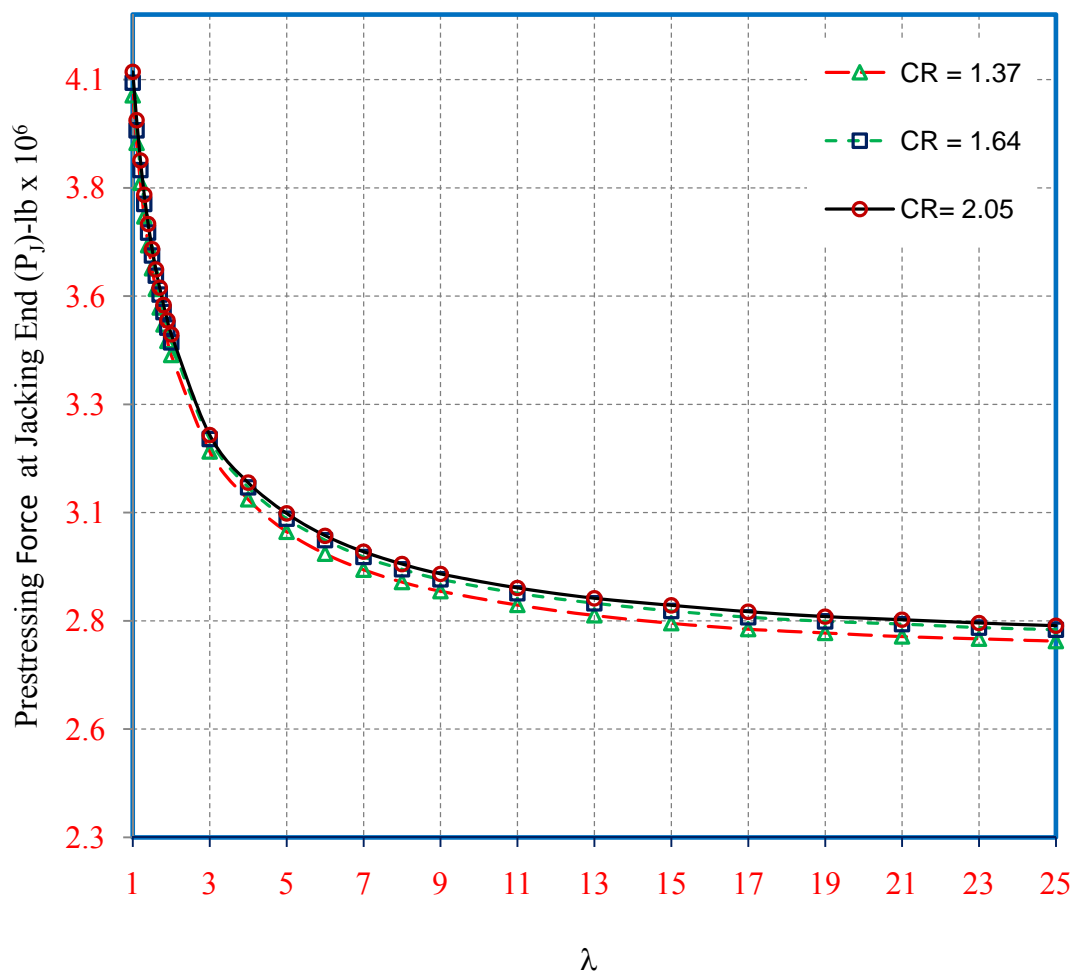1 = 2.43$ and $h_1/h_3 = 1.55$. The optimum tendon profile for is plotted in Figure 6.17. It has been observed that the optimum tendon profile is obtained when the values of design variables are at their upper limits, expect that at an interior span the design variables are below the upper limits.

The plot of the total material cost versus span ratio ε is shown in Figure 6.11, by nondimensionalizing the total material cost as C_{ti}/C_{t1}, where C_{ti} is the cost at $\varepsilon = \varepsilon_i$ (the ith step of iteration for ε) and C_{t1} is the cost at $\varepsilon = 1.0$ (equal spans). Figure 6.11 shows that the cost decreases rapidly with increase in ε up to about $\varepsilon = 1.34$, but thereafter the cost increases again with increase in ε, showing the influence of this important parameter on the cost.

The total cost of material versus the depth ratio h_2/h_1 is plotted in Figure 6.12, for three cases of h_1, $h_1 = 7.1$ *ft*, 9.1 *ft* and $h_1 = 11.1$ *ft*. The cost is nondimensionalized C_{ti}/C_{to}, where C_{ti} is the total cost of material at $h_2/h_1 = (h_2)_i/h_1$ (the ith step of iteration $(h_2)_i/h_1$) and C_{to} is the cost at the optimum values of $h_1 = 7.1$ *ft* with depth ratio $h_2/h_1 = 2.43$. It can seen that the total cost of material decreases initially with increases in the depth ratio h_2/h_1 up to a certain value and thereafter the total cost increases with further increases in

h_2/h_1. The minimum total cost of the bridge girder is achieved at a value of $h_1 = 7.1\ ft$ with depth ratio $h_2/h_1 = 2.43$. The change of the total cost of material versus the depth ratio h_1/h_3 is plotted in Figure 6.13, for the three values of h_1, by nondimensionalizing the total cost as C_{ti}/C_{to}, where C_{ti} is the cost at $h_1/h_3 = h_1/(h_3)_i$ (the ith step of iteration $h_1/(h_3)_i$) and C_{to} is the cost at the optimum values of h_1, h_2 and h_3. Both Figure 6.12 and Figure 6.13 show similar trend, revealing that h_2/h_1 and h_1/h_3 ratios change with different chosen value of h_1, unlike two-span bridge girders, when the ratio h_2/h_1 varied only marginally with chosen h_1. The plots also indicate that use of higher value of h_1 (higher than the optimum h_1) will lead to higher total cost.

For the optimum value of $\varepsilon = 1.34$, $h_1 = 7.1\ ft$, $h_2 = 17.27\ ft$ and $h_3 = 4.59\ ft$ (h_2/h_1 $=2.43$ and $h_1/h_3 = 1.55$), the change of prestressing steel cost with λ is plotted in Figure 6.14, to show the influence of λ on cost. The steel cost is nondimensionalized as C_{psi} $/C_{ps1}$, where C_{psi} is the cost of prestressing steel at $\lambda = \lambda_i$ (the ith step of iteration for λ) and C_{ps1} is the cost of prestressing steel at $\lambda = 1.0$. The plot has shown that the cost of prestressing steel decreases rapidly as λ increases up to about $\lambda = 9.0$, but thereafter the decrease is almost negligible as the C_{ps}-λ plot becomes essentially flat. The plot of the change of required prestressing force at the jacking end P_J versus λ is shown in Figure 6.15. The force of prestressing steel is nondimensionalized as before. The plot shows a similar trend as the steel cost C_{psi} $/C_{ps1}$ decreases.

From Figures 6.14 and 6.15, it can be noticed that while the force parameter of steel decreases slowly with value of $\lambda > 9.0$, the cost parameter of prestressing steel C_{psi}/C_{ps1} becomes essentially flat with higher λ. Thus, an economical design can be

attained with $\lambda \geq 9.0$, in this case. .

The variation of steel cost with span ratio ε is plotted in Figure 6.16, at the optimum values of h_1, h_2 and h_3. The steel cost is nondimensionalied as C_{psi}/C_{ps1}, where C_{psi} is the steel cost at $\varepsilon = \varepsilon_i$ (the ith step of iteration for ε) and C_{ps1} is the steel cost at ε =1.0. It can be observed that the minimum steel cost is attained at a value of span ratio ε = 1.34. The steel cost increases rapidly with $\varepsilon > 1.35$ and $\varepsilon < 1.30$.

Thus, it can be concluded that for three-span continuous structures of total length equal to 500 ft subjected to AASHTO HS-20 Bridge loading, the optimum total material cost can be achieved when ε lies within 1.3 to 1.4, and a combination of short and long tendons with $\lambda \geq 9.0$ is used. Figures 6.11 and 6.16 clearly highlight the significance of ε on the cost, signaling that the value of ε must be carefully chosen to seek an economical design.

6.3.2 Variation in Total Bridge Length

In order to study the influence of total length of bridge on the optimum span ratio, the optimum depth ratios and the optimum depth at interior support, several designs were made with different total length of bridge L from 300 *ft* to 600 *ft*. Optimum depth at interior support h_2 and depth ratios h_2/h_1 and h_2/h_3 versus the total length of bridge for HS-20 are plotted in Figures 6.18 and 6.19. Figures 6.20 and 6.21 show the change of total material cost versus ε of different bridge length L, by nondimensionalizing total material cost as before. It is clear that for a symmetrical three-span bridge girder of a given total length, the optimum value of the total cost of material is attained when ε lies

within 1.30 to 1.40. The required prestressing force at the jacking end P_J versus λ is plotted in Figure 6.22 for different total length of bridge L. It can be seen that the required prestressing force P_J declines slowly with higher value of $\lambda \geq 9.0$. For all spans, it can be concluded that, a low-cost design can be attained with $\lambda \geq 9.0$, a value that is seen also to be valid for two-span continuous girders.

6.3.3 Effect of Unit Costs on Optimum Solution

To study the effect of unit cost on the optimum values of ε, λ, h_2/h_1, h_2/h_3 and depth at interior support h_2 for three-span continuous bridge girder, several designs were performed for a bridge of total length L = 500 ft with different cost ratio CR from 1.37 to 2.05, in which CR is the ratio of the unit cost of concrete per volume to the unit cost of prestressing steel per weight.

The variation in the dimensions h_2 and depth ratios h_2/h_1 and h_2/h_3 resulting from change in the cost ratio CR are shown in Figures 6.23 and 6.24. The plots show that h_2/h_1, h_2/h_3 and h_2 change with different value of CR, unlike two-span bridge girders, where the ratio h_2/h_1 and h_2 varied marginally with CR (Figure 6.9). Figure 6.25 shows the change of total material cost versus span ratio ε for different values of CR, by nondimensionalizing the total cost. As seen from Figure 6.25, the optimum value of ε is range-bound within 1.30 to 1.35, regardless of the assumed value of CR. The variation of prestressing force at the jacking end P_J with λ is shown in Figure 6.26 for different values of CR. The plots in Figure 6.26 show that the required prestressing force P_J is lower with lower CR value and decreases slowly with higher value of $\lambda \geq 9.0$. The variation of prestressing force P_J with λ shows similar trend as noted for the total cost (Figure 6.25).
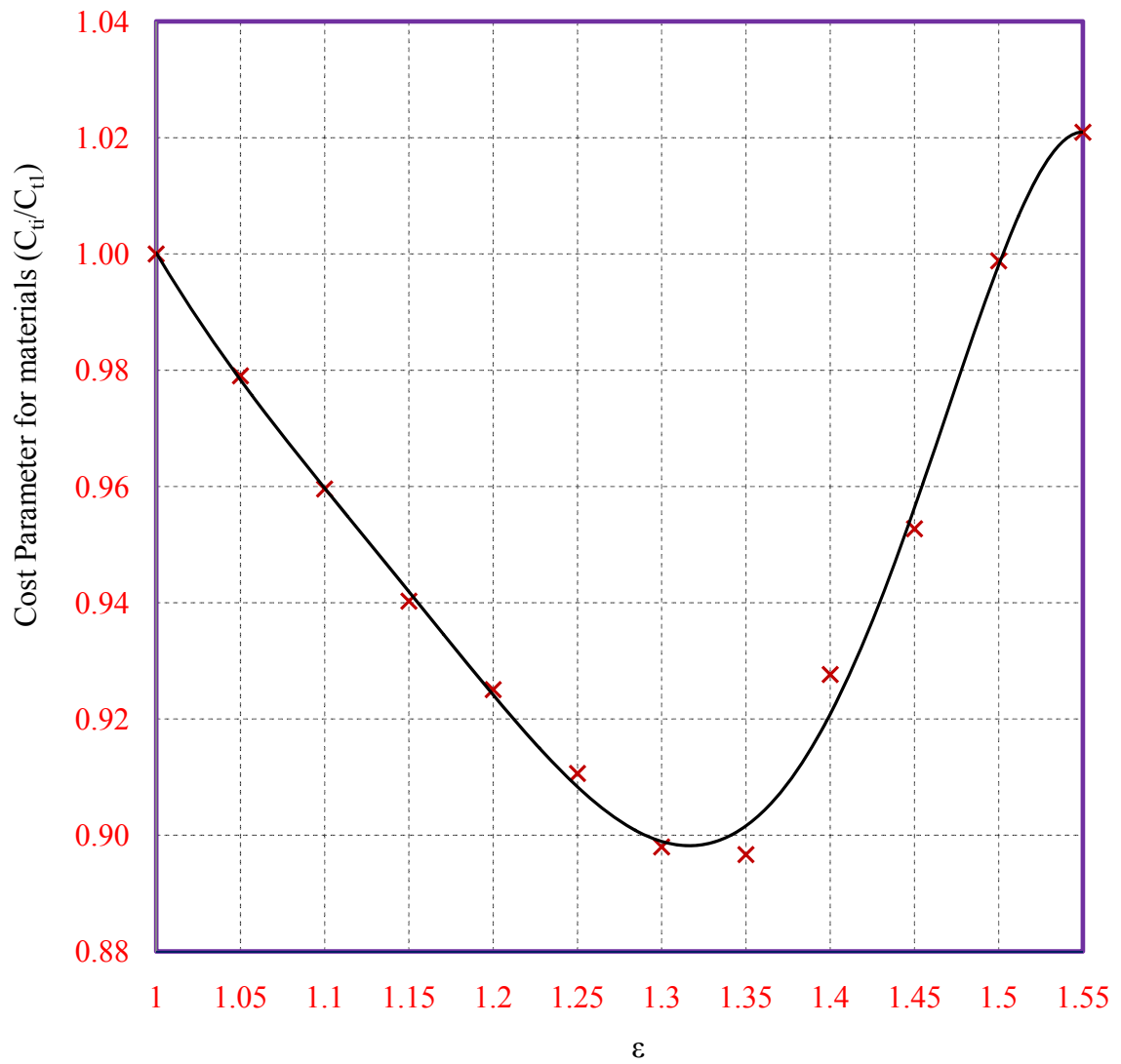
Figure 6.11 Plot of Total Cost versus ε (3-Span of Total Length (500 ft) and AASHTO HS-20 loads)
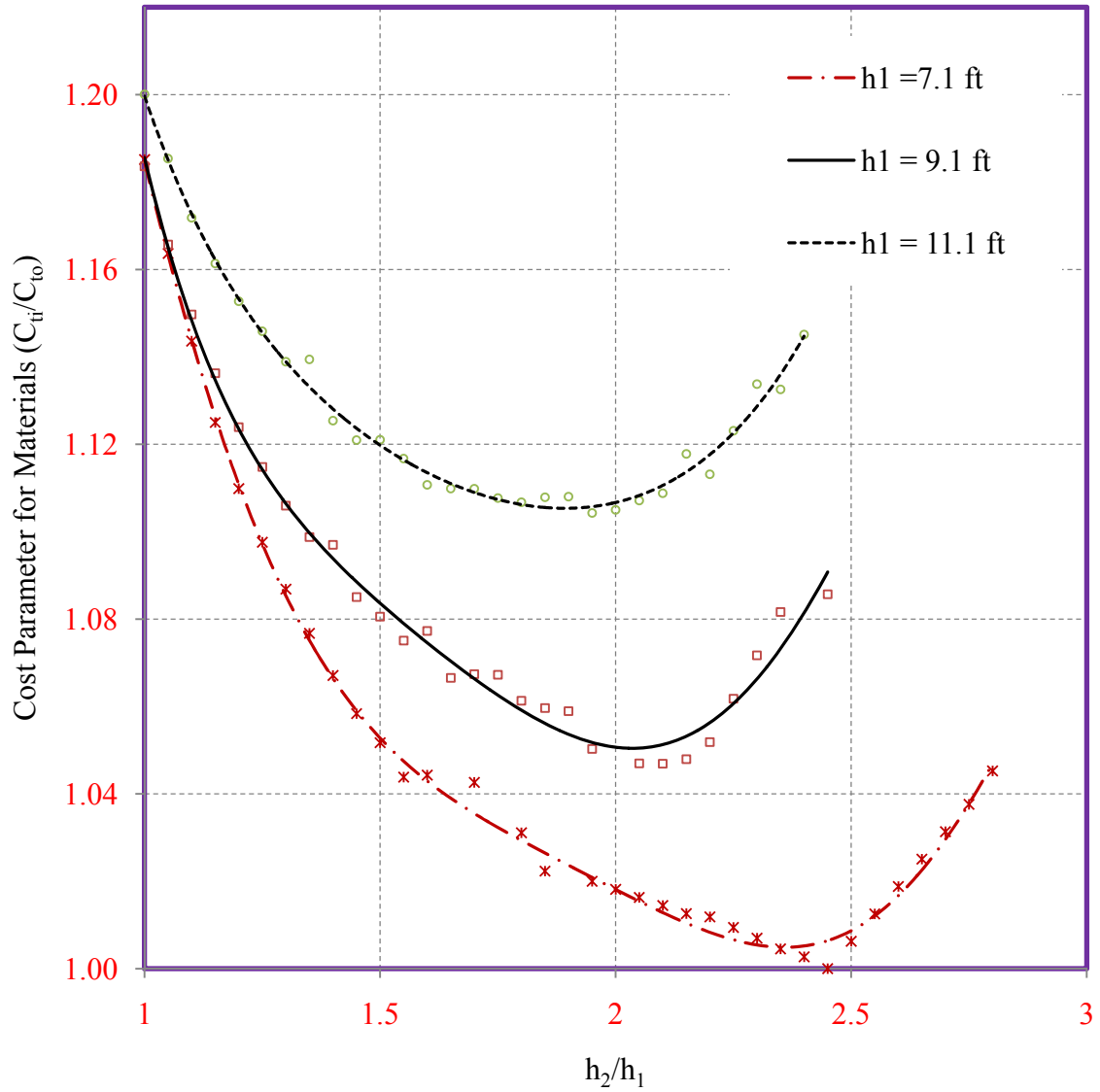
Figure 6.12 Plot of Total Cost versus h_2/h_1 (3-Span of Total Length (500 ft) and AASHTO HS-20 loads)
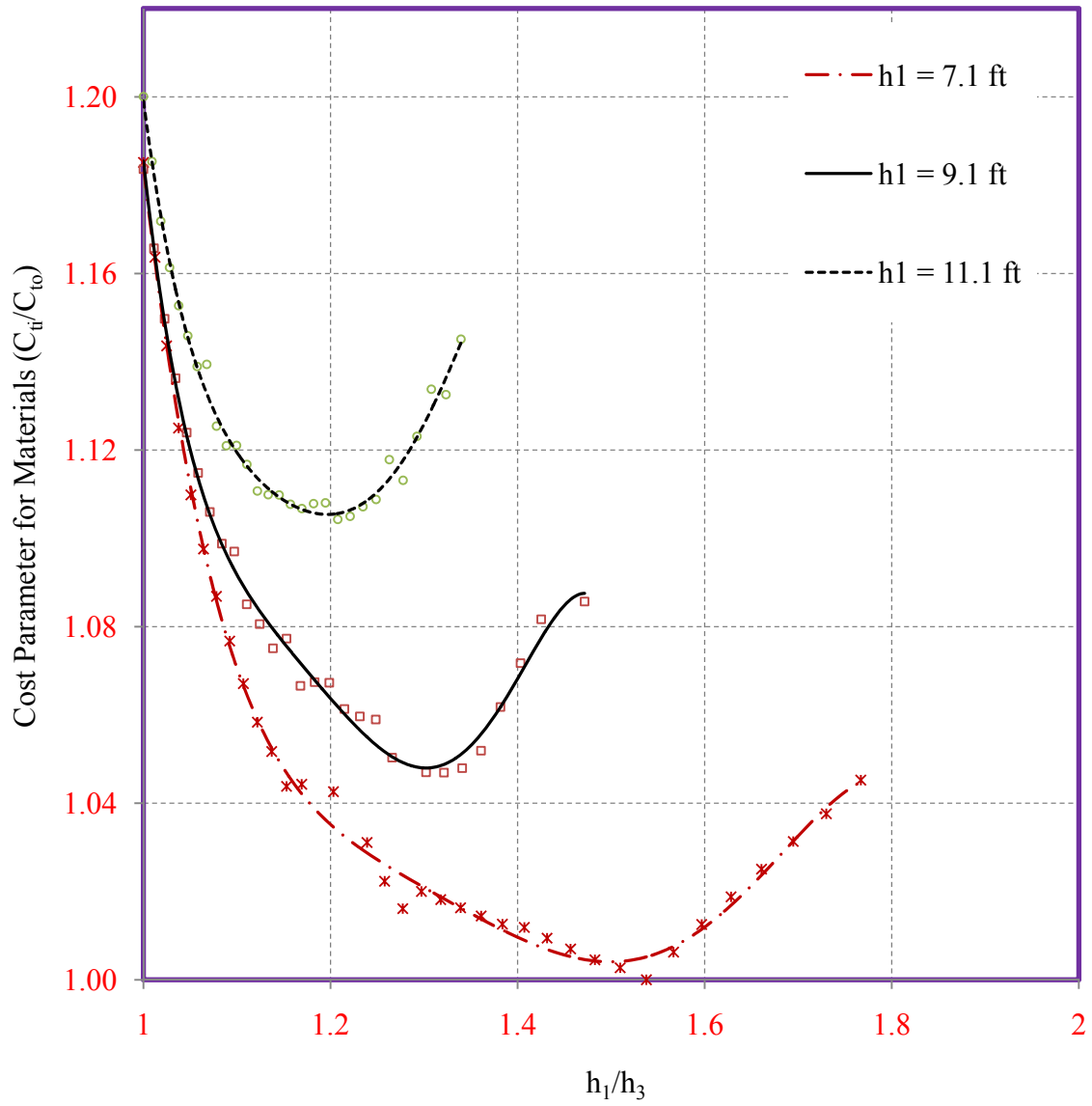
Figure 6.13 Plot of Total Cost versus h_1/h_3 (3-Span of Total Length (500 ft) and AASHTO HS-20 loads)
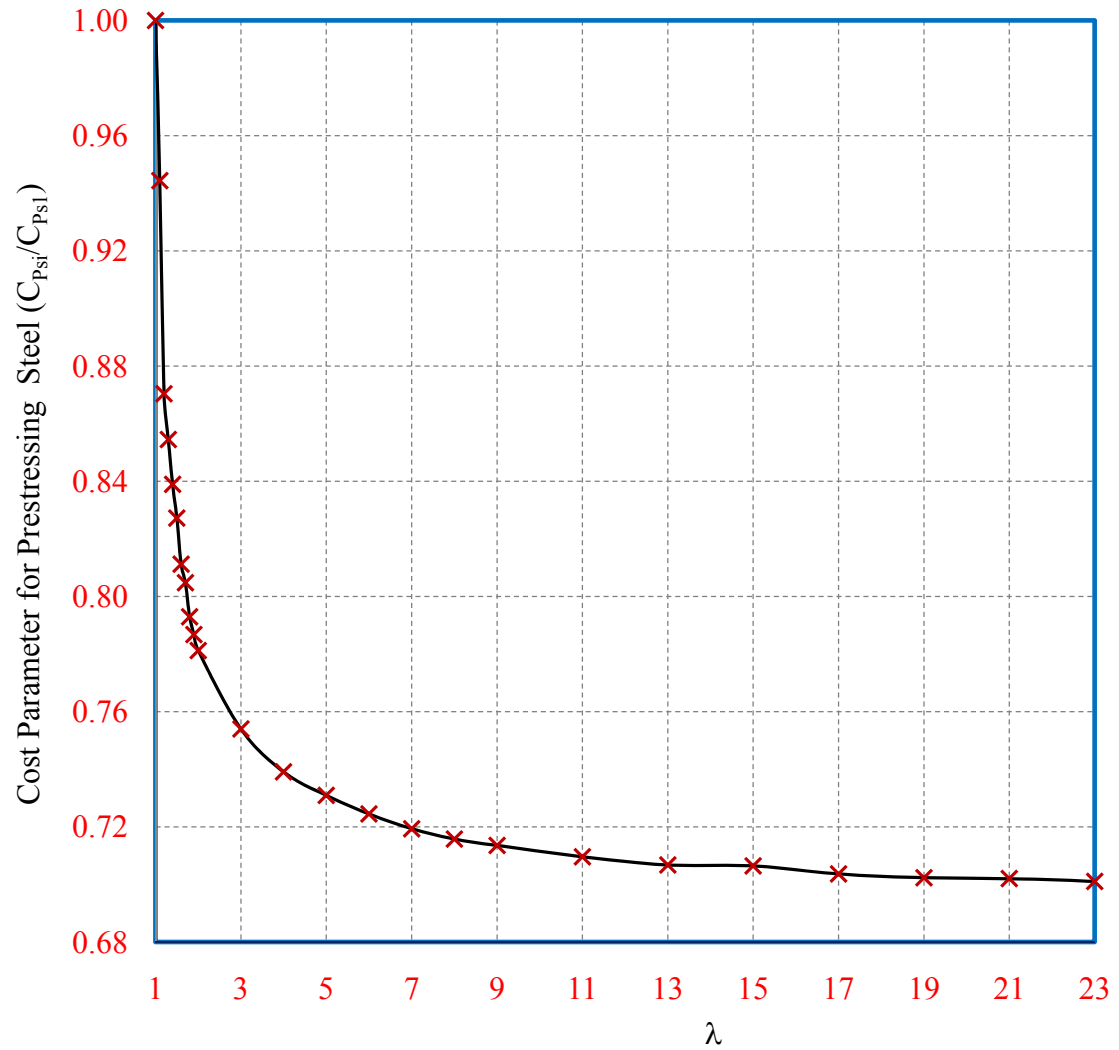
Figure 6.14 Plot of Steel Cost versus λ (3-Span of Total Length (500 ft) and AASHTO HS-20 loads)
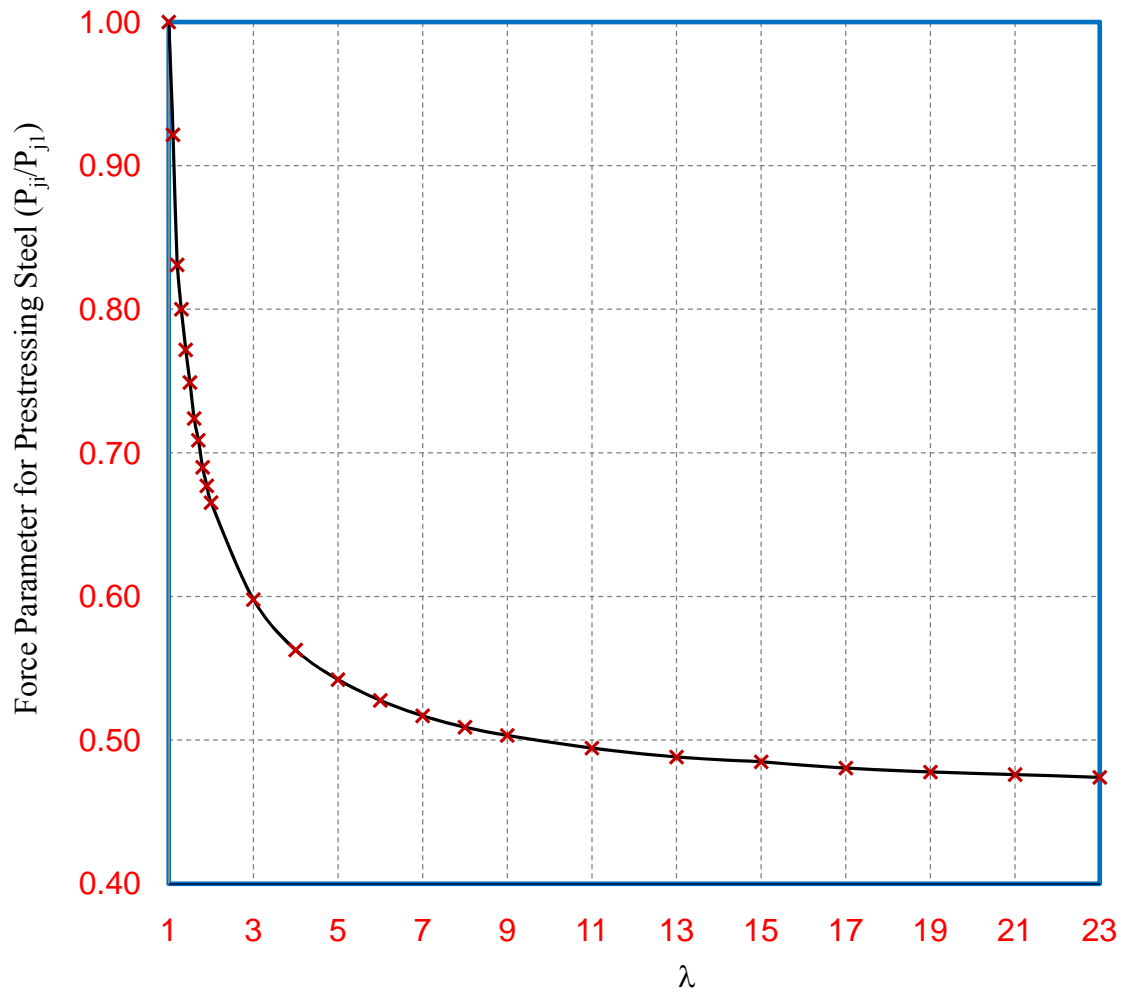
Figure 6.15 Plot of Required Prestressing versus λ (3-Span of Total Length (500 ft) and AASHTO HS-20 loads)
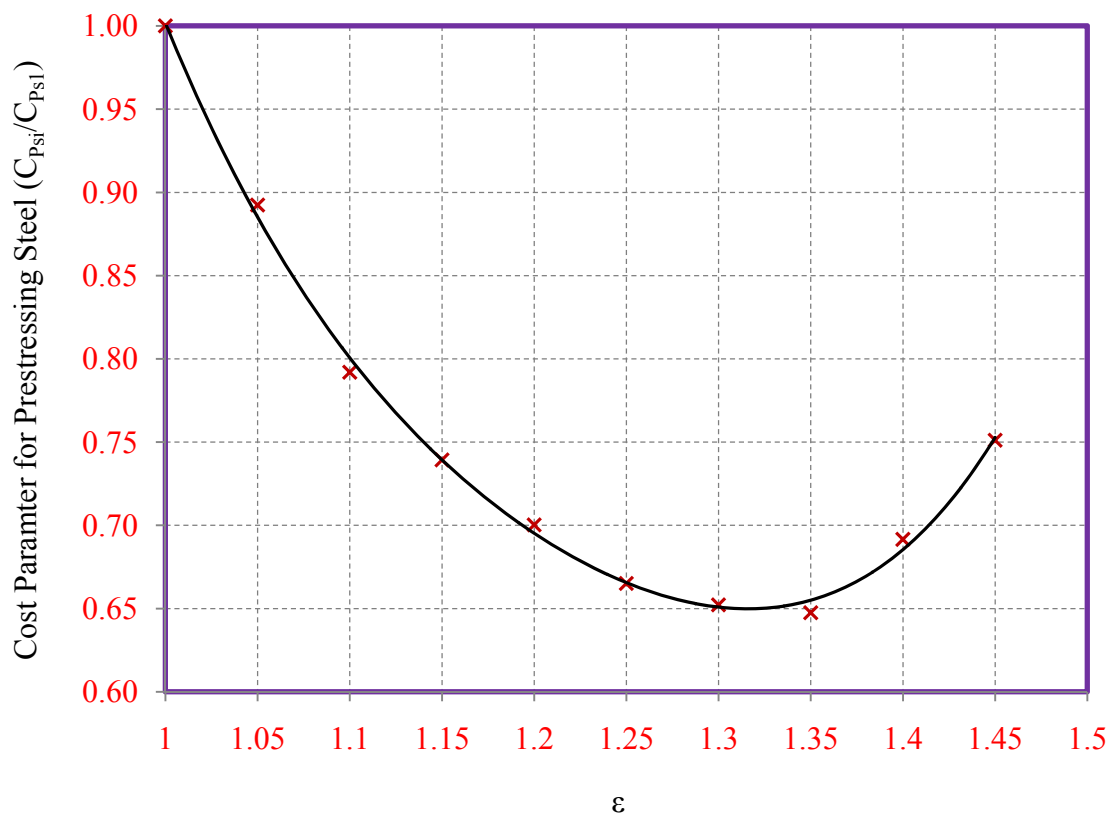
Figure 6.16 Plot of Steel Cost versus ε (3-Span of Total Length (500 ft) and AASHTO HS-20 loads)
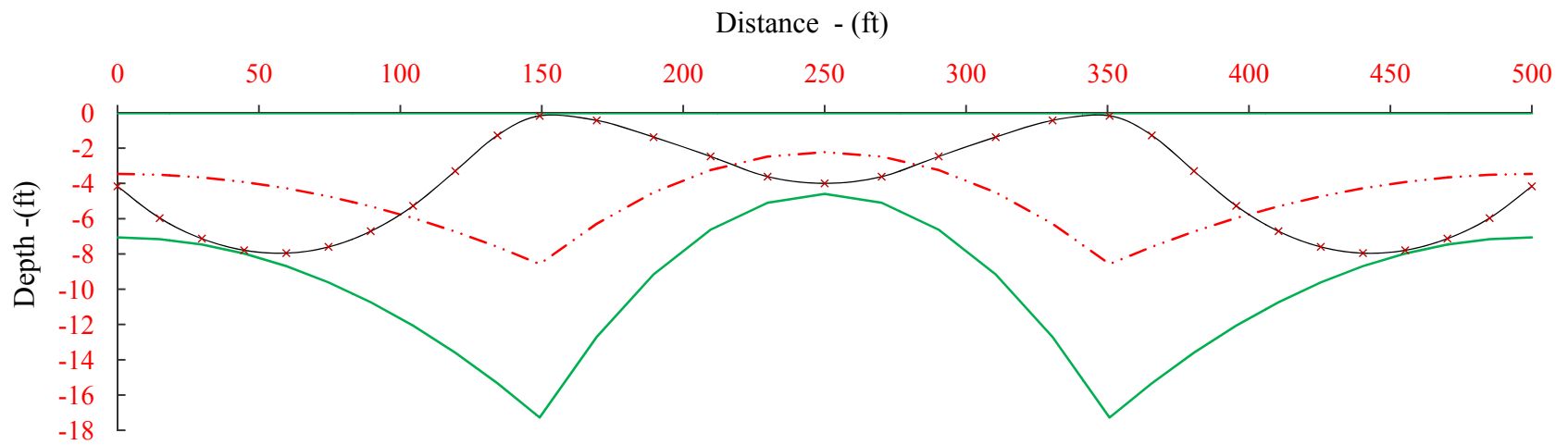
Figure 6.17 Plot of Optimum Tendon Profile (3-Span of Total Length (500 ft) and AASHTO HS-20 loads)
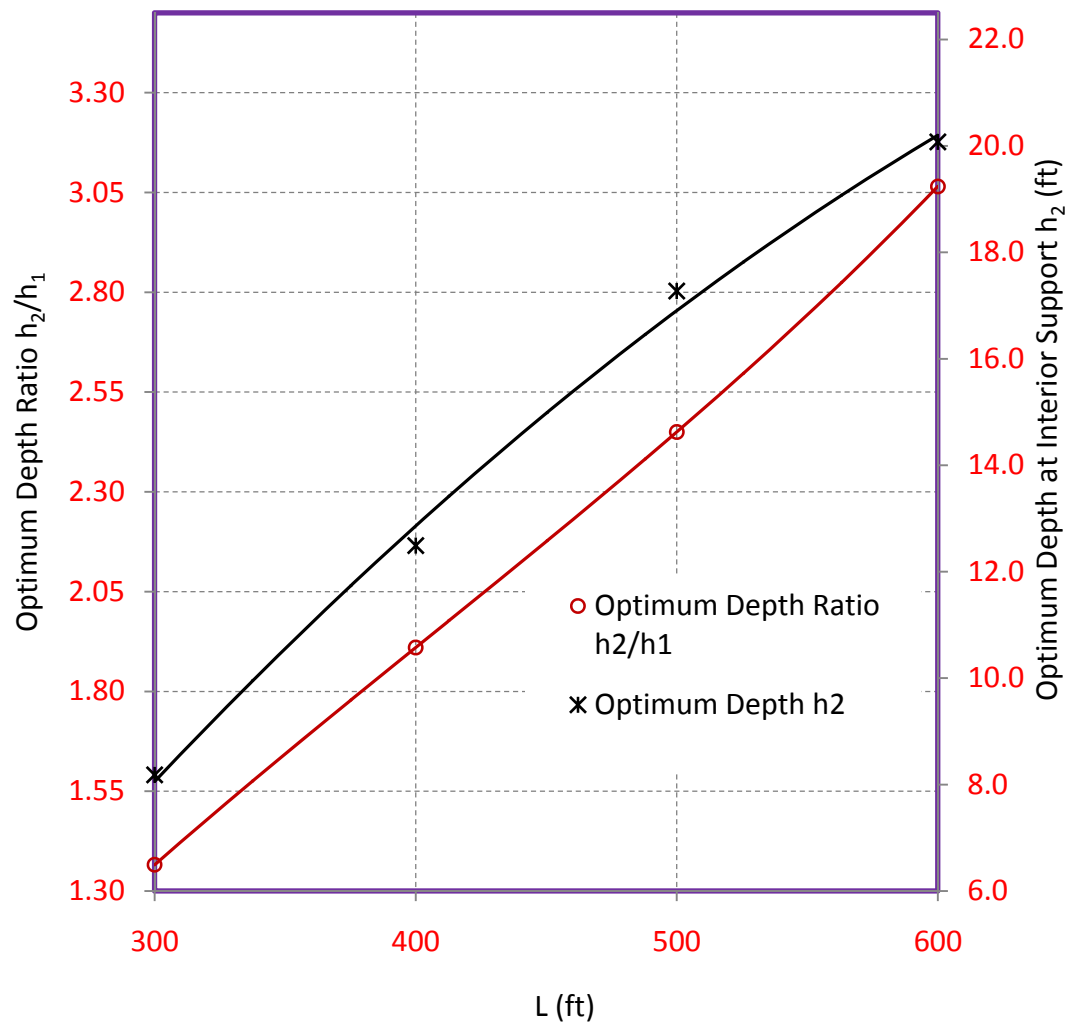
Figure 6.18 Plot of Optimum Value of Depth Ratio h_2/h_1 and Depth h_2 versus Total Length of Bridge Girder (3-Span AASHTO HS-20 loads)
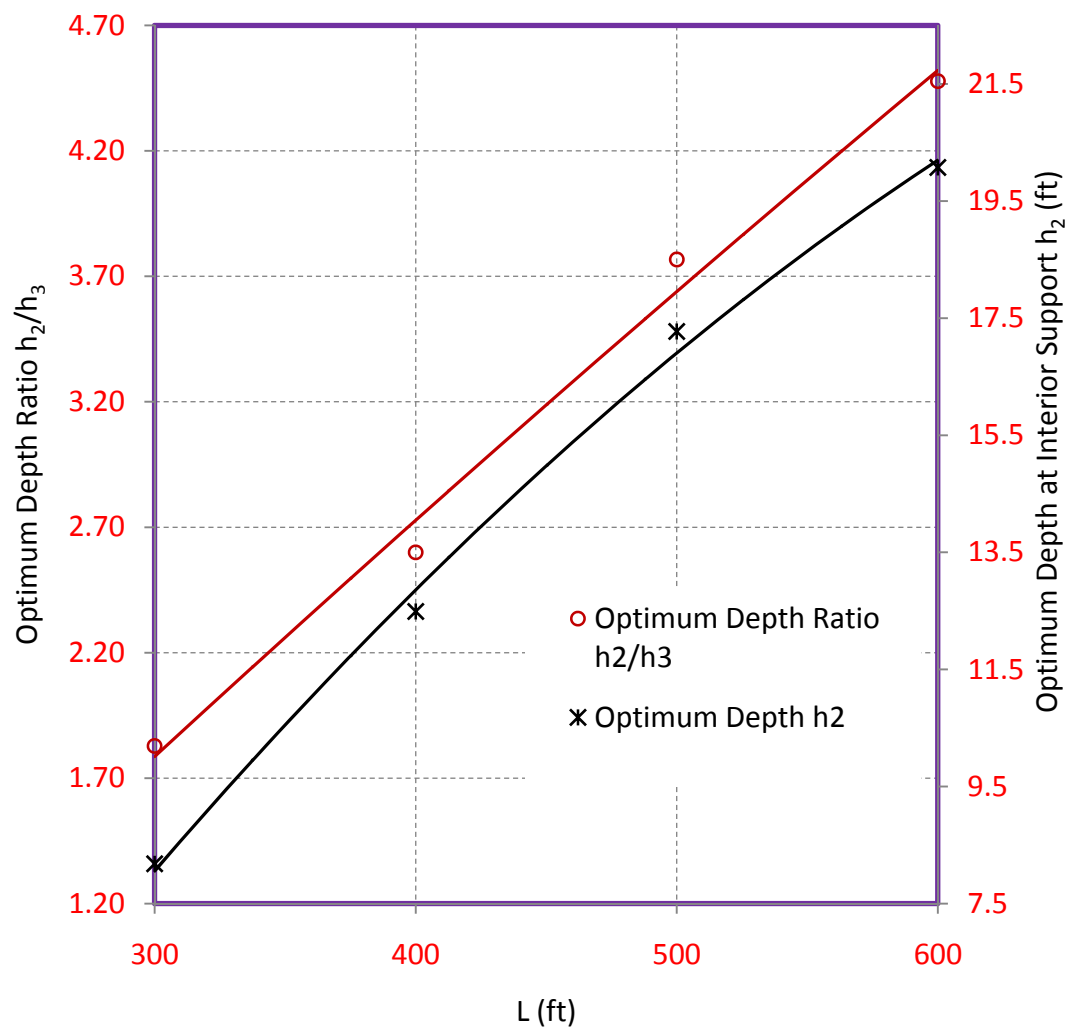
Figure 6.19 Plot of Optimum Value of Depth Ratio h_2/h_3 and Depth h_2 versus Total Length of Bridge Girder (3-Span AASHTO HS-20 loads)
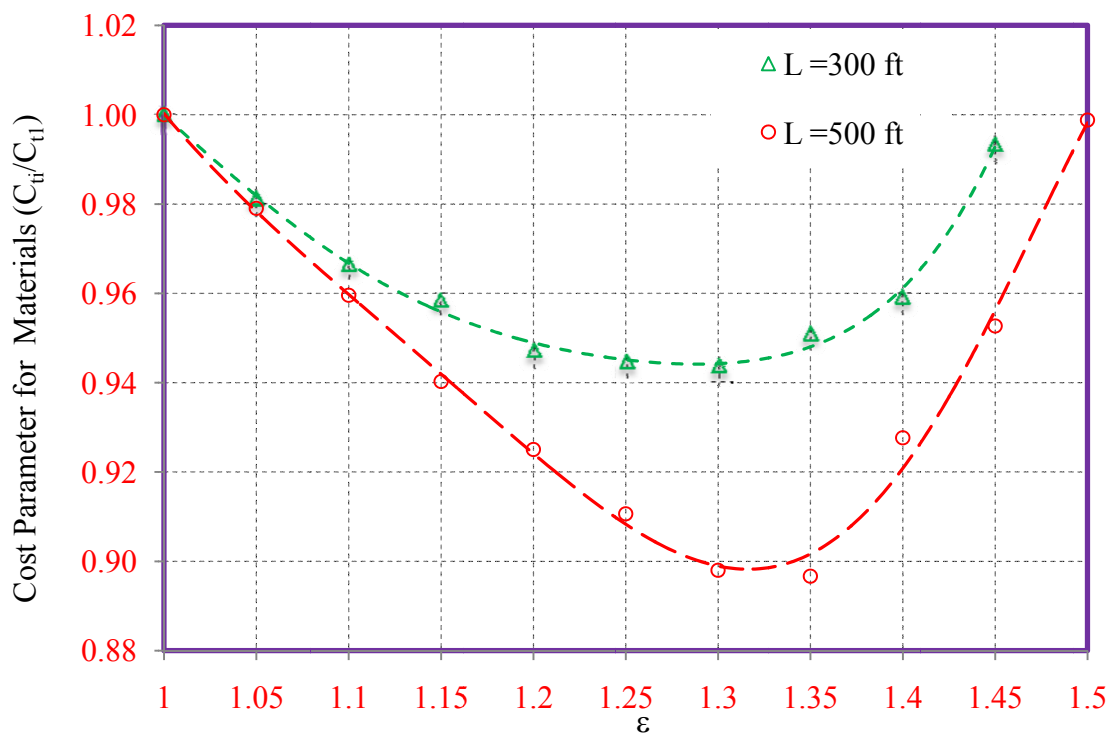
Figure 6.20 Plot of Total Cost versus ε (3-Span, AASHTO HS-20 loads, L= 300 ft and 500 ft)
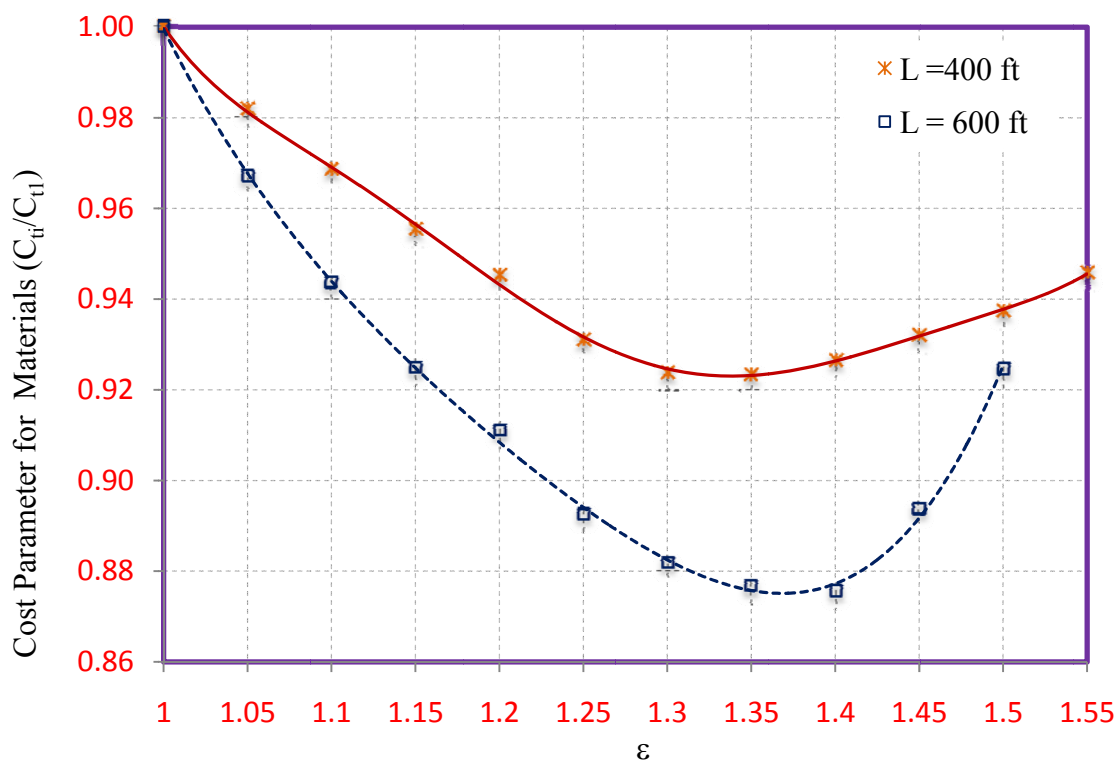
Figure 6.21 Plot of Total Cost versus ε (3-Span, AASHTO HS-20 loads, L= 400 ft and 600 ft)
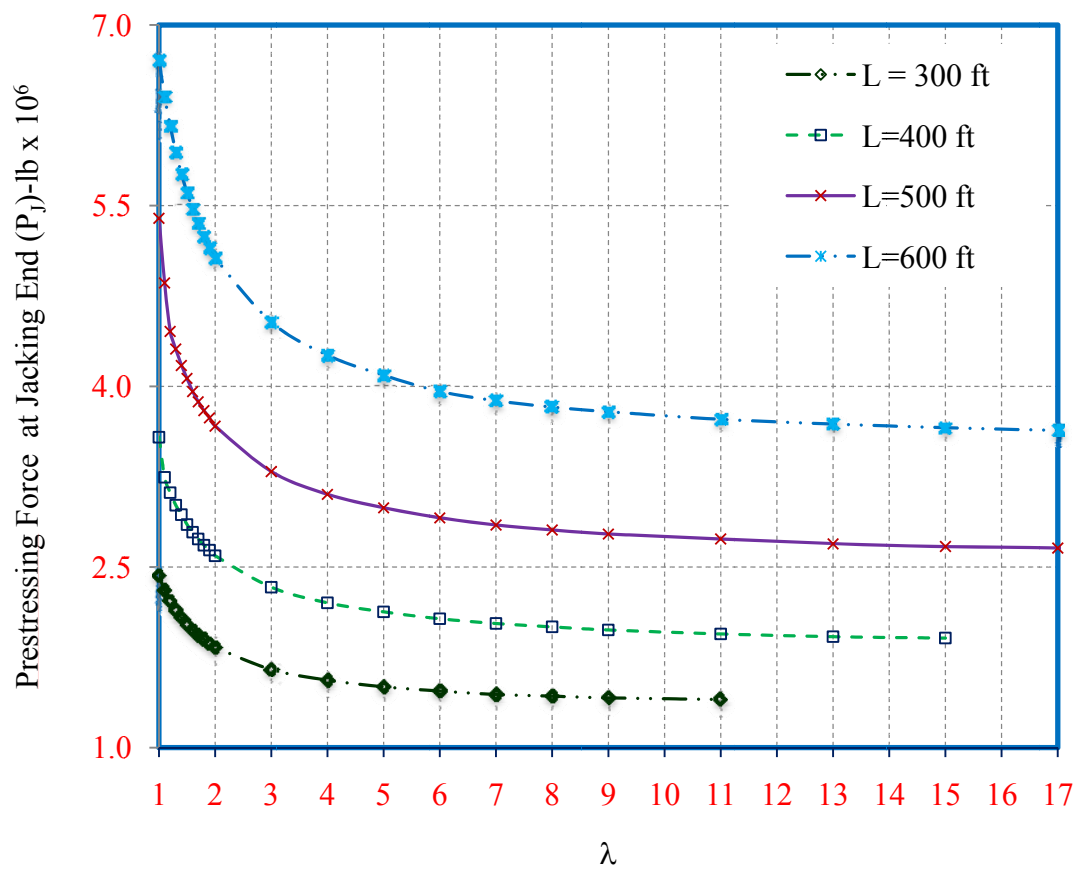
Figure 6.22 Plot of Required Prestressing (P_J) versus λ (3-Span and AASHTO HS-20 loads, L= 300 ft, 400 ft, 500 ft and 600 ft)
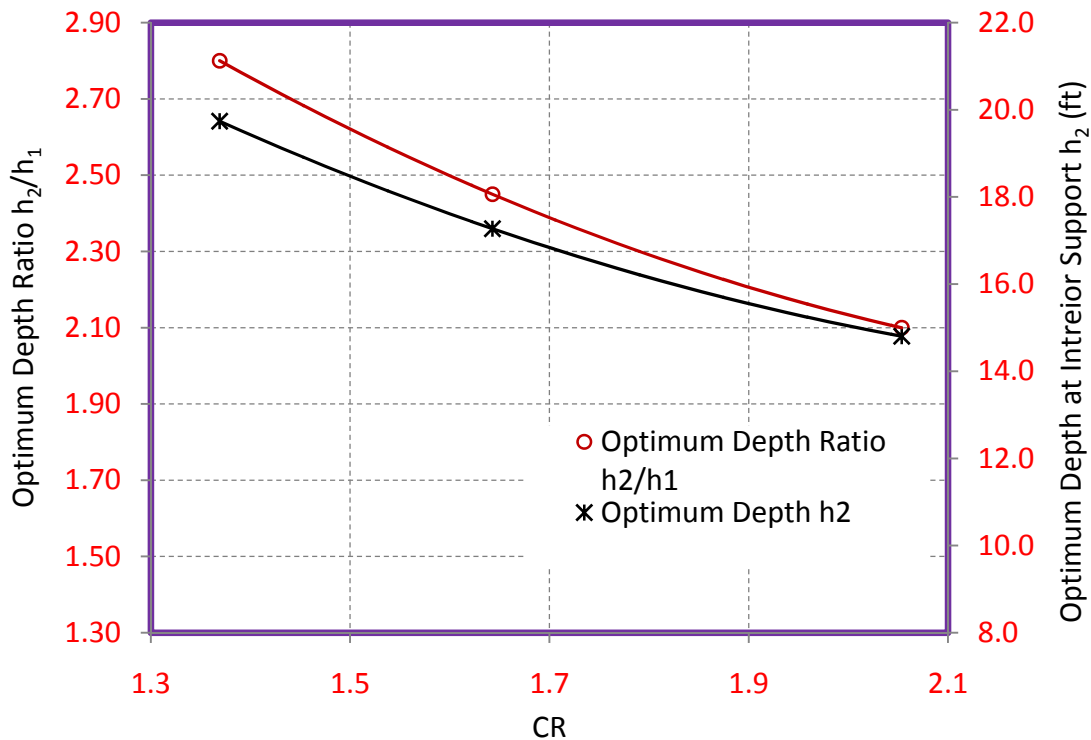
Figure 6.23 Optimum Value of Depth Ratio h_2/h_1 and Depth h_2 versus Ratio of Unit Cost CR(C_c/C_p) (3-Span of Total Length (500 ft) and AASHTO HS-20 loads)
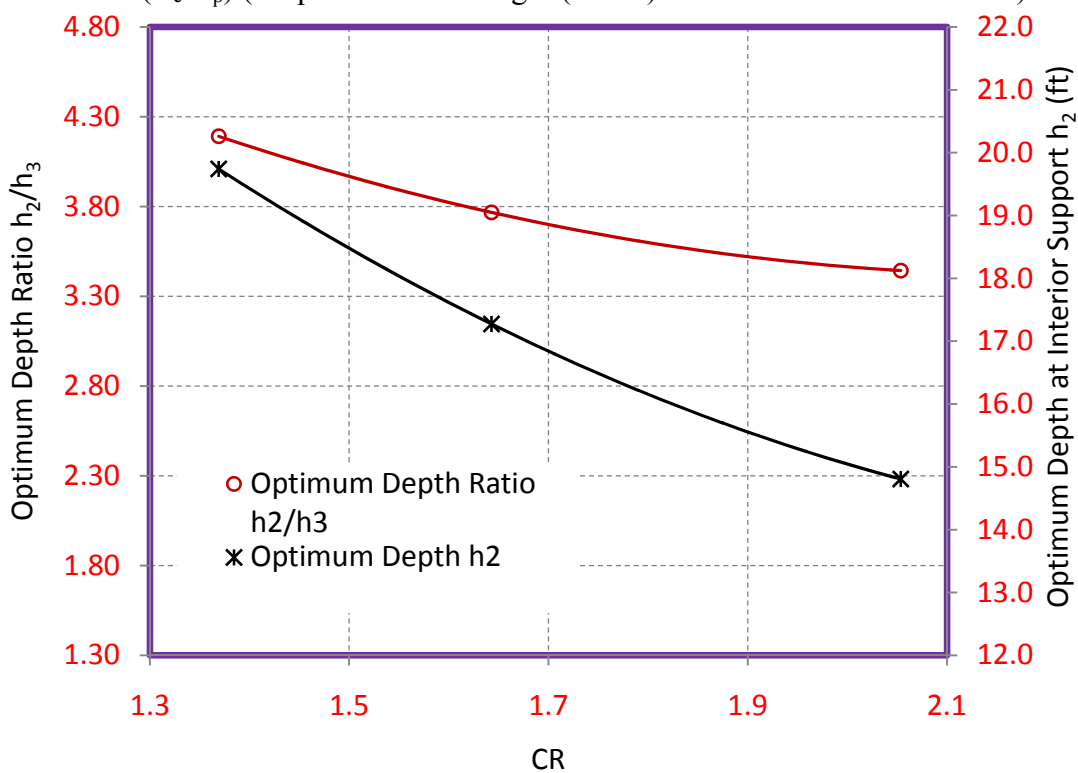
Figure 6.24 Plot Optimum Value of Depth Ratio h_2/h_3 and Depth h_2 versus Ratio of Unit Cost CR (C_c/C_p) (3-Span of Total Length (500 ft) and AASHTO HS-20 loads)
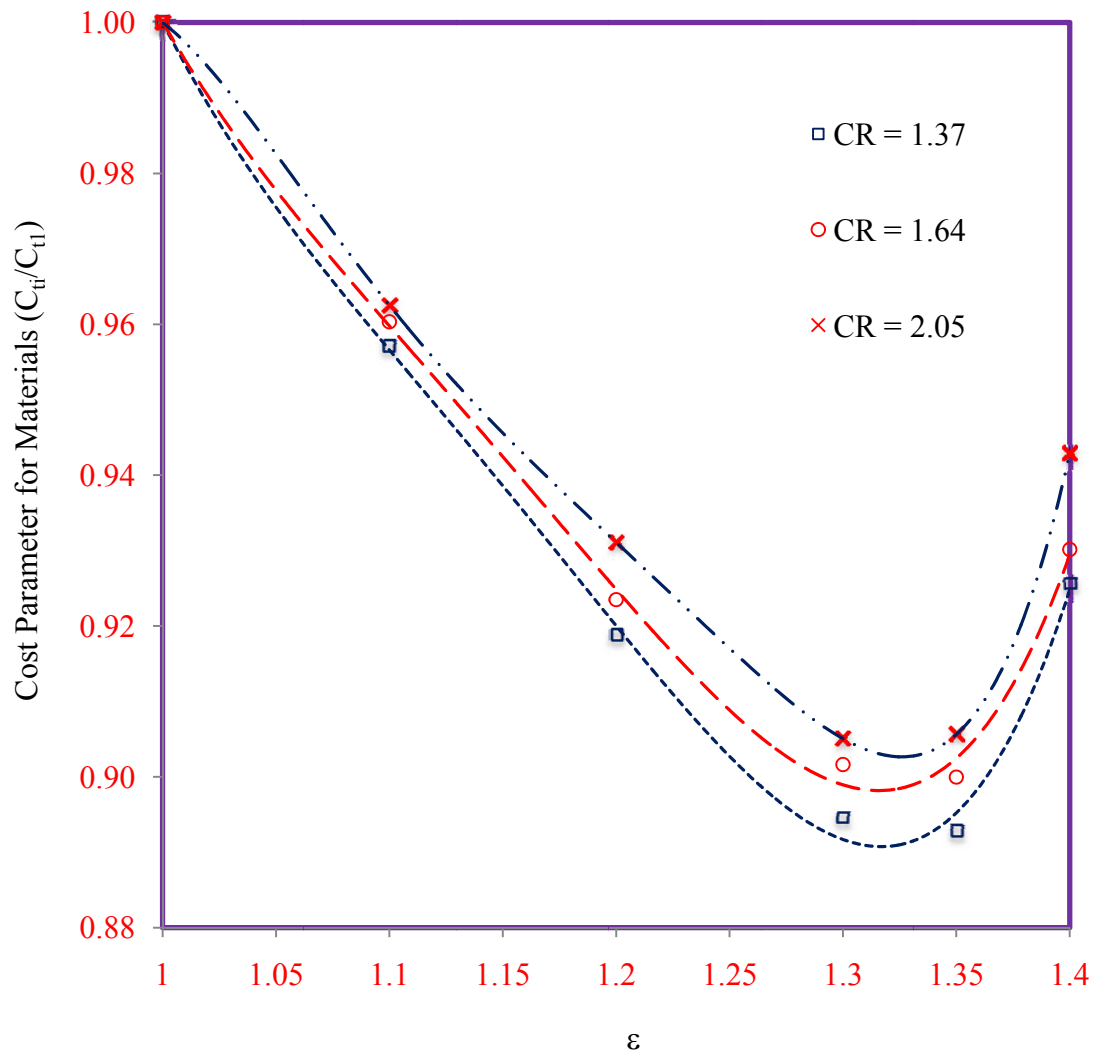
Figure 6.25 Plot of Total Cost versus ε for Different CR (C_c/C_p) (3-Span of Total Length (500 ft) and AASHTO HS-20 loads)
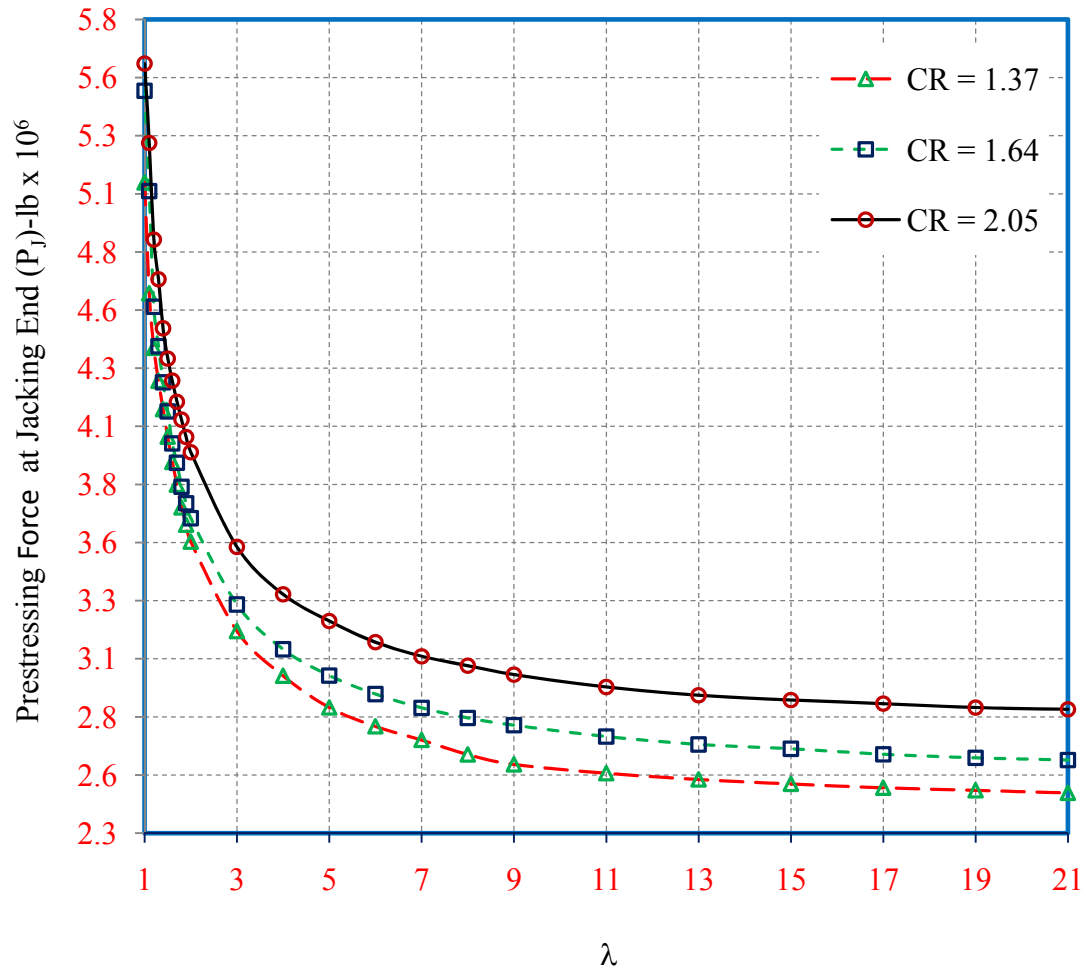
Figure 6.26 Plot of Required Prestressing P_J versus λ for Different CR(C_c/C_p) (3-Span of Total Length (500 ft) and AASHTO HS-20 loads)

6.4 General Observations

Based on the previous results presented for two and three-span continuous bridge girders, some observations that would help designers are made here:

1) The optimum value of ε for three-span continuous bridge girder lies within 1.30 to 1.4 regardless of the value of CR and total length of bridge girder L.

2) For a two-span continuous bridge girder, an economical design can be achieved with a right combination of long and short tendons even for non-optimum values of cross-sectional depths h_1 and h_2.

3) It has been observed that the optimum depth values are relatively insensitive to unit cost of prestressing steel and concrete for two-span continuous bridge decks. However, that would not be the case for three-span continuous bridge decks, for which optimum values of depths would depend on CR.

4) Lower prestressing steel cost can be attained with $\lambda \geq 9.0$ for both two-span and three-span continuous bridges, regardless of the value of CR and total length of bridge girder L.

5) The use of all full length tendons does not lead to economical design, and so a suitable combination of both long and short tendons ($\lambda > 1.0$) must be used.

CHAPTER SEVEN

CONCLUSIONS AND RECOMMENDATIONS

7.1 Conclusions

A generalized computer program PCPCBGND has been developed to readily determine the minimum cost design of non-uniform single-cell box girder bridge decks for two-span or three-span continuous bridges. The constrained non-linear optimization problem is solved iteratively by using a gradient search method to achieve a total solution which determines the deck profile along the length, the proportion of the long and short tendons, the required prestressing force and the tendon layout.

Based on this study, the following conclusions are made in order to achieve both economy and aesthetics of designing variable depth having single- cell box girders:

6) A generalized computer program PCPCBGND is developed to readily find the optimum design of a two-span or three-span of bridge girders of variable depth. The program automatically determines the optimum girder profile and the tendon layout with a combination of long and short tendons.

1) The combination of short and long tendons for either a two-span or a three-span bridge girder is always necessary to achieve economical design. When compared with all long tendons, an economical proportion of long and short tendons would always result in lower prestressing cost.

2) For a symmetrical three-span bridge girder of a given length, the minimum value of the total cost of material is achieved when ε lies within 1.3 to 1.4.

3) The optimum value of span ratio ε for three-span girder and λ are relatively insensitive to the ratio of unit costs of concrete and prestressing steel, *CR*.

4) As the results show that the cost of prestressing steel is insensitive beyond a value of $\lambda \geq 9.0$, an economical design can be attained with $\lambda \geq 9.0$ for all values of *L* considered in this study regardless of the value of unit cost ratio *CR*.

5) For three-span continuous bridge girders, the optimum values of h_1, h_2 and h_3 are sensitive to the change in the unit cost ratio *CR* of concrete and prestressing steel. However, for two-span continuous bridge girders, the optimum values of h_1 and h_2 are marginally impacted by *CR* value.

7.2 Recommendations for Future Research

The following recommendations can be made for further research in this area

1) In this research, only the material cost was considered in the objective function. Future work may include other costs in addition to material cost, such as the cost of prestressing steel anchorage, formwork and ordinary steel reinforcement.

2) Multi-cells box girders can also be studied for wider bridge decks.

3) This study can be extended to other cross-section types, such as solid and voided slab-type bridge decks.

REFERENCES

[1] Abul-Feilat E., ''Optimum Design of Continuous Partially Prestressed Concrete Beams.'' Master Thesis, King Fahd University of Petroleum & Minerals, Dhahran, Saudi Arabia, January 1991.

[2] ACI-ASCE Committee 343, Analysis and Design of Reinforced Concrete Bridge Structures, 1995.

[3] ACI Committee 435-R, Control of Deflection in Concrete Structures, 1995.

[4] ACI Committee 318, Building Code Requirements for Structural Concrete, 2005.

[5] Al-Gahtani A., Al-Saadoun S. and Abul-Feilat E., '' Design Optimization of Continuous Partially Prestressed Concrete Beams.'' Computers & Structures, Vol. 55, No.2, PP. 365-370, 1995.

[6] American Association of State Highway and Transportation Officials. (1996). "AASHTO Standard Specifications for Highway Bridges." 16th Edition. Washington, D.C.

[7] Arora J. S., ''Introduction to Optimum Design.'' McGraw-Hill, Inc., New York, N.Y., 2004.

[8] Azad A. K. and Qureshi M., ''Optimum post-tensioned for three-span continuous slab-type bridge decks.'' Engineering Optimization, Vol. 31, PP. 679-693, 1999.

[9] Azad A. K., ''Class notes for Prestressed Concrete course CE-522.'' King Fahd University of Petroleum & Minerals, Dhahran, Saudi Arabia, Fall 2006.

[10] Barakat S., Al Harthy A. and Thamer A., ''Design of Prestressed Concrete Girder Bridges Using Optimization Techniques.'' Pakistan Journal of Information and Technology, 1(2), PP. 193-201, 2002.

[11] Barakat S., Kallas N. and Tahab M., ''Single Objective Reliability-based Optimization of Prestressed Concrete Beams.'' Computers & Structures, Vol. 81, PP. 2501-2512, 2003.

[12] Barker R. and Puckett J., ''Design of Highway Bridge. ''John Wiley & Sons, Inc., Hoboken, New Jersey, 2007.

[13] Barr A. S., Sarin S. C., and Bishara A. G., ''Procedure for Structural Optimization.'' ACI Structural Journal, Vol. 86, No. 5, PP 524-531, September-October 1986.

[14] Caprani C., ''Prestressed Concrete'', 2006/7, Obtained from: http://www.colincaprani.com/files/notes/CED1/PSC%20Notes.pdf

[15] Cohn M. Z. and Lounis Z., ''Optimum Limit Design of Continuous Prestressed Concrete Beams.'' Journal of Structural Engineering, Vol. 119, No. 12, PP 3551-3570, December, 1993.

[16] Cohn M. Z. and Lounis Z., ''Optimal Design of Structural Concrete Bridge Systems.'' Journal of Structural Engineering, Vol. 120, No. 9, PP 2653-2674, September 1994.

[17] Erbatur F., Al Zaid R. and Dahman N., ''Optimization and Sensitivity of Prestressed Concrete Beams.'' Computers & Structures, Vol. 45, No.5/6, PP. 881-886, 1992.

[18] Gail S., ''Prestress Losses in Post-Tensioned Structures.'' Pit Technica1 Notes, Issue 10, September 2000.

[19] Hinkle S., ''Investigation of Time-Dependent Deflection in Long Span, High Strength, Prestressed Concrete Bridge Beams.'' Master Thesis, Virginia Polytechnic Institute and State University, August 2006.

[20] Hulse R. and Mosley W. H., ''Prestressed Concrete Design by Computer.'' Macmillan Education Ltd, London, 1987.

[21] Hussain A., and Bhatti M., ''Optimum Design of Continuous Prestressed Concrete Girders.'' Symposium of Electronic Computation, PP 168-179, 1986.

[22] Johnson F., ''An Interactive Design Algorithm for Prestressed Concrete Girders.'' Computers & Structures, Vol. 2, PP. 1075-1083, 1972.

[23] Karim A., ''Nonlinear Optimization, Theory and Practice.'', 2nd International Bhurban Conference on Applied Sciences and Technology Control and Simulation, Lahore University of Management Sciences, June 19 – 21, 2003

[24] Khachaturian N. and Gurfinkel G., ''Prestresssed Concrete.'' McGraw-Hill, Inc., New York, N.Y., 1969.

[25] Khaleel M. and Itani R., ''Optimization of Partially Prestressed Concrete Girders under Multiple Strength and Serviceability Criteria.'' Computers & Structures, Vol. 49, No.3, PP. 427-438, 1993.

[26] Kirsch U., ''Optimum Design of Prestressed Beams.'' Computers & Structures, Vol. 2, PP. 573-583, 1972.

[27] Kirsch U., ''A Bounding Procedure for Synthesis of Prestressed Systems.'' Computers & Structures, Vol. 20, No.5, PP. 885-895, 1985.

[28] Kirsch U., ''Two-level optimization of prestressed structures.'' Engineering Structure, Vol. 19, No.4, PP. 309-317, 1997.

[29] Kuyucular A., ''Prestressed Optimization of Concrete Slabs.'' Journal of Structural Engineering, Vol. 117, No. 1, PP 235-254, January, 1991.

[30] Lounis Z. and Cohn M. Z., ''Multiobective Optimization of Prestressed Concrete Structures.'' Journal of Structural Engineering, Vol. 119, No. 3, PP 794-808, March, 1993.

[31] Nawy E., ''Prestressed Concrete, A fundamental Approach.'' Pearson Education, Inc, 2006.

[32] Nilson A. H., Darwin D. and Dolan W. C., ''Design of Concrete Structures.'' McGraw-Hill, Inc., New York, N.Y., 2004.

[33] Ohkubo S., Dissanayake P. and Taniwaki K., ''An approach to multicriteria fuzzy optimization of a prestressed concrete bridge system considering cost and aesthetic feeling.'' Structural Optimization, Vol. 15, PP. 132-140, 1998.

[34] PCI Industry Handbook Committee. PCI Design Handbook – Precast and Prestressed Concrete (6th ed.). Precast/Prestressed Concrete Institute. Chicago, Illinois, 2004.

[35] Quiroga A. and Arroyo M., ''Optimization of Prestressed Concrete Bridge Decks.'' Computers & Structures, Vol. 41, No.3, PP. 553-559, 1991.

[36] Qureshi M., ''Optimization of continuous post-tensioned bridge decks of prescribed lengths.'' Master Thesis, King Fahd University of Petroleum & Minerals, Dhahran, Saudi Arabia, March 1995.

[37] Sirca G. and Adeli H., ''Cost Optimization of Prestressed Concrete Bridges.'' Journal of Structural Engineering, Vol. 131, No. 3, PP 380-388, March, 2005.

[38] Touma A. and Wilson F., ''Design Optimization of Prestressed Concrete Spans for High Speed Ground Transportation.'' Computers & Structures, Vol. 3, PP. 265-279, 1973.

[39] Utrilla M. and Samartin A., ''Optimized Design of the Prestressed in Continuous Bridge Decks.'' Computers & Structures, Vol. 64, No.1/4, PP. 719-728, 1997.

[40] Western Concrete Reinforcing Steel Institute, Post-Tensioning Committee, Concrete Reinforcing Steel Institute," Post-tensioned box girder bridges.'' 1971.

[41] Yu C.H., Das Gupta N.C., and Paul H., ''Optimization of Prestressed Concrete Bridge Girders.'' Engineering Optimization, Vol. 10, PP. 13-24, 1986.

APPENDIX A: Program Verification

Table A.1 Minimum Prestressing force P_J for Two-Span of Total Length 400 ft Using Excel Solver

| Ratio λ | Value of P_J Obtained From | | Ratio (PCPCBGND/Solver) |
| | PCPCBGND | Excel Solver | |
	P_J Kips x 10^3	P_J Kips x 10^3	
1	6.463	6.490	0.99584
1.1	6.281	6.279	1.000319
1.2	6.128	6.126	1.000326
1.3	6.005	6.006	0.999833
1.4	5.904	5.898	1.001017
1.5	5.816	5.805	1.001895
1.6	5.729	5.712	1.002976
1.7	5.653	5.629	1.004264
1.8	5.583	5.554	1.005221
1.9	5.520	5.488	1.005831
2	5.463	5.432	1.005707
3	5.106	5.083	1.004525
4	4.911	4.883	1.005734
5	4.786	4.753	1.006943
6	4.700	4.661	1.008367
7	4.639	4.597	1.009136
8	4.591	4.554	1.008125
9	4.554	4.521	1.007299
11	4.498	4.479	1.004242
13	4.458	4.451	1.001573
15	4.435	4.430	1.001129
17	4.413	4.414	0.999773
19	4.398	4.402	0.999091
21	4.386	4.388	0.999544

Table A.2 Bending Moment for Two-Span of Total Length 400 ft Using Staad-Pro Package

STATION	Value of B.M.F Obtained From					
	PCPCBGND			Staad-Pro		
	Kip.ft			Kip.ft		
No.	Min.LL	Max.LL	Self wt.	Min.LL	Max.LL	Self wt.
1	0.0	0.0	0.0	0.00	0.00	0.00
2	-137.226	1177.501	8252.356	-137.22	1177.44	8252.40
3	-274.448	2003.995	13965.52	-274.45	2003.95	13965.60
4	-411.668	2500.714	17139.43	-411.67	2500.69	17139.60
5	-548.894	2713.135	17774.18	-548.90	2713.12	17774.40
6	-686.118	2662.615	15869.78	-686.12	2662.61	15870.00
7	-823.349	2386.445	11426.19	-823.34	2386.44	11426.40
8	-960.578	1898.042	4443.403	-960.57	1898.02	4443.60
9	-1097.81	1252.031	-5078.512	-1097.81	1252.00	-5078.40
10	-1235.04	511.7026	-17139.65	-1235.01	511.67	-17139.60
11	-1372.27	0.0	-31740.01	-1372.24	0.00	-31740.00
12	-1235.04	511.7026	-17139.65	-1235.01	511.67	-17139.60
13	-1097.81	1252.031	-5078.512	-1097.81	1252.00	-5078.40
14	-960.578	1898.042	4443.403	-960.57	1898.02	4443.60
15	-823.349	2386.445	11426.19	-823.34	2386.44	11426.40
16	-686.118	2662.615	15869.78	-686.12	2662.61	15870.00
17	-548.894	2713.135	17774.18	-548.90	2713.12	17774.40
18	-411.668	2500.714	17139.43	-411.67	2500.69	17139.60
19	-274.448	2003.995	13965.52	-274.45	2003.95	13965.60
20	-137.226	1177.501	8252.356	-137.22	1177.44	8252.40
21	0.0	0.0	0.0	0.00	0.00	0.00

Table A.3 Computed Flexural Stresses for Two-Span (L= 400 ft, λ = 25, h₁ = 8.95 ft and h₂ = 13.0 ft)

Station	Flexural Stress, *f* (Psi)	
	Bottom	Top
Initial Stage (Self-Weight Bending Moment +Prestressing Force)		
1	-640.8995	-846.0278
2	-703.5483	-729.437
3	-704.845	-667.5983
4	-669.7285	-637.7239
5	-618.3036	-618.3773
6	-528.9006	-630.2209
7	-374.8642	-705.9083
8	-207.512	-808.515
9	-193.1864	-1485.066
10	-318.2923	-1301.142
11	-761.7043	-798.139
Final Stage (Max. Bending Moment +Prestressing Force)		
1	-512.7196	-676.8223
2	-312.7807	-826.0346
3	-148.1304	-937.4014
4	-40.15674	-991.3176
5	2.44E-04	-975.3138
6	-0.3719482	-915.3726
7	-6.782959	-850.1688
8	-45.78683	-764.0422
9	-222.7255	-1121.484
10	-512.5251	-788.7589
11	-1260.993	-0.5142822
Final Stage (Min. Bending Moment +Prestressing Force)		
1	-512.7196	-676.8223
2	-434.8928	-707.6206
3	-359.8041	-732.0527
4	-307.6393	-731.6538
5	-291.0704	-692.4998
6	-286.4944	-637.0691
7	-264.5041	-599.1882
8	-257.3388	-557.7562
9	-389.4524	-958.6883
10	-680.702	-624.323
11	-1260.993	-0.5142822

Table A.4 Computed Flexural Stresses for Two-Span (L= 400 ft, $\lambda = 25$, $h_1 = 10.95$ ft and $h_2 = 15.90$ ft)

Station	Flexural Stress, *f* (Psi)	
	Bottom	Top
Initial Stage (Self-Weight Bending Moment +Prestressing Force)		
1	-506.1884	-715.2472
2	-560.2944	-614.1479
3	-560.1973	-561.6698
4	-528.0643	-537.5235
5	-482.0065	-522.5867
6	-411.1202	-526.9332
7	-298.57	-572.7827
8	-182.5658	-634.3641
9	-148.087	-1182.284
10	-230.7604	-1047.832
11	-595.9606	-629.2662
Final Stage (Max. Bending Moment +Prestressing Force)		
1	-404.9507	-572.1978
2	-252.9057	-681.818
3	-123.5569	-766.0171
4	-35.79614	-807.4462
5	-0.3017578	-794.4496
6	-0.6032715	-742.5157
7	-12.93542	-679.3234
8	-56.48276	-595.2414
9	-177.9536	-887.4877
10	-394.8144	-631.8754
11	-988.9254	0.00E+00
Final Stage (Min. Bending Moment +Prestressing Force)		
1	-404.9507	-572.1978
2	-343.6553	-593.3126
3	-280.8564	-612.5555
4	-234.5497	-613.436
5	-216.5449	-583.2145
6	-213.1087	-534.751
7	-204.266	-492.0777
8	-213.4462	-441.467
9	-301.6173	-766.2037
10	-519.5293	-509.4245
11	-988.9254	0.00E+00

VITA

Name   Mohammed Ali Mohammed Al-Osta

Date of Birth 2^{sd} May 1975

Education

University   Obtained B.E in Civil Engineering from Sana'a

                      University, Yemen, 1999

                      Obtained M.S in Structural Engineering from King Fahd

                      University of Petroleum & Minerals,   Dhahran, KSA, 2009.

Work Experience

2001 to 2004   Assigned as instructor in Sana'a University in Yemen.

                      I still worked in Sana'a University.

Major Achievements and Awards

                      Received First Honor Awards in all the semesters in the BS

                      program.

                       Obtained the highest GPA (3.97/4.00) among the graduate Civil

                      and Applied Civil Engineering students.